Role of cAMP-PDE4b-CREB Signaling in Controlling the Function of Alveolar Macrophages

BY

Ian Rochford
B.S., University of Nebraska at Lincoln, 2012
M.S., University of Missouri at Kansas City, 2014

THESIS
Submitted as partial fulfillment of requirements
for the degree of Doctor of Philosophy in Pharmacology
in the Graduate College of the
University of Illinois at Chicago, 2021

Chicago, Illinois

Defense Committee
Dolly Mehta, Chair and Advisor
Kostandin Pajcini
Yulia Komarova
Shekhar Reddy, Pediatrics
Kiwook Kim

Dedication

This thesis is dedicated to my parents, who nurtured my love of science from the time I was little, and to my sister, Caitlin, who reminded me how to be smart after I had forgotten.

Acknowledgments

First and foremost, I would like to extend my gratitude to Dolly Mehta, for allowing me to join her lab and complete my PhD journey. Her lab has been a place of scientific curiosity that has allowed me to explore my own path through a diverse array of fields within biomedical science. Central to both the running of the Pharmacology department and motivating the cohort of graduate students is Dr. Malik. I greatly appreciate his role in my receiving of the T32 Lung Biology training grant.

I am grateful for the other members of my research committee, Drs. Yulia Komarova and Konstandin Pajcini. Their constructive critique and suggestions were instrumental in making my project what it is. Similarly, I am grateful for the advice, resources, and suggestions given to me by members of their respective labs.

Early on in my time in the lab, I was under the wing of Pascal Yazbek, who spent time acclimating me to the lab and whom I thank for sharing the various secrets and tricks that only come with experience. I would like to give special thanks to Drs Jagdish Joshi and Rayees Sheikh for their assistance and dedication to my project, as well for giving me a chance to contribute substantively to their projects during my time in the lab. My first co-authorships were on their papers, officially making me a published scientist, and I greatly value their partnership. While I thank all the other members of the Mehta lab, I would also like to give credit to Somenath Banerjee for always being available for my questions and lively discussions about macrophages and flow strategies.

I owe a great debt of gratitude to the members of the Flow Core for their assistance in running my many hundreds of flow cytometry experiments. Not only have Balaji Ganesh and Suresh Ramasamy helped me design experiments, but many times they have stayed late or come

early to accommodate my experiment schedule. Their kindness and guidance were central to my mastery of flow cytometry techniques.

Table of Contents

List of Tables

List of Figures

List of Abbreviations and Nomenclature

AC – Adenylate cyclase
AKAP – A-kinase anchoring protein
ALI – Acute lung injury
AMP – Adenosine monophosphate
AMϕ – Alveolar macrophages
ARDS – Acute respiratory distress syndrome
ATM – Adipose tissue macrophage
ATP – Adenosine triphosphate
BMDM – Bone marrow-derived macrophages
cAMP – Cyclic adenosine-monophosphate
cGAMP Cyclic guanosine-adenosine mono phosphate
cGMP – Cyclic guanosine monophosphate
COPD – Chronic obstructive pulmonary disease
CREB – cAMP response element binding protein
DAMP – Damage associated molecular pattern
DT – Diphtheria toxin
DTR – Diphtheria toxin receptor
EPAC – Exchange protein activated by cAMP
FAO – Fatty acid oxidation
GFP – Green florescent protein
GLUT – Glucose transporter
GM-CSF -Granulocyte/macrophage colony stimulating factor
GMP – Guanosine monophosphate
GPCR- G protein coupled receptor
HDAC - Histone deacetylase
IFN – Interferon
IL –Interleukin
IMϕ – Interstitial macrophages
iNOS – Inducible nitric oxide synthase
IRAK - Interleukin-1 receptor-associated kinase 4
IRF – Interferon regulator factor
LDTF – Lineage defining transcription factor
LPS - Lipopolysaccharide
M-CSF- Macrophage colony stimulating factor
Mo-Mϕ – Monocyte derived macrophages
NFAT – Nuclear factor activator of T-cells
NFkB – Nuclear factor kappa B
NLPR3 - NLR family pyrin domain containing 3
PAMP – Pathogen associated molecular pattern
PDE - Phosphodiesterase
PDH - Pyruvate dehydrogenase
PDK – Pyruvate dehydrogenase kinase

PPAR – Peroxisome proliferator-activated receptor
PKA – Protein kinase A
PKG – Protein kinase G
sAC – Soluble adenylate cyclase
SDTF – Signal dependent transcription factor
SMC – Smooth muscle cell
STAT – Signal transducer and activator of transcription
STING – Stimulator of interferon genes
TANK – TRAF family member-associated NF-kappa-B activator
TBK – TANK binding kinase
TCA - Tricarboxylic acid cycle
TGF – Transforming growth factor
TLR – Toll-like receptor
TNF – Tumor necrosis factor
TRAF1 – TNF receptor-associated factor 1
UCR – Upstream constant region

Summary

Acute lung injury (ALI) is a debilitating condition that results from excessive inflammatory stimulation of the immune system. If left untreated, ALI can progress to a fatal clinical exacerbation known as acute respiratory distress syndrome (ARDS). Under healthy conditions, the lungs permit non-threatening pathogens or irritants to be cleared away by the immune system without triggering inflammatory cascade reactions. This tolerogenic environment is maintained by populations of lung resident macrophages. But during lung injury, cytokines produced by macrophages induce the weakening of the lung vascular endothelial barrier, leading to the accumulation of edema fluid in the alveolar airspace and the impairment of gas exchange. Ultimately, macrophages then resolve acute lung injury by shifting from a pro-injury inflammatory state to an anti-inflammatory state and restore lung fluid homeostasis. As master regulators of both the induction and resolution of inflammatory injury, understanding macrophage state transitions is essential to develop medical interventions to severe lung disease.

This thesis begins by describing the plasticity and molecular signaling underlying macrophage behavior generally and in the context of lung disease. This background also supports previously published work by the Mehta lab describing how monocyte-derived macrophages educate resident lung macrophages by dampening activation of the STING complex through non-receptor mediated activity of S1P. Other important published work investigated the role of cAMP signaling in the tuning of alveolar macrophage (AMϕ) inflammatory responses by inhibiting calcium influx regulated cytokine production. Based on this prior established work, I developed the hypothesis that cAMP signaling was required to induce the pro-resolution functionality of lung resident AMϕ.

The testing and exploration of this hypothesis are covered in four sections. The first begins with an examination of the dynamic changes alveolar and interstitial/monocyte-derived macrophages undergo over the time course of reversible acute lung injury. Flow cytometric analysis showed that AMϕ diminish as a percentage of the total lung resident macrophage pool and transition to a $CD11b^{+}$ phenotype. To further characterize the transcriptional profile of lung resident macrophages over the course of lung injury, the total macrophage pool was isolated during the basal, inflamed, and resolved injury states and used for RNA sequencing. By focusing on genes that were related to the cAMP signaling pathway we identified the gene PDE4b, a negative regulator of cAMP signaling, as correlating with the transition between injury states. Analysis of the promoter for PDE4b revealed several binding sites for NFAT, a potential regulator for PDE4b expression. Pharmacological inhibition experiments demonstrated that NFAT signaling was required for increased PDE4b gene expression at both the mRNA and protein levels. Further experiments showed that NFAT both bound to the promoter of PDE4b and that gene activation occurred in response to LPS and NFAT activation.

In the second part of the study, we sought to determine how inhibition of PDE4b enzymatic function affected the dynamics of lung resident macrophages as well as the progression of lung injury. Intratracheal administration of the PDE4 specific inhibitor rolipram accelerated the resolution of acute lung injury as measured both by edema formation and vascular barrier permeability. During this accelerated resolution, the lung resident macrophages also exhibited an altered phenotype. The decrease of AMϕ as a fraction of the total macrophage pool and their transition to $CD11b^{+}$ was reversed by PDE4 inhibition. Flow cytometric quantification showed that this change in proportion was, in fact, due to an increase in the total number of AMϕ.

In the third part of this study, we isolated AMϕ from rolipram-treated mice and adoptively transferred them into injured mice. The enhanced injury recovery seen in these rolipram-treated cell recipient mice demonstrated that enhanced cAMP signaling programs AMϕ into a pro-resolution phenotype. We next made use of a mouse model which allowed us to selectively deplete CD11b expressing monocytes and macrophages to show that rolipram was not effective at resolving injury in the absence of recruited monocytes. By tracing the adoptively transferred monocytes we found that they were recruited into the airspace and became phenotypically similar to resident AMϕ.

The fourth section of this study is a preliminary look at the role of the cAMP-regulated transcription factor CREB on the functionality and generation of AMϕ. We show that mice that lack the CREB gene in myeloid cells exhibit a defect in the homeostatic maintenance of vascular barrier integrity and are insensitive to the accelerated injury resolution by PDE4 inhibition. In addition, CREB is shown to be responsible for the expression of PDK4, a kinase that regulates the transition of metabolites from glycolysis to the TCA cycle.

The conclusion of this work discusses our conclusion that cAMP is responsible for programming monocyte-derived macrophages in the airspace to a pro-injury resolution phenotype by activation of a CREB dependent transcriptional program. The implications of this regulatory pathway and future studies are addressed in a reflection on planned projects stemming from this work.

Abstract

Increased lung vascular permeability and neutrophilic inflammation are hallmarks of acute lung injury. Recent studies indicate that AMϕ, the predominant immune cell type in the airspace, die off while fending off pathogens and are replaced by recruited monocytes. These new AMϕ facilitate the resolution of injury, but the mechanisms regulating this reparative phenotype have not yet been defined. Cyclic AMP (cAMP) is an immunosuppressive second messenger in many cell types. Here, we subjected mice expressing GFP under the control of the Lysozyme-M promoter (LysM-GFP mice) to the LPS model of rapidly resolving lung injury to address investigate changes in cAMP signaling in the initiation and mobilization of reparative AMϕ. RNA-seq analysis of flow-sorted Mϕ identified PDE4b as the top LPS-responsive cAMP-regulating gene. We observed that the cAMP negative regulator PDE4b expression sharply increased at the time of peak lung injury (4 h) and then decreased to below the basal level during the resolution phase (24 h). Activation of transcription factor NFATc2 was required for transcription of PDE4b in Mϕ. Inhibition of PDE4 activity after injury induction using *i.t.* rolipram increased cAMP levels, augmented the reparative AMϕ pool, and accelerated injury resolution. This response was not seen following conditional depletion of monocytes, thus establishing airspace-recruited monocytes as the source of reparative AMϕ following enhanced PDE4 inhibition. Interestingly, adoptive transfer of rolipram-educated AMϕ into injured mice resolved lung edema. The transcription factor CREB was shown to be required for rolipram-induced injury resolution and maintenance of basal lung fluid homeostasis. We propose that enhanced CREB signaling through suppression of PDE4b is an effective approach to promote reparative AMϕ generation from monocytes for lung repair.

Hypothesis:

cAMP signaling is required for the generation and programming of reparative alveolar macrophages.

Specific Aims:

Specific Aim 1: Evaluate the role of cAMP signaling genes in the conversion of alveolar macrophages from an enflamed to reparative phenotype.

Specific Aim 2: Determine whether cAMP reprograms alveolar macrophage reparative phenotype *in vivo.*

Specific Aim 3: Determine whether CREB plays a role in alveolar macrophage reparative phenotype *in vivo.*

Literature Review

1. Macrophages

Macrophages are the principal immune sentinels of the body. While different lineages of lymphocytes facilitate the adaptive immune system, these leukocytic cells are the central regulators of the innate immune system. Macrophages are seen as professional phagocytes, patrolling tissues and eliminating cell fragments and foreign debris by engulfment[1]. Meanwhile, a suite of receptors on their surfaces detects various common pathogen or damage-associated molecular patterns (PAMPs and DAMPs)[2]. Unlike antibodies, which are specific for foreign antigens, PAMP receptors recognize a broad range of stereotypical molecules produced by pathogens or damaged cells. In response to these signals, macrophages secrete a range of cytokines and growth factors in response to environmental cues to instruct neighboring cells appropriate to the threat. Macrophages respond to infection by secreting such as complement proteins and reactive oxygen species generating enzymes used to target unwanted pathogens[3]. In response to tissue damage, macrophages can also facilitate wound healing and tissue regeneration[4]. This huge array of functions is possible only because of the incredible plasticity of macrophage phenotype and identity. Different macrophages from different tissues, or even within the same tissue, will exhibit different phenotypes and responses to stimuli. Recent research has begun to define three primary factors which contextualize macrophage identity: 1) origin and ontogeny; 2) residency; and 3) polarization.

The first aspect which defines macrophages is their origin and ontogeny **(Fig 1A)**. Macrophages subpopulations are typically derived from a common lineage descended from embryonic precursors[5] or adult monocytes[6], while other tissue-specific subpopulations are

transiently derived from differentiated monocytes[7]. A complex system of epigenetic regulation permits the signature plasticity of macrophages. PU.1 is the lineage-defining transcription factor (LDTF) for macrophages. When coupled with transcriptional effectors such as C/EBP, PU.1 binds to numerous macrophage-specific gene promoters and enhancers, opening them up for transcription[8,9]. It is suggested that many 'latent enhancers' are made available within the constellation of macrophage-specific sites opened by PU.1 but are not active until a secondary stress signal is initiated activates signal-dependent transcription factors (SDTFs)[10]. In this hierarchical system, the LDTF PU.1 makes the full repertoire of macrophage-related genes available while a second wave of SDTFs activate subsets of this repertoire depending on extrinsic signals.

The second factor governing macrophage identity is the unique phenotype which is necessary to fulfill the specific functions related to maintaining tissue homeostasis and is dependent on the specific tissue microenvironment signals **(Fig 1B)**. Macrophages that reside within tissues in the basal state are considered 'resident' to that tissue. A suite of SDTF induced by the tissue environment activate the genes necessary for the macrophage to perform its homeostatic functions for that tissue[5,11]. For instance, splenic red pulp macrophages activate the transcription factor Spi-C in response to heme exposure, inducing their erythrocyte degradation functions[12]. Signals unique to the peritoneal cavity induce the transcription factor GATA6, unlike other resident macrophage populations, to facilitate the self-renewal of peritoneal macrophages[13].

The third and most complex factor defining macrophage identity is the activation state acquired by stress-related signaling which can lead to induction of inflammatory signaling, or "acute state functionality"[14]. Researchers have conceptualized this activation as macrophages 'polarizing' along an axis between two states in response to different cytokine and

microenvironmental signals **(Fig 1C)**. One polarization state, M1, or 'classical activation' is generally considered pro-inflammatory, characterized by the secretion of cytokines which further stimulate the inflammatory response in other myeloid cells and induction of anti-microbial protein secretion. The M2, or 'alternatively activated', state is considered anti-inflammatory, as it induces the cessation of inflammatory signaling and initiates wound healing and regenerative processes[15]. The idea of a linear axis between M1 and M2 is increasingly considered to be an oversimplification of the *in vivo* process of macrophage responses to physiological changes. Canonical M1 and M2 markers are consistent *in vitro* given a narrow range of stimuli, but the inflammatory responses of *in vivo* macrophages will deviate from these expected patterns across different resident tissue populations and across different times following stimulation[16,17].

But in spite of this challenging complexity, transcriptional regulation of acute stress signaling pathways has been well characterized *in vitro*. The essential pro-inflammatory transcription factor induced by numerous PAMP and DAMP receptors is NFκB. In the case of the PAMP receptor TLR4, activation by the bacterial product LPS leads to the activation of NFκB[18]. This signal path relies on MyD88, which couples to the active TLR4 receptor complex and IRAK-4[19] but also acts through a MyD88 independent pathway which leads to the activation of IRF3. The TIR-containing adaptor protein TRIF also binds to the active TLR4 receptor complex and recruits TRAF3 to activate IRF3 by associating with TANK/TBK1. Activation of IRF3 by TBK1 initiates the expression of interferon type-1 genes in addition to the cytokines induced by NFκB[2]. IFN-γ, an inflammatory cytokine, can then amplify M1 signaling through activation of STAT1 and IRF1, where LPS predominantly leads to the activation of NFκB and IRF1[2]. The bifurcation and later overlap of this activation pathway create points of regulation to tailor inflammatory responses to specific stimuli.

Polarization to the M2 state generalizes a number of different functionalities, including suppression of inflammatory signaling, responses to helminth infection, and fibrosis[20]. The anti-inflammatory cytokine IL-4 activates IRF4 and STAT6[14]. Inflammatory and anti-inflammatory signaling can antagonize each other. IL-4, an M2 signal can activate STAT6, which can suppress STAT1 signaling activated by IFN-γ [21]. Conversely, IFN-γ can suppress IL-4 induced gene expression through STAT1[22]. This reciprocity suggests that macrophage signaling is a balancing act between inflammatory directives which shift over the course of stress as signals are integrated into feedback loops.

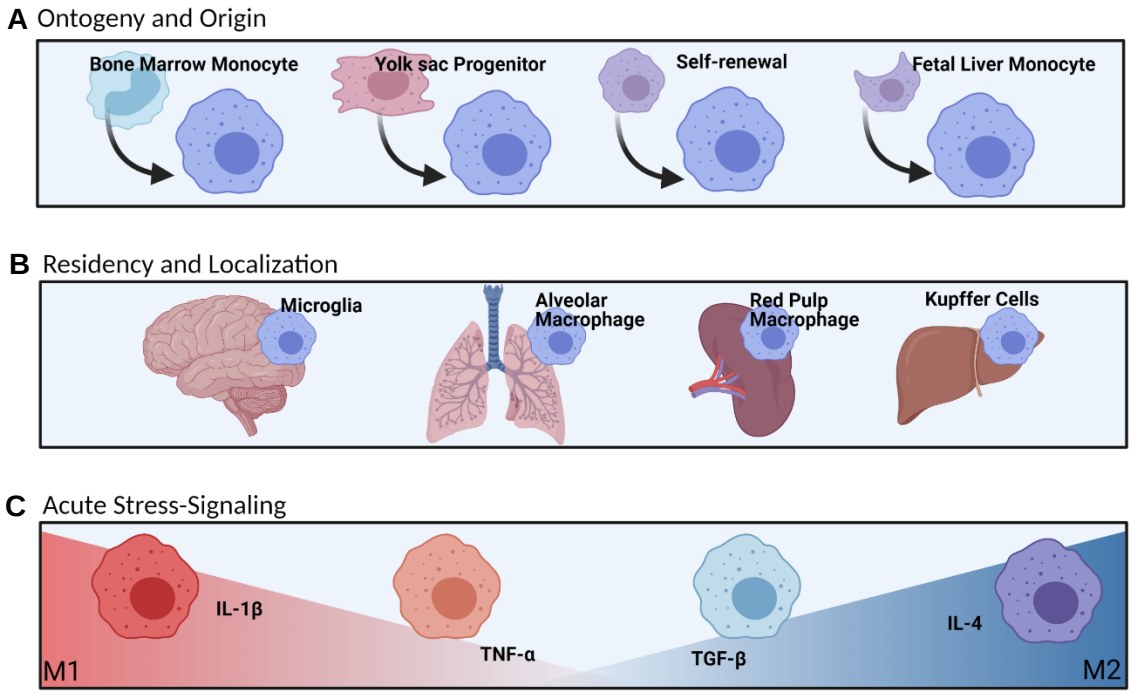

Figure 1. The three dimensions that contextualize macrophage plasticity. Macrophage identity is determined by the life history of the cell. Ontogeny is defined by paths of differentiation from precursors cells (A). During development, fetal monocytes or macrophage progenitors colonize developing tissues and become tissue-resident macrophages. During adulthood, these populations maintain either through adult monocyte differentiation or self-renewal of existing cells. Residency is defined by the organ or tissue in which the macrophage resides (B). Each organ has multiple resident macrophage populations which display distinct functions. Acute stress is defined as a rapid and reversible change due to pathological signals (C). Cytokines released by neighboring cells activate pro- or anti-inflammatory cascades and initiate specific functions in macrophages.

1.1. Pulmonary Resident Macrophages

In an immunological context, the lungs are an extremely dynamic and sensitive organ. Because the pulmonary epithelium is directly exposed to all the airborne contaminants and pathogens that are breathed in, the lungs must maintain a state of tolerance to low-level irritants which pose no threat but must also remain vigilant for any dangerous pathogens. To this end, the lungs harbor several distinct populations of resident macrophages which are responsible for maintaining tissue homeostasis and coordinating inflammatory responses during various disease states[23,24]. These populations are distinguished from one another and from other myeloid cells in the lung by their expression of different surface markers through flow cytometry **(Table 1)**.

Alveolar macrophages (AMϕ) are the first line of defense in the lung. These resident cells occupy the interior of the alveolar lumen, within the layer of surfactant supporting the alveolus and in direct contact with the alveolar epithelium[25]. AMϕ are easily identifiable in the lung due to their distinguishing surface markers and location. AMϕ can be distinguished from other non-macrophage cell populations by their expression of the Fc receptor CD64, which binds to G-type immunoglobin, and expression of MER receptor tyrosine kinase, MerTK[26,27]. The sialic-acid binding lectin SiglecF is the established canonical surface marker for AMϕ in the basal state, as all non-AMϕ in the lung are SiglecF negative. AMϕ also differ from other macrophage populations in the lung due to their high autofluorescence and expression of the integrin CD11c and CD206 in the basal state[28], while also being uniquely negative for the integrin CD11b, which is expressed by most other myeloid populations in the lung[29]. AMϕ have been well studied in the context of their role in the inflammatory responses to pathogens, and therefore the development of pulmonary inflammatory diseases[30–32]. Their importance to understanding disease is belied by the fact that,

due to their location, these cells are readily isolated via bronchial-alveolar lavage and are therefore the most well studied pulmonary resident macrophage population.

Aside from the AMϕ population, other resident macrophage populations in the lung are less well defined. In both mice and humans, a smaller subset of macrophages called interstitial macrophages (IMϕ) are understood to reside outside the alveolar lumen. Contrary to the readily accessible AMϕ, these cells are identified through differential tissue digestion or flow cytometric analysis of whole lung tissue[28,33], but defining their exact location in-situ presents some challenges. While IMϕ have been described in the human alveolar interstitial space between the alveolar wall and the capillary, an analogous IMϕ population in mice has been difficult to pinpoint. Just as AMϕ are defined by their physiological location, distinct non-AMϕ populations have been defined by their location in the interstitial spaces of the parenchyma and bronchiolar regions[25,34,35], but biomarker identification of these interstitial populations remains controversial[36]. Recent studies using histological labeling of MerTK+ cells in CX3CR1$^{GFP/+}$ mice described three IMϕ subpopulations which were distinguished from each other by turnover rate, phagocytic activity, and surface expression of Lyve-1, CD206, CD11c, CCR2, and Major Histocompatibility Complex class II[34]. The exact role of each of these subpopulations has yet to be unraveled. In addition to the non-AMϕ population, a population of classical monocytes constantly patrol the lung in the steady state[37]. While research into more detailed characterization is ongoing, as a whole, this population is easily separated from AMϕ by their surface markers[28].

The developmental origins of the AMϕ and IMϕ are also distinct. Primitive monocytes from the fetal liver colonize the developing lung at E13.5 where they differentiate into AMϕ over a period from E17.5 to after birth, at which point the alveolar niche is fully formed[38]. The first breath the newborn takes could be considered the first ‘wound’ which forces the embryonic

monocytes to react by differentiating. In both the developing and adult lung, the AMϕ phenotype is induced and maintained by levels of GM-CSF produced by alveolar type II epithelial cells and TGF-β produced in an autocrine manner[39]. This signaling drives the expression of the transcription factor PPARγ, which is required for AMϕ identity. Genes required for fatty acid metabolism are controlled by PPARγ, suggesting the catabolism of pulmonary surfactant potentiates AMϕ identity [40,41]. BTB domain and CNC homolog 2, BACH2, deficiency results in changes in lipid handling by AMϕ, interfering with their homeostatic function and inducing alveolar proteinosis. This defect is more severe in BACH1/BACH2 double knockouts but is absent in BACH1 knockout mice[42]. IMϕ are derived from yolk-sac macrophages which emerge without undergoing a monocyte stage and colonize the lung during organ development between E10.5 and E12.5[38].

Table 1. surface marker expression of resident myeloid cell populations in naïve mouse lung

	Neutrophils	Dendritic Cells	Alveolar Macrophages	Interstitial Macrophages	Mo-Macs
CD45	+	+	+	+	+
CD11b	+	+/-	-	+	+
CD11c	-	+/-	+	+/-	+
SiglecF	-	-	+	-	-
CD64	-	-	+	+	+
Ly6c	-	-	-	-	+/-
F4/80	-	-	+	+	+
Ly6g	+	-	-	-	-
MerTK	-	-	+	+	+/-
CD24	-	+	-	-	-
CD68	-	-	+	_	+
CD206	-	-	+	-	-
MHCII	-	+	+/-	+	-
CX3CR1	-	+/-	-	+/-	+/-
CD14	-	-	+/-	+	-/(+)

2. Acute Lung Injury

Acute lung injury is characterized by enhanced permeability of pulmonary endothelial and epithelial barriers, leading to protein-rich edema fluid building up inside the airspace, leading to impaired gas exchange and hypoxia **(Fig 2B)**[43–45]. Inflammatory cytokines released by innate immune cells residing in the lung drive the recruitment of other immune cells such, as neutrophils, monocytes, and lymphocytes, into the lung[46]. Acute lung injury is, in part, propagated by the death and cytokine release of alveolar epithelial cells[47,48]. These processes can lead to a cascade of inflammatory signaling which can drive further barrier breakdown and amplification of the inflammatory cytokine response. Untreated, this will lead to a clinical exacerbation of ALI referred to as Acute Respiratory Distress Syndrome (ARDS)[49]. Physicians diagnose ARDS using criteria proscribed by the 'Berlin definition.' Presently, this definition includes (1) an acute onset within one week, at most, of the initial insult; (2) bilateral infiltrates; and (3) reduced arterial oxygen content. The condition is further classified by a PO_2/FiO_2 between 200 and 300 for a mild condition, 100 and 200 for moderate condition, and below 100 for severe condition[50].

Because of their delicate architecture and critical role in gas exchange, the lungs are incredibly sensitive to inflammatory injury. Lung insult leading to ALI and ARDS can be direct, such as gastric aspiration, smoke inhalation, or viral pneumonia, or they can be indirect, such as cases of bacterial sepsis, pancreatitis, or severe third-degree burns. In the case of injuries distant from the lung, high systemic levels of inflammatory mediators or cytokines in the blood lead to activation of localized lung inflammation. This phenomenon contributes to the high incidence and difficulty in treating ALI and ARDS[45].

Lipopolysaccharide (LPS), a heterogeneous glycolipid present on the outer membrane of gram-negative bacteria, is often used as an inducer of acute lung injury in mouse models[51,52]. In

gram-negative bacterial infections, LPS is an important mediator of sepsis. Induction of ALI by administration of LPS has many benefits, it is highly reproducible, and it mirrors many of the pathological hallmarks of ALI such as neutropenic accumulation, increase in alveolar vascular permeability, and production of inflammatory cytokines[51].

2.1. Pulmonary Macrophage in the Basal Lung

Each population of lung resident macrophages plays a specialized role in the maintenance of tissue homeostasis and the development of disease. Under basal conditions, AMϕ are more efficiently phagocytic compared to IMϕ[33]. IMϕ have been shown to highly express the immunomodulatory cytokine IL-10 during basal conditions and enhanced IL-10 production through TLR4/MyD88 activation during house mite dust induced asthma model in order to dampen Th2 responses and neutrophilic accumulation[53].

AMϕ perform many essential functions for the maintenance of lung homeostasis; most importantly, the clearance of surfactant and the engulfment of inhaled contaminants **(Fig 2A)**. Intra-vital microscopy has revealed that AMϕ can migrate between alveoli using pores of Kohn. This is crucial, as typically there are more alveoli than AMϕ in the lung and inhaled contaminants must be identified and engulfed by AMϕ to cloak them from triggering an immunological alarm and driving recruitment of neutrophils[54]. Some research has suggested that there are at least two subsets of AMϕ: One subset is sessile and communicates directly with the alveolar epithelium through connexin43 channels. These channels propagate a steady calcium wave signal which modulates the lung microenvironment and maintains homeostasis. The other subset is non-sessile and thus is more easily removed via branchial alveolar lavage[55].

While inflammatory regulation is, to a large degree, mediated by myeloid cells communicating with other cells, the alveolar epithelium also signals to macrophages to maintain the tolerogenic environment through CD200. Airway macrophages express CD200R, which ligates to CD200 expressed by airway epithelial cells. Loss of CD200 results in enhanced macrophage activation and sensitivity to viruses, to the point at which minor survivable infections in wildtype mice lead to death in CD200 null mice[56]. Elimination of AMϕ entirely by intratracheally administered clodronate loaded liposomes results in an enhanced immune response[57].

2.2. Macrophages in the Enflamed Lung

Both resident macrophage populations maintain the tolerogenic environment of the lung to prevent non-pathogenic or commensal organisms from eliciting an inappropriate immune response. But the innate immune system must rapidly switch modes in situations where harmful pathogenic organisms gain a foothold in the lung. Due to their location, AMϕ are typically the first to sense pathogens through receptor-mediated recognition of PAMPs. The intracellular signaling which leads to the production of the first wave of cytokines and chemokines in response to infection has been well characterized[2,18,58].

Under inflammatory conditions, IMs produce inflammation-enhancing cytokines IL-6 to propagate inflammatory signaling beyond the local area[33]. Whereas, AMϕ perform two critical localized functions: First, AMϕ transition to an anti-microbial phenotype by producing more reactive oxygen species, nitric oxides, and antimicrobial proteins to directly attack bacteria or viruses within the alveolar lumen. The second role is to perpetuate inflammatory signaling through programmed cell death and the release of mature IL-1β.

These two roles are not mutually exclusive. AMϕ actively recognize and internalize bacteria and then initiate programmed cell death, both to release inflammatory mediators as well as to destroy the bacteria[59,60]. Unlike normal apoptosis, pyroptosis results in the leakage of cellular contents into the milieu. Cellular DNA, ATP, and other signals go on to activate other immune cells pyroptosis[61]. When AMϕ pyroptosis is inhibited the resulting inflammatory injury is attenuated[58]. Pyroptosis is induced by two sequential signals, LPS/TLR4 induced transcription of the precursor pro-IL-1β and formation of the NLRP3 inflammasome[62]. IL-1β is a key instigator of acute lung injury by way of strongly disrupting endothelial barrier integrity and activating macrophages[63]. Signals of cell stress or infection induce oligomerization of NLRP3, which serves as a platform for activated caspases. The newly assembled inflammasome then cleaves the precursor of IL-1β to its mature form which is released from the cell either by inflammasome-activated gasdermin pores or by pyroptotic loss of cell integrity[64,65].

2.3. Macrophages in the Resolving Lung

The timely resolution of ALI is essential to preventing the incidence of ARDS and other clinical complications. As the physiological state of the lung changes so drastically over the course of injury, the role of the innate immune sentinel cells, namely tissue-resident macrophages and recruited monocytes, must also change to coordinate the transition back to a homeostatic state. This process of recovery is not simply a restoration of lung homeostasis, but an active repair process aimed at reversing damage caused by the immune system. Emigration of neutrophils from the blood must be ceased, vascular barrier integrity must be restored, and edema fluid must be removed from the airspace[44]. This process is mediated largely by lung resident macrophages[66].

Under basal conditions, a Na^+ gradient is maintained across the epithelial barrier of the alveolus by Na, K-ATPases on the basolateral side of the epithelium. During injury, water leaks through the disrupted vascular endothelial barrier into the alveolar lumen. Once the endothelial barrier is restored, the epithelium removes excess edema fluid from the lumen through increased expression and activity of Na^+ channels (ENaC). This increases the transepithelial Na^+ gradient and passively drives water to move across the barrier by osmotic pressure and into the lung parenchyma[67,68]. Growth factors secreted by AMϕ can increase both the expression and activity of ENaC[69].

Studies point to AMϕ being required for injury resolution[70]. They play a critical role in clearing away cellular debris and apoptotic cells left over from the peak of lung inflammation **(Fig 2C)**. This often in cases of ALI takes the form of dead neutrophils[71]. Apoptotic cells are identified and removed by two processes, receptor-mediated phagocytosis of large particles or a receptor signal-recognition mediated process of smaller particles called efferocytosis. In both cases, foreign particles are engulfed by the cell and digested within acidic phagosomes[72]. When engulfment is impaired, the buildup of apoptotic cell fragments in the airspace causes exacerbations of existing inflammation and ultimately a failure to resolve inflammatory injury[73]. Phagocytosis of apoptotic cell fragments also serves as a survival signal in macrophages[74]. While PPARγ defines the AMϕ phenotype under basal conditions, enhancing PPARγ expression increases the pro-resolution phenotype of activated AMϕ[75,76]. Activation of PPARγ through stimulation of AMϕ by apoptotic fragments induces enhancement of efferocytosis and further pro-resolving cytokine expression[77].

Resolving factors secreted by AMϕ have a strong effect on the regeneration of alveolar epithelial cells[78]. In fact, secretion of vascular endothelial growth factor (VEGF)[79,80], hepatocyte growth factor (HGF)[81], epidermal growth factor (EGF)[82], by AMϕ has been specifically shown to

be induced by phagocytosis of dead cell fragments. While VEGF can encourage the regeneration of the endothelial barrier, HGF can enhance the survival and proliferation of alveolar type II cells[82]. To counter IL-1β, AMϕ produce the anti-inflammatory cytokine IL1ra, a soluble decoy receptor for IL-1β. Researchers used CCR2-/- mice to demonstrate that production of IL-1ra was primarily through monocyte-derived AMϕ[83]. This negation of IL-1β also acts to inhibit the decrease in ENaC expression in the lung parenchyma.

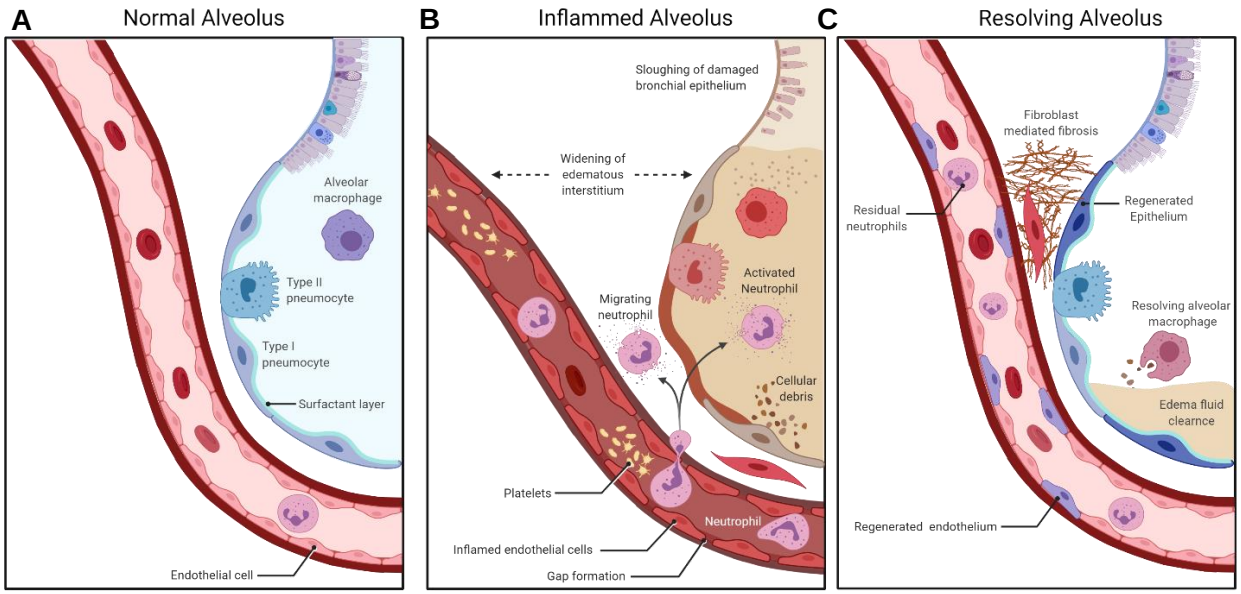

Figure 2. Schematic of alveolus during healthy conditions, during acute inflammation, and during the resolution phase of acute inflammation. In the naïve state (A), the alveolar architecture is defined by the single cell thick alveolar epithelium composed of type-1 and type-2 pneumocytes. The alveolus is separated from the pulmonary capillary by a thin interstitial protein matrix. Alveolar macrophages reside in the alveolar lumen. In the inflamed lung (B), cytokines produced by AMϕ increase the permeability of the capillary endothelium, leading to the leakage of protein-rich fluid into the alveolar lumen, bringing in monocytes, neutrophils, and lymphocytes. Disruptions of the endothelial and epithelial barrier compromise the alveolar architecture. During the resolution phase of injury (C), macrophages phagocytose cellular and bacterial debris, edema fluid is removed from the airspace, and the vascular and epithelial barrier regenerate. Architectural disruption is repaired by fibrosis instigated by fibroblasts.

2.4. Lung Resident Macrophage Dynamics

The sequential ontogeny of lung resident macrophages represents a hotly debated topic. It is well established that IMs derive from recruited monocytes[84,85] and that, the adult healthy lung, AMϕ exhibit a low turnover rate, renewing their population through proliferation with minimal contribution from bone marrow monocytes[86]. These monocyte-derived AMϕ persist across the entire lifespan[87]. But questions remain as to whether IMϕ can migrate to the alveolar space and take on an AMϕ phenotype after AMϕ death during severe injury. Or if it is only monocytes that differentiate directly into canonical AMϕ[88]. Studies support the idea that both occur, but it is unknown how different physiological or pathological conditions affect which lineage predominates and how AMϕ of different lineages compare in terms of functionality.

Lineage tracing experiments have identified IMϕ as a putative intermediate stage between monocytes recruited into the lung and differentiate into macrophages before entering the alveolar space to become true AMϕ[89]. During inflammatory lung injury, the line between the AMϕ and IMϕ populations blurs substantially. In addition to the two primary resident macrophage populations seen in basal conditions, acute inflammation drives the recruitment of monocytes, which can differentiate into new resident macrophages or continue to act as monocytes[90]. When these cells have been isolated via flow cytometry they were shown to arrive into the airspace highly expressing genes involved in neutrophil chemoattraction, lysosomal proteases, and LPS signaling[91]. After injury, some pulmonary resident macrophage populations are reconstituted by bone marrow-derived $CCR2^{+}$ monocytes which arrive by following CCL2 gradients to the lung as well as IL-13 produced by lung lymphoid cells[92]. Depletion of AMϕ which are derived from monocytes has been shown to dampen the fibrotic response to bleomycin-induced lung injury[87]. Several lines of evidence suggest that as embryonically derived AMϕ are replaced by monocytes

derived AMϕ over the lifespan due to minor lung injury the capacity of the lung to maintain itself diminishes[23]. But, overall, studies looking at the changing ontogeny of lung resident macrophages and their role in disease progression have been hampered by the complex nature of macrophage replacement which occurs during different disease models.

As ARDS and ALI are characterized by out-of-control inflammation, the essential role of AMϕ is to reestablish tissue homeostasis. AMϕ are generally thought to be immunosuppressive, but after inflammatory stimuli AMϕ may contribute to inflammatory propagation. At this point, many studies have examined the immunophenotype of AMϕ to distinguish their inflamed and resolving behavior from their basal condition. These studies have pointed to the fact that AMϕ, normally CD11b negative, begin to express CD11b on their surface in the inflamed lung. What remains to be clarified, however, is if $CD11b^{+}$ AMϕ are derived from cells recruited into the lung airspace or are resident $CD11b^{-}$ AMϕ which have switched on CD11b expression. It is suggested that high CD11b expression represents a marker of AMϕ activation, correlating with higher pro-inflammatory cytokine generation, though researchers cannot definitively categorize these cells as being a purely pro-inflammatory cell[93]. $CD11b^{hi}$ AMϕ examined in an inhaled silica model also shows high phagocytotic functions and a role in the creation of granulomas. The expansion of $CD11b^{lo}$ AMϕ was induced by IL-1a, after which these AMϕ transitioned into $CD11b^{hi}$ and enhanced granuloma development[94]. Interestingly, examination of CD11b expression in human alveolar macrophage samples suggests a continuum of CD11b expression, with low $CD11b^{hi}$ AMϕ correlating with lower disease burden and inflammation[95].

One useful tool for studying the dynamics of lung myeloid cells during different injury models is the macrophage/monocyte-specific inducible Diphtheria-toxin receptor (DTR) mouse strain. Mice are not affected by diphtheria toxin (DT), but a mouse strain carrying the human

diphtheria toxin receptor gene under the control of the macrophage/monocyte specific CD11b promotor has been generated. By injecting DT into these mice, the $CD11b^+$ macrophages and monocytes can be selectively depleted by inducing apoptosis, without affecting other CD11b expressing cells such as neutrophils and dendritic cells[96]. One study demonstrated using the CD11b-DTR mouse strain that $CD11b^+$ IMϕ are crucial to neovascularization after ischemic injury. Under normal conditions, the $CD11b^+$ macrophage population in the lung expands in number after induction of left lung ischemia as new blood vessels are formed. Following the depletion of $CD11b^+$ IMϕ this neovascularization did not occur. When isolated, these cells were able to induce proliferation in cultured endothelial cells in vitro[97]. Due to the structure of the lung, the localization of these intestinal macrophages within the parenchyma may allow secreted vascular regeneration factors to reach the hypoxic tissues, as AMϕ are too isolated within the airspace. This indicates localization of resident macrophage populations correlates with functional specialization.

The inflammatory state of resident AMϕ can also be influenced by monocytes recruited into the lung during injury. Recent studies have illustrated that recruited monocytes require sphingosine kinase 2 (SPHK2) to facilitate the resolution of ALI. CD11b-DTR mice which have been depleted of native $CD11b^+$ macrophages and monocytes are unable to resolve lung injury. This function was restored when $CD11b^+$ bone marrow monocytes were adoptively transferred back into depleted mice via intravascular injection. But if monocytes that lack the SPHK2 gene are transferred the mice are unable to resolve lung injury. It was determined that sphingosine-1-phosphate (S1P), the product of SPHK2, allosterically inhibited the STING complex and prevented it from initiating downstream signaling[98]. STING binds to cGAMP, a messenger produced by cGAS upon sensing free double-stranded DNA and initiates activation of type-2 interferon signaling[99,100]. This IFN-β signaling programmed existing AMϕ to perpetuate inflammation. As

the inhibition of STING was reliant on exogenous cells which differentiated, in part, into macrophages in situ, this indicates that AMϕ responses are programmed by monocyte-derived macrophages. Interestingly, while AMϕ do express CD11b after LPS exposure, they were not affected by DT in these studies.

3. cAMP Signaling Pathway

G-protein coupled receptors (GPCRs) comprise the largest group of signaling receptors in nature. These complexes transmit intracellular signals through ligand-activated releases of heterotrimeric G-proteins. As shown in the top half of **figure 3**, two G-protein subunits, $G\alpha_S$ and $G\alpha_i$, activate and inhibit the enzyme adenylate cyclase (AC), respectively[101]. AC cyclizes ATP to produce the secondary messenger cyclic adenosine monophosphate (cAMP). While most AC isoforms are regulated by GPCR signaling, soluble AC (sAC) instead responds to changes in pH by directly binding to bicarbonate ions[102].

The universal secondary messenger cAMP propagates a cellular signal by activating numerous other pathways which lead to cellular responses, shown in the bottom half of **figure 3**. One well-recognized path is the activation of protein kinase A (PKA). Normally bound to inhibitory subunits, PKA is activated by cAMP directly binding to the inhibitory subunits, causing their release. The now active kinase can phosphorylate its targets and propagate signaling[103]. Besides PKA, cAMP also acts through a pair of cAMP sensors called Epac1 and Epac2. These proteins act as nucleotide exchange factors for the Rap subfamily of RAS-like small GTPases[104]. Historically, the cAMP pathway has been interrogated by researchers using the AC agonist forskolin[105]. Derivatives of forskolin have been used in the development of other cAMP generating drugs aimed at treating a wide range of human disease[106,107].

Despite the coupling of cell surface receptors to cAMP signal propagation, cAMP is utilized by multiple parallel pathways which diverge spatially. Internalization of GPCRs and attendant G-proteins by β-arrestin and other endocytic machinery can lead to the negative regulation of this signaling[108]. While the canonical schematic of GPCR-AC-cAMP signaling occurs at the plasma membrane, many studies have identified the role of relocalization of various components to subcellular domains to regulate effectors with greater spatial specificity. Different AC isoforms exhibit distinct trafficking capabilities. For instance, AC9 traffics to the endosomes after activation by G_s while AC1 remains at the plasma membrane[109]. Controlled localization of PKA holoenzyme through A-kinase-anchoring proteins (AKAPs) allows for signaling microdomains within these specific cellular areas[110]. This intracellular trafficking of pathway components allows cAMP to act over short distances and for discrete cellular microdomains to discriminate signaling from the cell surface, and thus produce different responses, using the same messenger molecule[111].

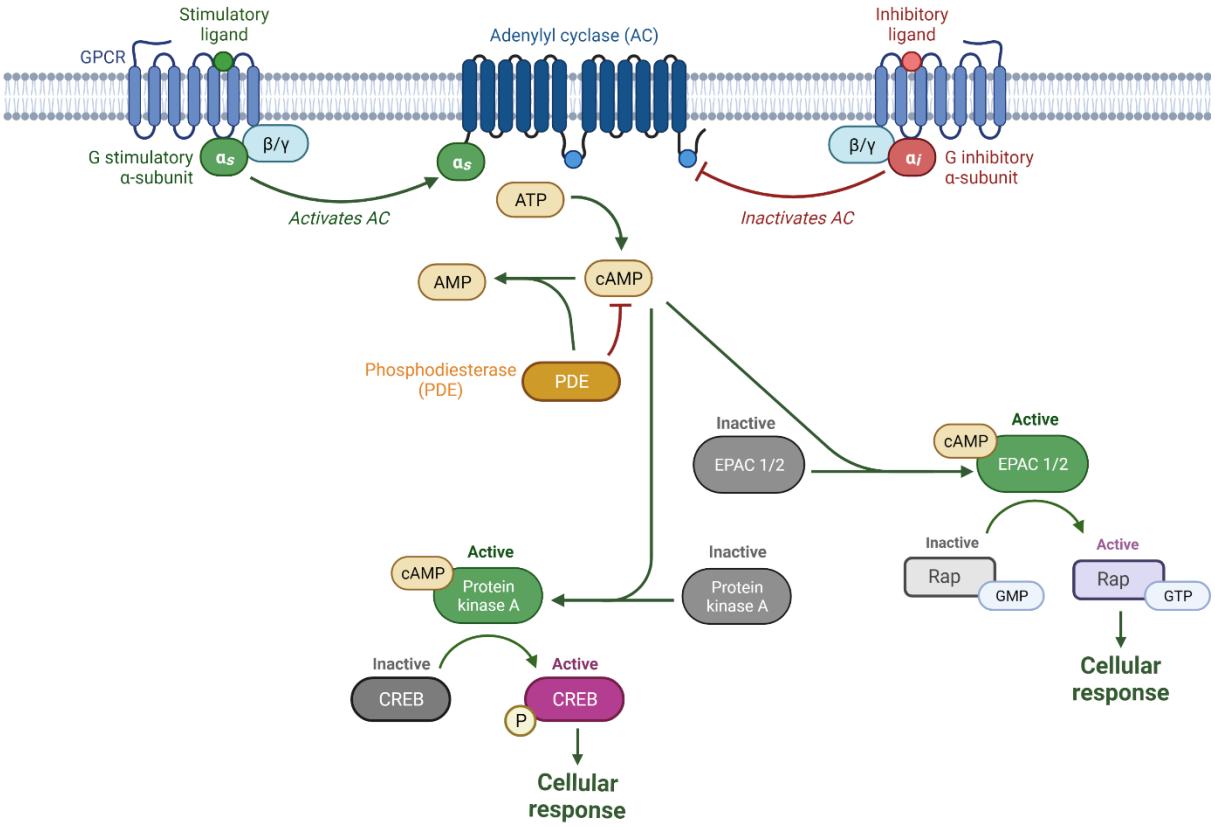

Figure 3. Schematic of the cAMP signaling pathway. Adenylate cyclase mediated by conversion of ATP to cAMP is inhibited by $G\alpha_i$ signaling and activated by $G\alpha_s$. cAMP goes on to activate downstream signaling by binding to EPAC1/2 and binding to inhibitory subunits of PKA complex, which release from the now active PKA. cAMP signaling is inhibited by phosphodiesterase enzymes, which convert cAMP into AMP.

3.1. Regulation of cAMP by phosphodiesterase

Because cAMP is used as a messenger in many different pathways, the level of cAMP in the cell must be tightly controlled to prevent signal overflow. This negative regulation is done by a large family of intracellular phosphodiesterase (PDE) enzymes. PDEs are responsible for modulating cAMP signaling through the enzymatic decyclization of cAMP into AMP[112].

The ubiquity of cAMP necessitates that the regulatory system of PDEs be incredibly complex. The superfamily of PDEs is made up of 11 families, each with its own protein structure and cyclic nucleotide specificity. Several PDE families have multiple subtypes, each with their own encoding gene, totalling 21 PDE genes in mammals. Moreover, due to alternative splicing, there are over 100 distinct PDE gene products[112]. All PDEs share a common catalytic domain, but alternative splicing products can result in widely varying regulation. Most PDE splice forms have an N-terminal regulatory domain, such as GAFs (cGMP binding PDE domains) calmodulin binding domains, upstream conserved regulatory (UCR) domains[113].

Each family of PDE enzymes exhibits different specificities for cAMP and cGMP, with some being specific for cAMP (PDE4, PDE7, PDE8) some specific for cGMP (PDE5, PDE6, and PDE9), and others able to target both cAMP and cGMP (PDE1, PDE2, PDE3, PDE10, and PDE11)[114]. Many duel specific PDEs have a preferential bias towards one over the other or are regulated by one of their substrates For instance, cGMP can bind to PDE2, a dual specific PDE, at an allosteric regulatory site, leading to a 10-fold increase in its affinity for cAMP while not affecting the affinity for cGMP[115].

PDE4 has a unique system of gated regulatory functions not present in any other PDE family. Isoenzymes of PDE4 possess two UCR domains, UCR1 and UCR2. Basally activity of PDE4 is negatively regulated by these domains, as removal of either domain results in an increase

in PDE4 catalytic activity[116]. Unlike other PDEs, PDE4 also possesses an autoinhibitory domain at its C-terminal end[117]. When cAMP levels are low, PDE4 exists as a dimer with the autoinhibitory domain covering the active site of the enzyme[117,118]. This C-terminal autoinhibitory domain is also able to bind to β-arrestin or other scaffold proteins. This association frees the active site of PDE4 from the autoinhibitory domain, thus activating the enzyme[119,120]. As a homodimer, the UCR domains also serve to regulate PDE4 activity. An alpha-helix in the UCR2 of one PDE4 monomer can cover the active site of the other monomer, rendering half of the homodimer inactive. Partial capping of the second active site may account for reduced activity in the other monomer[121]. Phosphorylation at serine 54 of the UCR2 domain by PKA can prevent the occlusion of the active site by UCR2, leaving both halves of the dimer catalytically active. While phosphorylation of the autoinhibitory domain by ERK results in inhibition of PDE4 activity[122,123].

That cAMP-activated PKA can increase PDE4 activity and prolonged activation of cAMP signaling can upregulate expression of PDE4[124] illustrates the tight feedback loop required for normal signaling cAMP. Additionally, regulation of PDE4 localization and enzymatic activity by partner and anchor proteins, such as XAP2, myomegalin, and DISC1[114], also play a critical role in its temporal and spatial regulation of cAMP signaling within the cell. Subcellular localization of various PDEs aid in the compartmentalization of cAMP, which is a component of multiple distinct signaling cascades[125]. Scaffolding proteins can bring together PDE4 to localized cell surface microdomains to regulate GPCR signaling. The reversal of autoinhibition by β-arrestin allows PDE4 to be brought into proximity to the β2-adrenoceptor after activation by β2-agonist. This allows PDE4 to degrade cAMP at the β2-AR/AC site of production, preventing activation of PKA and thereby the phosphorylation and desensitization of β2-AR[126].

3.2. Role of cAMP in Macrophage Phenotype

Despite the ubiquity of cAMP signaling pathways, many are known to converge on cell responses linked with inflammatory regulation. During inflammatory injury, activation of the TLR4 pathway and several cytokine-stimulated GPCRs occurs simultaneously on macrophages. These signaling pathways converge at several points, but multidimensional analysis of transcriptional patterns elicited co-stimulation of a cAMP analog and TLR4 specific agonist shows non-additive effects where one pathway suppresses genes activated by the other[127]. In this case stimulation of TLR4 prevented cAMP-mediated downregulation of many inflammatory genes, while also not affecting genes positively regulated by both agonists.

Death of myeloid cells is a normal part of both the initiation and resolution of inflammatory injury[128]. Beyond the mediating effects of cytokines, cAMP signaling is also heavily implicated in the regulation of cell death and autophagy and through these pathways, injury resolution. Enhanced cAMP signaling has been shown to inhibit programmed cell death through multiple mechanisms, namely by inhibiting the formation and of apoptotic inflammasomes through direct binding to NLRP3[129], enhancing pro-survival signals through increasing Ca^{+} signaling[130]. Studies have into this pathway support the idea that pyroptotic cell death plays a functional role in antimicrobial defense, as inhibition of cell death decreased bacteria killing[60] and truncates the inflammatory response[59,131].

In microglia, microphage-like cells that reside in the brain, increasing cAMP levels by blocking PDE activity leads to anti-inflammatory activity though increasing autophagic activity. The formation of inflammasomes is prevented by this autophagy, leading to inhibited caspase signaling and preventing the proteolytic activation of pro-IL-1β. Without inflammasome-mediated cell death, the activated IL-1β is not readily released into the microenvironment[132]. Some

studies have examined the converging roles of PKA and Epac1/2 in the downstream mediation of cAMP signaling. In the case of the anti-inflammatory cytokine IL-1a, both pathways activate its expression, but only PKA is linked to the enhanced IL-1a expression observed after PDE4 inhibition[133]. Use of Epac specific cAMP analog has shown that while cAMP mediates the activation of monocyte and macrophage effector functions such as synthesis and release of cytokines, phagocytosis, chemotaxis, the Epac-Rap1 pathway does not participate in the regulation of these pathways[134].

The significance of cAMP signaling in immune cells is highlighted by the use of PDE inhibitors to alter inflammatory signaling. PDE4 has a role in regulating the expression of cytokines in macrophages. Induction of PDE4b is essential for TNF-α generation in macrophages and monocytes exposed to LPS[135,136] *in vitro*. While, conversely, the inhibition of PDE4 enhances macrophage induction of anti-inflammatory factors such as arginase[137]. The exact mechanism by which PDE inhibition systemically reduces inflammation has been difficult to isolate in part due to the huge number of independent pathways regulated by cAMP across different cell types, inflammatory activation states, and intracellular locations. Despite performing the same enzymatic action, specific inhibition of different PDE family members can result in very different responses within the same tissue or even within the same cell type[138,139].

4. Cyclic-AMP Response Element Binding protein (CREB)

The zinc-finger transcription factor CREB is responsible for regulating a wide array of cellular and physiological functions, ranging from memory[140] to tissue development[141], as well as, critically, immune function[142]. CREB recognizes the Cyclic AMP Response Element (CRE) site palindromic motif TGACGTCA. These motifs exist at over 41,000 sites in the mouse genome,

~40% of which are located within 2kb of the transcription start site of a gene[143]. Most of these sites are occupied under basal conditions, as CREB will bind to DNA in its inactive dephosphorylated state but will not initiate transcription[144]. This requires phosphorylation of serine 133 by one of several possible kinases, including AMPK[145] and PKA[144], after which phosphorylated CREB will associate with CREB binding protein (CBP)[146] and further recruited different transcriptional effectors which regulate the specificity of CREB activated genes.

CREB plays a role in the development and proliferation of myeloid cells. Overexpression of CREB is seen in human cases of acute myeloid leukemia and is associated with worse clinical outcomes. CREB overexpression induced can lead to the development of myeloproliferative/myelodysplastic syndrome in myeloid lineage cells over time[147]. But this lag indicates that overexpression of CREB is not sufficient to induce leukemia. Later studies using retroviral insertional mutagenesis revealed Sox4 as a transcription factor that can cooperate with CREB to induce abnormal cell survival and proliferation[148].

CREB has been categorized as anti-inflammatory signals in macrophages[142]. CREB is responsible for the expression of IL-10, a cytokine essential to the repression of inflammatory activation in the lung due to allergen or pollutant exposure[149,150]. CREB in macrophages induces the expression of KLF4 following cAMP stimulation, which in turn induces the production of the anti-inflammatory paracrine hormone PGE2[151]. Early signaling studies suggest macrophages undergo a transition from M1 to a pro-resolution phenotype which shares some markers of classical activation, namely iNOS, but express lower levels of pro-inflammatory cytokines while secreting higher levels of IL-10, and that this transition is dependent on cAMP[152].

Activated CREB has also been known to compete for transcriptional co-activators. In alveolar macrophages, induction of CD200 diminished M1 markers in vitro while increasing M2

markers. This effect was reliant on C/EBP-β. As a part of the inflammatory cascade, NFκB partners with C/EBP-β to activate the transcription of pro-inflammatory genes. But activated CREB can compete for access to this transcriptional co-activator and thereby diminish cytokine production while inducing its own anti-inflammatory genes[153] Activation of CREB during TLR activation may also act to modulate pro-inflammatory signaling given the ability of CREB to compete with NFκB for their shared transcriptional effector CREB-binding protein, or CBP[154].

5. cAMP and PDEs in Lung Disease

As cAMP signaling has been shown to regulate several processes with a positive effect on health, PDEs have been popular pharmacological targets to treat numerous conditions. Asthma and COPD are both characterized by chronic inflammation, which can lead to remodeling of the small bronchial airways, causing obstruction and impaired breathing[155,156]. Inflammation in COPD is mediated by high recruitment of macrophages, neutrophils, and $CD8^+$ lymphocytes, while asthma is mediated by the recruitment of eosinophils, mast cells, and $CD4^+$ lymphocytes[156]. Standard treatments for COPD include β2-adrenoceptor agonists, anticholinergics, and theophylline, a nonspecific PDE inhibitor. In cases of severe COPD, these treatments are combined with a PDE4 specific inhibitor such as roflumilast as an add-on treatment[157].

Many PDEs have dual specificity for both cAMP and cGMP, coupled with variation in expression patterns within different tissue have created a variegated field of pharmacological treatments involving PDE inhibiors[158]. Inhibitors of PDE5 and PDE3 have been widely explored in situations of pulmonary hypertension and excessive bronchoconstriction. These drugs work by preventing the degradation of cGMP, thereby allowing smooth muscle cells (SMCs) to be responsive to nitric oxide[159,160]. Activation of PKG, a cGMP sensitive kinase, limits cellular

contraction through inhibition of calcium influx and deactivation of myosin light-chain kinase[160,161]. Through this relaxation mechanism, the blockbuster drug sildenafil, a PDE5 inhibitor, became the first drug to treat erectile dysfunction[162,163]. Blockage of smooth muscle contraction also inhibits excessive proliferation of SMCs, which can lead to hyperplasia and tissue disruption[159].

Dual treatment combining anti-inflammatory effects of PDE4 inhibition and the bronchodilation effects of PDE3 inhibition has been studied in clinical trials in inflammatory lung disease. Early results show that dual PDE3/PDE4 inhibitor treatment has greater efficacy than either drug along[164,165]. Combined PDE3/PDE4 inhibition has also been studied in the case of glucocorticoid resident COPD and was shown to both decrease activation of AMϕ and increase responsiveness to glucocorticoid by preventing inhibition of HDAC by oxidative stress[166]. Proliferation and pro-fibrotic mediator secretion by fibroblasts were strongly inhibited by simultaneous inhibition of β2 receptors and PDE4, while inhibition of PDE4 did not effectively prevent activation of fibroblasts. Another study showed that PDE4 and PDE3 inhibition was required to prevent inflammatory cytokine production in human lung microvascular cells. While the combination of PDE4 inhibitor with a β2 receptor inhibitor, though not either inhibitor alone, prevented adhesion of neutrophils to activated endothelial cells[167].

Inhibitors of PDE4 have been used to treat numerous lung diseases related to immune signaling, including COPD[168,169], pulmonary fibrosis[170], and emphysema[171]. Rolipram, and other PDE4 inhibitors, have been well studied in their effect on several models of acute lung injury.[172–174]But despite the ubiquity of PDE4 inhibitors in treating lung disease and studies demonstrating that blockade of PDEs limits lung inflammation[175] there is a significant gap in our understanding of the mechanism underlying their effects.

The use of PDE inhibitors to treat a wide arrange of lung diseases supports the understanding of cAMP signaling as immunomodulatory. COPD patients are at risk of further loss of lung function through the continual immune medicated remodeling of the lung architecture, an adherent 'wound healing' process, as well as exacerbations of acute infections, an overactive inflammatory response. PDE4 inhibitor treatment can improve both of these conditions by preserving the remaining lung architecture and dampening excessive inflammatory reactions to pathogens[168]. While very promising for their anti-inflammatory activity, oral PDE4 inhibitors have a limited therapeutic window and often lead to gastrointestinal side effects due to PDE4 being active in many tissues and organs[164]. Long-term treatment with roflumilast fully prevented the development of chronic cigarette smoke-induced emphasyma[176].

Inflammatory activation of AMϕ is at least in part dictated by cAMP signaling. Protease-activated receptor 2 (PAR2), as a GPCR stimulated by proteolytic cleavage of a peptide ligand from its extracellular terminal domain. The PAR2 activating peptide can be freed to activate PAR2 by many proteases, such as elastase and tryptase, but it can also be activated by thrombin, a protease produced during inflammatory lung injury, or transactivated by activated PAR1[177]. Activation of PAR2 by thrombin in AMϕ was shown to lead to an increase in cAMP, this cAMP then suppressed activation of the TRPV4 calcium channel. This led to a dampening on the increase in intracellular calcium and thus diminished activation of the calcium-sensitive transcription factor NFAT. In the case of PAR2 knockout AMϕ, the lack of cAMP-mediated inhibition of NFAT activation allowed NFAT to synergize with activated NFκB to enhance the expression of several pro-inflammatory cytokines[178]. While the inflammatory injury was not suppressed by PAR2, this study shows its role in 'tuning' the inflammatory response to match the degree and context of the injury.

There is evidence that PDE inhibition through intravascular administration of inhibitors both reduces recruitment of neutrophils to the lung and delays apoptosis of neutrophils within the lung after inflammatory stimuli[169,179]. In vitro studies of T-lymphocytes treated with PDE4 inhibitors show a decrease in NFκB and NFAT activation, while activation of CREB and AP-1 were increased[180,181]. But these effects do not fully explain the role of PDEs in myeloid cells over the course of lung injury.

6. Macrophage Metabolism

When macrophages polarize to an M1 or M2 state their metabolisms also undergo a transition to support cellular functions. During the activation of macrophages by LPS or IFN-γ, drive a shift to glycolysis and a redirecting of the TCA cycle. A key signaling factor controlling this shift is mTOR, which regulates autophagy, protein synthesis, and cell survival[182]. LPS will also drive the relocalization of glucose transporter GLUT1 to the surface of the cell to increase glucose intake[183]. During inflammation, macrophages generate large quantities of reactive oxygen species through iNOS or decoupling of ATP production to the TCA cycle in order to kill pathogens[184]. This process has the secondary effect of damaging the mitochondria of the macrophage. If severe enough, M1 polarization induces sufficient oxidative stress to damage the mitochondria and prevent the metabolic transition to an M2 state, prolonging inflammatory signaling[185]. The immunomodulatory cytokine IL-10 can induce autophagy in LPS stimulated macrophages, removing damaged mitochondria and dampening inflammatory signaling[186].

A two-stage metabolic switch occurs, beginning with the inhibition of isocitrate dehydrogenase, leading to the buildup of prior TCA cycle intermediates, namely citrate, which is funneled into the production of itaconate. Succinate dehydrogenase is inhibited by itaconate, this

truncation of the TCA cycle allows more free oxygen to stabilize hypoxia-inducible factor 1α (HIF-1α) and subsequent expression of PDK3[187]. By inhibiting PDHC by PDK3 flux of pyruvate by way of acetyl-CoA through the TCA cycle is reduced[188].

In the context of anti-inflammatory signaling mediated by IL-4/STAT6 enhanced FAO and oxidative phosphorylation and increased utilization of glucose through cooperative activation of IRF4 with M-CSF[189]. This coincides with the shift in macrophage polarization seen in macrophage-specific IRF4 knockout mice given a high fat diet. Adipose tissue macrophages (ATMs) generated increased inflammatory gene expression and had higher insulin resistance compared to controls, despite no difference in adiposity[190]. Energy balance seems to have a great impact on macrophage polarization state, even under basal conditions, as ATMs have been shown to exhibit greater basal expression of M1 markers in the case of diet-induced obesity[191]. Exposure to IL-25 can shift ATMs to an M2 state through activation of lipolysis and enhanced mitochondrial respiratory capacity[192]

6.1. Role of PDK4 and PDC Axis

Pyruvate dehydrogenase kinase 4 (PDHK4) is a critical regulator of the multimeric pyruvate dehydrogenase complex (PDHC). The irreversible metabolic step of converting pyruvate into Acetyl-CoA is performed by PDHC. This activity is decreased after PDHC is phosphorylated on its E3 subunit by one of four pyruvate dehydrogenase kinase enzymes[193]. As illustrated in **Figure 4**, PDHC functions as a metabolic bottleneck for the flux of molecules from glycolysis into the TCA cycle[194]. High fatty acid oxidation (FAO) can activate PDKs and drive the inhibition of glucose oxidation. While high levels of pyruvate will inhibit PDKs, allowing PDH to drive production of acetyl-CoA and glucose oxidation[195]. [196]. Recent studies have suggested that the

pyruvate dehydrogenase complex can translocate into the nucleus itself, whereby local acetyl-CoA production can be utilized by histone-modifying enzymes to enact epigenetic changes[197,198]. Deactivation of PDKs using small molecular inhibitors such as dichloroacetate has already been shown to dramatically alter epigenetic profiles[199].

Macrophage metabolism has been shown to dramatically shift depending on the stress signals in the local environment. The degree of inflammatory polarization is greatly influenced by the metabolic state. In the case of macrophage polarization PDHC is important for the metabolic reprogramming which occurs during the transition between inflammatory states. Previous understanding that M1 macrophages rely on glycolysis while M2 macrophages rely on oxidative phosphorylation though the TCA cycle has recently been recontextualized. PDH is active in LPS stimulated macrophages, but glucose-derived pyruvate is oxidized via PDH to produce citrate, but this metabolite is shunted through different pathways to drive other functions[196]. By inhibiting PDHC by PDK3 flux of pyruvate by way of acetyl-CoA through the TCA cycle is reduced[188].

Studies in Kupffer cells using an endotoxemia model show that this PDK dependent shift towards glycolysis has a negative effect on the expression of IL-10. PDK inhibition increased AMPKα1 activity and CREB phosphyorylation[200]. Conversely, the PDK-PDH-lactic acid axis was implicated in inflammatory pain. Inhibition of PDK2/4 limited localized lactic acid production and pro-inflammatory activation of macrophages[201]. Essential macrophage functions during inflammatory activation such as migration rely on this transition, as formation and cycling of filopodia and lamellipodia require rapid glycolytic ATP synthesis. Synthesis of PDK1 by HIF-1α drives this shift as macrophages enter into low oxygen zones within inflamed tissues[202].

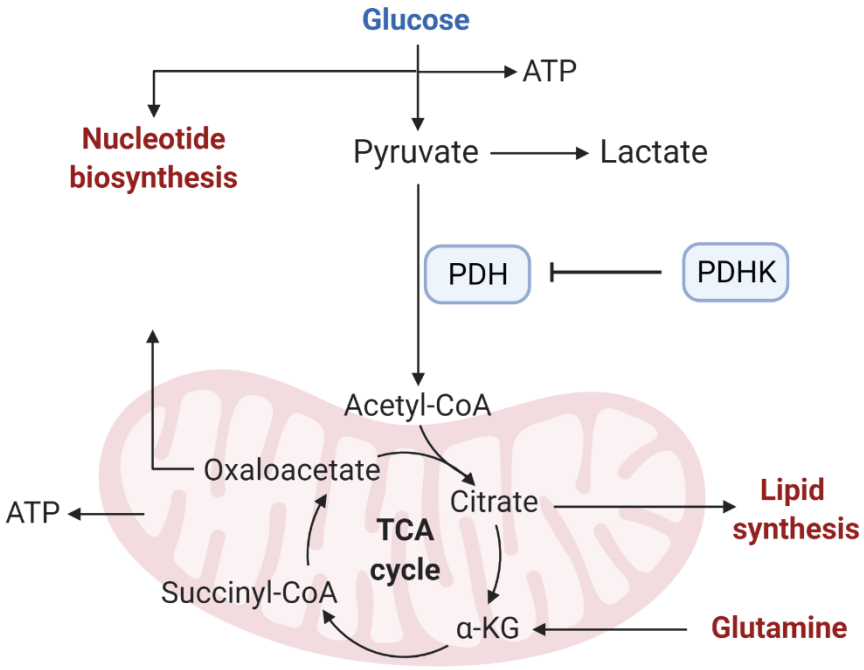

Figure 4. Role of pyruvate dehydrogenase in the alternation between glycolysis and the TCA cycle. The end-product of glycolysis, pyruvate, is converted into Acetyl-CoA by the enzyme complex Pyruvate dehydrogenase, whereby it enters the TCA cycle within the mitochondria. Pyruvate dehydrogenase is inhibited by pyruvate dehydrogenase kinase. Pyruvate dehydrogenase kinase serves as a junction between metabolic systems.

Methods and Procedures

A. Experimental Animals

All animal work was approved by the Institutional Animal Care and Use Committee of the University of Illinois. CD11b-DTR, LysM-Cre, CREB Flox, and wildtype mouse strains were obtained from Jackson Laboratory (Farmington). LysM-GFP mice were provided by Dr. Klaus Ley (La Jolla Institute for Immunology, UCSD). Breeding colonies of all strains were maintained in a pathogen-free housing facility at the University of Illinois at Chicago. All mouse strains were of a C57Blk/6J background. Both male and female (6-8 weeks old) mouse were used in a pairwise manner throughout the study.

B. Non-invasive intratracheal instillation

Monocytes or macrophages suspended in the 50 µl of volume were endotracheally instilled in the airway. Briefly, mice were anesthetized by injecting ketamine and xylazine (100 mg/kg and 12 mg/kg) and hung in the supine position by securing the lower jaw teeth with thread. The tongue was grasped with the help of forceps and pulled outside towards the forward direction after which 50 µl cell suspension or rolipram was injected into the oropharynx. Nostrils were closed for 5-10 seconds and observed for the inhalation of cells/drug suspension by the mice. Mouse nostrils were then opened, and the animal returned to its cages.

C. Drug Administration

Rolipram (Millipore Sigma) or PBS vehicle was administered via non-invasive intratracheal instillation method as described above. Rolipram was dissolved in DMSO and diluted in PBS to working concentration. Diphtheria toxin isolated from Corynebacterium diphtheriae (Millipore Sigma,) was dissolved in sterile PBS and administered via *i.p.* injection (25ng/kg).

BrdU, 5-Bromo-2′-deoxyuridine, (Sigma Aldrich) was dissolved in PBS (15mg/ml) and 100µL and administered via *i.p* injection.

D. Induction and assessment of lung vascular permeability

To induce acute lung injury, mice were exposed to a nebulized 1mg/ml solution of lyophilized *E. coli* LPS (Sigma Aldrich) dissolved in sterile saline for 50 minutes in an enclosed space. Lung edema and vascular permeability were quantified by measuring Evans Blue accumulation and extravasation (EBAE) and lung wet-to-dry weight ratio. For EBAE, 100µL Evan's blue-labeled albumin was injected retro-orbitally 45 minutes before measurement. Right lung lobes were extracted and used for EBAE measurement while the left lung lobe was excised and completely dried in an oven at 55°C overnight for calculation of lung wet-dry-weight ratio as previously described[98,178].

E. Bronchoalveolar lavage

Bronchioalveolar lavage (BAL) was performed on euthanized mice using an 18-gauge needle, as previously described[98,178]. Briefly, a tracheotomy was performed, and 1 ml of cold PBS was slowly injected into the lungs, aspirated back into the syringe, and collected. This procedure was repeated for a total of 4 ml of fluid. BAL fluid was then centrifuged at 1250rpm for 10 min and the supernatant discarded. Cell pellets were used in further experiments.

F. Isolation and culture of bone marrow-derived macrophage

Mouse bone marrow-derived macrophages (BMDMs) were generated from wildtype mice as described[98]. Mouse femur and tibia were extracted and flushed with RPMI media containing 1% antibiotic/antimycotic, 10% Fetal Bovine Serum (FBS), and 25 ng/ml M-CSF (R&D Systems) and cultured at 37 °C in 5% CO_2 incubator for 5 days. On the third day, the media was replaced

with fresh M-CSF free RPMI containing 10% FBS and antibiotic/antimycotic; cells were incubated for additional 2 days. For each experiment, BMDMs were serum starved in RPMI media containing 1% FBS for 30 min before stimulation with LPS (1 µg/ml). For inhibitor experiments, serum starved cells were preconditioned with 25 µM INCA-6 (Millipore Sigma) for 15 minutes before LPS stimulation.

G. Luciferase Assay

A Gaussia Luciferase construct containing the PDE4b promotor was obtained from Genecopoeia (Rockville, Maryland) (Product ID: MPRM43245). BMBMs were transfected with 1.5 µg plasmid using Amaxa Nucleofector electroporation system (Lonza, Basel, Switzerland) and stimulated with LPS and INCA-6. Cell lysates were analyzed using a Secrete-pair dual luminescence assay kit (Genecopoeia) using the manufacturer's protocol.

H. Monocyte isolation from bone marrow

Purified $CD11b^{+}$ monocytes were isolated using CD11b magnetic microbeads (Miltenyi). Mouse femur and tibia were flushed with autoMACS buffer (Miltenyi,). Cell number was quantified by hemocytometer. Cells were pelleted and resuspended in autoMACS solution (90ul per 10^7 cells) and incubated with a proscribed (10ul bead solution per 10^7 cells) number of magnetic microbeads and incubated on ice for 20 min. A magnetic separator was first washed with 500ul of autoMACS buffer while in magnetic fitting followed by the cell suspension, the effluent was discarded. Cells within the column were washed 3x with 500ul autoMACS buffer and then eluted by removing column from magnetic fitting and pushing 500ul rinsing solution through the column with a syringe plunger. Cells were quantified again and used for experiments.

I. ELISA Assay

BAL fluid from each mouse was collected as described previously and directly poured onto plastic dishes. Cells were allowed to adhere for 1h, dishes were then vigorously rinsed with sterile PBS to remove non-adherent cells. cAMP was determined using ELISA kit (Sigma Aldrich, following the manufacturer's instructions.

J. Florescence associated cell sorting

Lungs were surgically harvested following perfusion of the heart with cold PBS. Lung tissue was minced and enzymatically digested with 1 mg/mL collagenase A (Roche, Indianapolis, IN) for 50 min at 37°C. Digested tissue was washed twice following centrifugation at 1250 rpm for 4 min and cells were resuspended in FACS buffer (1% BSA in PBS). A single cell suspension was prepared by forcing minced tissue through a narrow cannula as previously described[98]. The washed cell suspension was passed through a 75-µm nylon filter. Red blood cells were lysed using diluted 10 x RBC lysis buffer (Invitrogen). The cell suspension was then incubated with Fc blocking CD13/CD32 antibody (Invitrogen) for 30 minutes on ice followed by the addition of fluorochrome-labeled antibody cocktail for 30 minutes on ice. Dead cells were identified using 7AAD (Biolegend, San Diego, CA) staining. Samples were washed 2x with 1 ml FACS sample buffer and fixed using IC Fixation Buffer (Invitrogen). Samples were analyzed using a CytoFlex flow cytometer (Beckman Coulter, Brae, CA). All data were processed using Flow Jo software (TreeStar, Inc, Ashland, OR). All antibodies used for flow cytometry were specific for mouse antigens and are listed in Table 1.

K. Immunoblotting

Cells were lysed in 2x Laemmli buffer. For each sample, 20µl of lysate were ran on SDS-PAGE gels and transferred to nitrocellulose membrane. Membranes were Western blotted using primary antibodies as listed in Table 2, diluted in TBST with 3% BSA. Anti-rabbit (Santa Cruz Biotechnology) or anti-mouse (Santa Cruz Biotechnology) IgG-HRP (1:10000 dilution) were used as secondary antibodies. β-actin was used as a loading control. Chemiluminescent signal was recorded on the ChemiDoc XRS Biorad Imager (Biorad Laboratories, Hercules, CA) and data were analyzed using ImageJ software (NIH, Bethesda, MD). All antibodies used for immunoblotting are listed in Table 2.

L. Quantitative Real-time Reverse Transcriptase-PCR

Total RNA was collected from the BMDMs or flow-sorted macrophages using TRIzol reagent (Invitrogen). RNA was isolated via ethanol precipitation and quantified using Biodrop. Reverse transcription reaction was carried to generate cDNA using the High-Capacity cDNA Reverse Transcription Kit (Applied Biosystems) according to the manufacturer's instructions. Forward and reverse primer pair sequences are listed in Table 3. Experiments were run on Viia7 Real-Time QPCR system (Thermofisher). Fold change was calculated by using the delta-delta-CT value based on housekeeping gene controls.

M. Immunohistochemistry and microscopy

Lungs were harvested following perfusion of the heart with cold PBS and embedded in optimal cutting temperature compound (OCT) and frozen at -80^{o}C before cryosectioning by the UIC Histology Research Core. Each 12-micron section was fixed in 2% paraformaldehyde and stained with appropriate primary and secondary antibodies or fluorochrome tagged primary

antibody. Lung sections and cytospin slides were analyzed using an LSM880 confocal microscope (Carl Zeiss). Hematoxylin/eosin staining was performed using Hema 3 Stat pack (Fisherbrand) according to manufacturer's instructions, slides were analyzed on an Echo Rebel hybrid visible light microscope (Echo).

N. Phagocytosis Assay

To assess phagocytic capacity, BAL from LysM-GFP mice was plated on glass-bottom 35 mm dishes containing RPMI media and 10% FBS. After 1 h, all non-adherent cells were removed through vigorous washing with PBS. Cells were incubated with fluorescently labeled latex beads (Millipore Sigma) for 2h, after which cells were washed with PBS to remove residual beads and fixed with 2% paraformaldehyde solution. Visualization of bead internalization was done using an LSM880 confocal microscope (Carl Zeiss).

O. Pyruvate Dehydrogenase Activity Assay

Measurement of Acetyl-CoA production by pyruvate dehydrogenase enzyme activity was performed using PDH activity assay kit (Sigma Aldrich). Cell lysates were generated from either cultured BMDMs or flow isolated cells. Experiments were performed according to the company's instructions.

P. Oligo-immunoprecipitation

Wildtype BMDM pretreated with INCA and LPS as indicated were washed with PBS and lysed using RIPA lysis buffer. Equal amounts of lysates protein (100-150 µg) were incubated with Poly IC compound (Sigma Aldrich) (40 ng/µl) in 500 µl binding buffer (HEPES 12mM, Tris 4mM, KCl 60mM, Glycerol 5% of final volume, EDTA 500uM, DTT 1mM, and Protease Inhibitor cocktail). Annealed biotinylated oligo (2µg) was then added and the mixture was mixed by

constant rotation at 4°C overnight. The next day, protein-oligo complexes were incubated with pre-washed Streptavidin beads for an additional 4-6 h. Complexes were centrifuges, washed x4 and resuspended in 25-30 µl of 4x Laemmli buffer. These complexes were heated at 90-95°C for 10 min and Western blotted as described above. Oligo sequences are listed in Table 4.

Q. RNA Sequencing and Bioinformatics:

RNA from flow-sorted cells was collected and submitted to Northwestern University NUseq research core for Illumina NextSeq 50075SE High Output RNA sequencing and bioinformatics analysis. Analysis of the PDE4b promoter was done using Gene Runner (https://generunner.net) and the eukaryotic promoter database (https://epd.epfl.ch//index.php). These data have been deposited at the Gene Expression Omnibus under accession number GSE174532.

R. Statistical Analysis

Results are expressed as means ± SD from three to five independent experiments. One-way ANOVA followed by post-hoc Tukey's multiple comparisons test and unpaired parametric t-test was used to compare groups using Graph Pad Prism version 7.0 (GraphPad Prism Software, Inc, San Diego, CA). Data represented as *P < 0.05, **P < 0.01, ***P < 0.001, and ****P<0.0001 to denote significant difference between treatment and vehicle control groups at the same timepoint, while # P < 0.05, ## P < 0.01, ### P < 0.001, and #### P<0.0001 to denote significant difference between baseline and after LPS exposure.

Table 2. Fluorescently labeled antibodies used in flow cytometry experiments.

Target	Clone #	Fluorochrome	Company	Cat #	Host Species	Dilution
CD64	X54-5/7.1	PEcy7	Biolegend	139314	Mouse	1/200
CD11b	M1/70	APC	eBioscience	17-0112-82	Rat	1/200
CD11b	M1/70	ef450	eBioscience	48-0112-82	Rat	1/200
CX3CR1	SAA011F11	PEcy7	Biolegend	149016	Mouse	1:70
Ly6c	HK1.4	PERCPcy5.5	eBioscience	45-5932-82	Rat	1/400
Ly6g	1A8	BV785	Biolegend	127645	Rat	1/200
SiglecF	S17007L	PE	Biolegend	155506	Rat	1/400
SiglecF	S17007L	APC	Biolegend	155508	Rat	1/400
CD45	30F11	PEcy7	Biolegend	103114	Rat	1/200
Brdu	Bu20a	APC	Biolegend	339808	Mouse	1/20
CD62L	MEL-14	APC	Biolegend	104411	Rat	1:200

Table 3. Unconjugated antibodies used in histology experiments.

Target	Company	Cat #	Host Species	Dilution
PDE4b	Invitrogen	MA5-25677	Mouse	1/1000
GFP	GenTex	GTX113617	Rabbit	1:50
p-NFATc2 ser54	Invitrogen	44-944G	Rabbit	1/1000
NFATc2	Cell Signaling	4389S	Rabbit	1:1000
Actin	Thermofisher	MA5-15739-HRP	Rabbit	1/1000

Table 4: Primer sequences used in RT-QPCR experiments.

Gene	Forward Primer Sequence (5'-3')	Reverse Primer Sequence (3'-5')
Actin	CGTTGACATCCGTAAAGACCT C	AGCCACCGATCCACACAGA
PDE4A	CAAGCGCCAGAAGCAGAG	CATAGTCTTCAGGTCAGCCAGA
PDE4B	AATGTGGCTGGGTACTCACA	AAGGTGTCAGATGAGATTTTAAACG
PDE4C	ATGGGGACTTGATGTGTTCA	TCTTGAGGAGGTCTCGTTCC
PDE4D	CGTTTTCCGAATAGCAGAGC	TTTTAAACGTTTTTAACAAATCTCG
IL-6	AGTCCGGAGAGGAGACTTCA	TTGCCATTGCACAACTCTTT
iNOS2	TGCATGGACCAGTATAAGGCAAGC	GCTTCTGGTCGATGTCATGAGCAA
IFN-y	TGAACGCTACACACTGCATCTTGG	CGACTCCTTTTCCGCTTCCTGAG
PDHK1	GACTGTGAAGATGAGTGACCG	CAATCCGTAACCAAACCCAG
PDHK2	AAGAGATCAACCTGCTTCCTG	GCATCTGTGAACTGGCTTAGAG
PDHK3	CGCCATTACAAGACCACTCC	CAGAGACTTCAGAGACAGCAC
PDHK4	AGTGACTCAAAGACGGGAAAC	GTGTGAGGTTTAATTCTGGCG
GAPDH	GTGAAGGTCGGTGTGAACGG	TCATGAGCCCTTCCACAATG
CREB1	ATTTGTAAATTGTTGGGGGAAATG	ACTGAATGAAGAAGCAACAACTGC

Table 5: Oligonucleotide sequences for oligo-immunoprecipitation experiment.

Oligos (Containing NFATc2 Binding sites)	
Forward Primer	GACTTGTCCTGAGAAGTGAAAAATAGCTTTCCAATCACAGCTA GATATATGATCTTGAAT
Reverse Primer	ATTCAAGATCATATATCTAGCTGTGATTGGAAAGCTATTTTTCA CTTCTCAGGACAAGTC
Control Oligos (No NFATc2 Binding sites)	
Forward Primer	GACTTGTCCTGAGAAGTGATAAAAAGCTTTCCAAGAACAGCTA GATATATGATCTTGAAT
Reverse Primer	ATTCAAGATCATATATCTAGCTGTGACCAAAAAGCAAAAAGTC ACTTCTCAGGACAAGTC

III. Results

A. Specific Aim 1: Evaluate the role of cAMP signaling genes in the conversion of alveolar macrophages from an enflamed to reparative phenotype

Results

LPS induces a dynamic shift in lung AMϕ during injury and repair.

We have shown that nebulized LPS induces inflammatory lung vascular injury within 4 h and that the injury resolves within the next 24 to 48 h[52]. Thus, we implemented this model of ALI in LysM-GFP mice[203], in which all myeloid cells express GFP (green). We used the gating strategy and ALI timecourse described in **Fig 5 and Fig. 6A** to investigate dynamic alterations in lung-resident Mϕ phenotype over the course of injury and repair. As expected, LPS induced lung edema 4 h post-injury, which was sustained for up to 16 h and then resolved by 24 h (**Fig 6B**). We found that AMϕ, operationally defined as $GFP^+/Ly6g^-/CD64^+/SiglecF^+$, accounted for ~60% of total lung macrophages, defined as $GFP^+/Ly6g^-/CD64^+$, under basal conditions **(Fig 6C and 6D)**. We grouped the other pool of resident Mϕ, namely the interstitial Mϕ (IMϕ) and monocyte-derived Mϕ (Mo-Mϕ), as ($CD11b^+/SiglecF^-$) together and found them to constitute ~40% of the total number of macrophages in naïve lungs **(Fig 6C and 6E)**. The AMϕ pool sharply declined ~20% at 16 and 24 h **(Fig 6C and 6D)**. We also noted that at 16 h (overlapping with the injury phase), the $SiglecF^+$ population bifurcated into two subpopulations, namely, $CD11b^{med}$ and $CD11b^{high}$ (16 h) **(Fig 6C and 7A)**. In the resolution phase, i.e., 24 h post-LPS challenge, the $SiglecF^+$ pool shrank to ~20% of the total Mϕ pool and almost entirely switched to $CD11b^+$ expression by 24 h **(Fig 6C, 6D)**. IMϕ and Mo-Mϕ remained $SiglecF^-/CD11b^+$ in all phases of injury and repair and proportionally increased to about 80% of the total number of macrophages at 16 h and 24 h **(Fig 6C and 6E)**. To examine the distinction between these two populations, we next flow-sorted AMϕ

from mice 16 h after LPS challenge and found that CD11b^{lo} and CD11b^{hi} AMϕ were structurally distinct, with most of the CD11b^{hi} AMϕ proving to be smaller and rounder in shape and higher in cytoplasmic density than CD11b^{lo} AMϕ, which were bigger than CD11b^{hi} AMϕ and had a well-defined cytoplasm **(Fig. 7B)**.

LPS induces PDE4b expression in AMϕ at the time of peak injury.

To assess how the phenotypic shift in Mϕ is related to alteration in their transcriptomics, we flow-sorted GFP^{+}/Ly6g^{-}/CD64^{+} lung cells at baseline, time of peak injury, and resolution phase and performed panRNA sequencing. We focused on genes associated with cAMP signaling due to its role in regulating anti-inflammatory and pro-resolution macrophage signaling[151,204]. We found PDE4b, which specifically degrades cAMP, to be one of the most highly expressed cAMP-related genes in Mϕ (**Fig 8**). Interestingly, PDE4b expression sharply increased at the time of peak injury and then dropped below baseline during the resolution phase (**Fig. 8**). We validated these findings using flow-sorted AMϕ and IM/Mo-Mϕ. As shown in **Fig. 9A-B,** at the time of peak injury, PDE4 mRNA increased ~3-fold in AMϕ but only ~1.8 fold in IM/Mo-Mϕ. In both populations, PDE4b expression decreased to below basal levels within 16 h-24 h. There are four members of the PDE4 gene family[13]: PDE4a, PDE4b, PDE4c, and PDE4d. However, PDE4b has been indicated to play an essential role in inflammatory lung disease[136]. Indeed, a comparison of the Critical Threshold (CT) values for each PDE4 gene in AMϕ by RT-QPCR confirmed PDE4b to be a highly expressed PDE4 family member, with lower CT values indicating higher expression (**Fig. 9A**). Whereas PDE4d was very modestly expressed in AMϕ, we failed to detect PDE4a and PDE4c mRNA (**Fig 9C**). In IMϕ and Mo-Mϕ, we only detected PDE4b mRNA but not PDE4a, PDE4c, or PDE4d (**Fig 9D**).

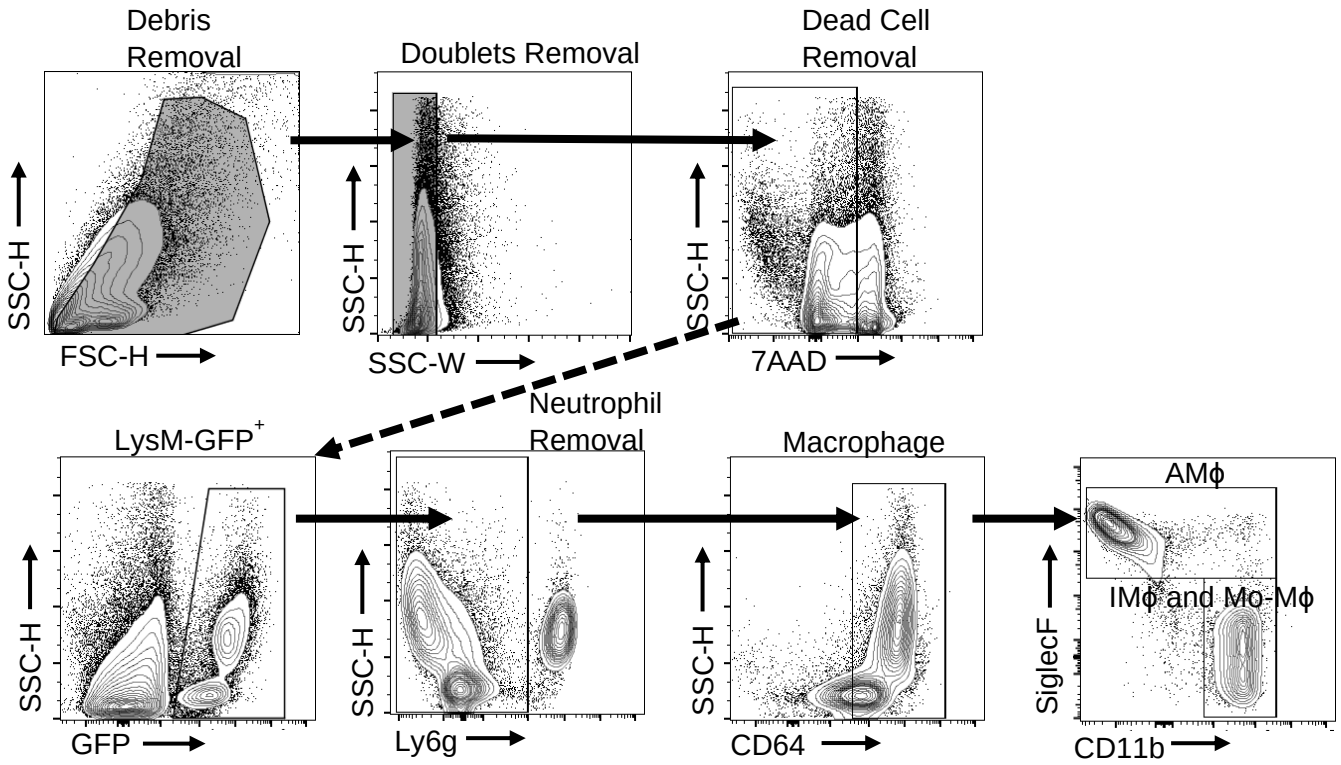

Figure 5. Gating strategy for assessing pulmonary macrophage populations in a LysM-GFP mouse. Single cell lung suspension is first gated to remove debris and doublets. Cells that are positive for 7AAD (dead cells) are excluded while 7AAD negative cells are gated onto GFP for selection of myeloid cells. Neutrophils ($Ly6g^+$) were next excluded from myeloid cells while all $CD64^+$ Mϕ and monocytes were further gated onto CD11b and SiglecF to define AMϕ ($SiglecF^+$) and IM/Mo-Mϕ ($SiglecF^-/CD11b^+$).

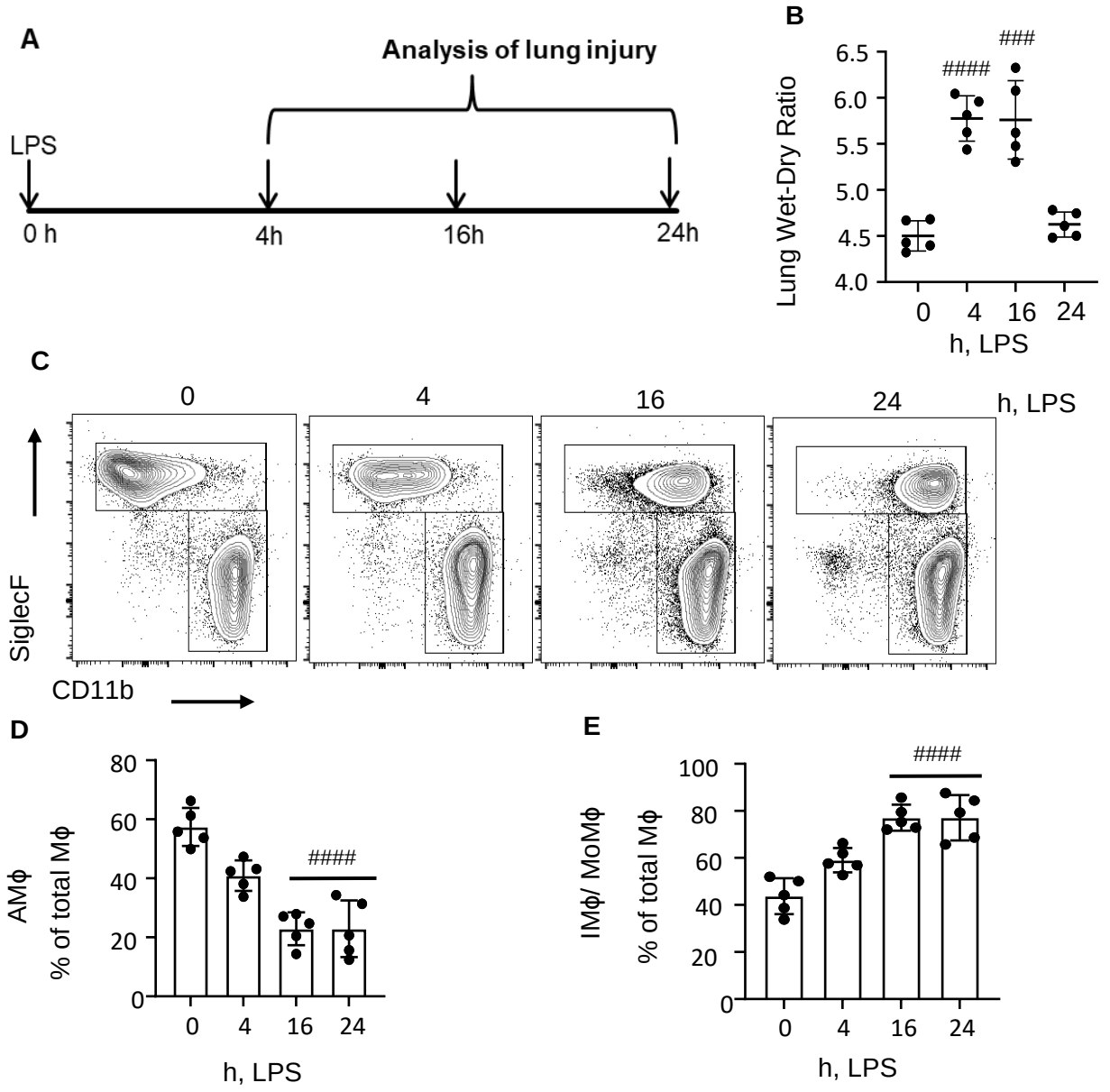

Figure 6. Tracing the phenotypic shift of pulmonary macrophages following LPS-induced acute lung injury. A) Schematics of assessment of lung injury and Mϕ phenotype following LPS induced injury. **B)** LysM-GFP mice were exposed to nebulized LPS (1 mg/ml) for 45 min. Lungs were harvested at indicated times and lung injury was determined by measuring lung wet-dry ratio. n=5 mice/group. **C-F)** Lung cells were stained with SiglecF, CD11b, CD64, Ly6g antibodies and gated as described in **Figure 1**. Flow cytometry analysis was performed to define AMϕ or IM/Mo-Mϕ populations. N=5 mice/group. A representative dot plot of pulmonary Mϕ subpopulations at indicated time is shown in **C. D)** Plot shows AMϕ number ($GFP^+/Ly6g^-/CD64^+/SiglecF^+$) as % of total Mϕ pool ($GFP^+/Ly6g^-/CD64^+$). **E)** Plot shows IMϕ/Mo-Mϕ ($GFP^+/Ly6g^-/CD64^+/SiglecF^-/CD11b^+$) as a percent of total Mϕ pool. Data in figure **B, D-E** are represented as individual scatter along with mean ± SD while ### $P < 0.001$ and #### $P<0.0001$ to denote significant difference between LPS exposed and 0 h unexposed mice.

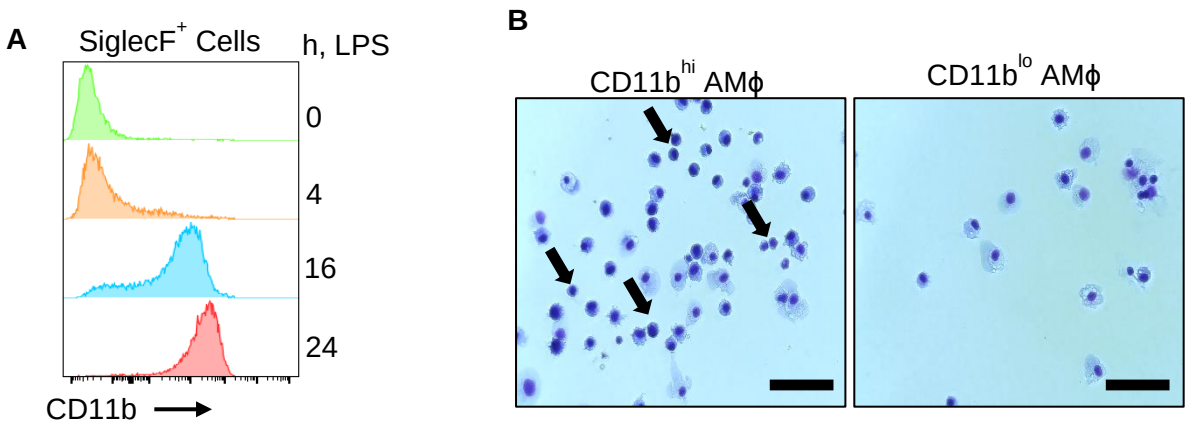

Figure 7. Tracing the phenotypic shift of pulmonary macrophages following LPS-induced acute lung injury. A) Representative histograms showing CD11b surface expression on AMϕ at indicated timepoints following LPS challenge. **B)** Flow sorted AMϕ were centrifuged onto glass coverslips. Cells were stained with hematoxylin and eosin and analyzed using light microscope. Scale bar, 70 μm.

NFATc2 induces PDE4b expression during lung injury.

While PDE4b is well studied in the setting of various lung diseases[172,205,206], the mechanisms regulating PDE4b expression during lung injury are unknown. We, therefore, analyzed the PDE4b promotor to identify key transcription factors that may activate PDE4b expression during injury. We found that the PDE4b promoter contains multiple binding sites for the Ca^{2+}-dependent transcription factor NFAT near the transcription start site (**Fig 10A**). We recently showed that LPS increases intracellular Ca^{2+}, which then activates NFATc2[178]. Activated NFATc2 then cooperates with NFκB to augment inflammatory signaling in AMϕ, thereby impairing the resolution of lung injury. Hence, we tested the possibility that NFATc2 synthesizes PDE4b to counter the anti-inflammatory activity of cAMP generated during injury. For this purpose, we used bone marrow-derived macrophages (BMDM) and the small molecule inhibitor INCA-6, which inhibits NFAT transcriptional activity[207]. LPS increased NFATc2 ser54 phosphorylation, a measure of NFATc2 activity in the nucleus[207], within half an hour, while preconditioning cells with INCA-6 for 15 min before LPS exposure prevented NFAT phosphorylation at phospho-serine54 (**Fig. 10B-C).** LPS also increased PDE4b protein expression in association with increase in NFATc2 activity in an INCA-6 sensitive manner (**Fig. 10B and 10D**). Moreover, we also found that LPS also increased PDE4b mRNA and protein expression when BMDM were stimulated over a longer time course (**Fig. 10E-G**). However, LPS failed to induce PDE4b mRNA and protein expression in BMDM treated INCA-6 (**Fig. 10E-G**).

We next used oligo immunoprecipitation and Western blotting to investigate whether NFATc2 directly binds to the PDE4b promotor after activation by LPS. BMDM were left unstimulated or stimulated with LPS and preconditioned with INCA-6 for the indicated times, after which cell lysates were incubated with biotinylated oligonucleotide sequences matching the

PDE4b promotor containing or lacking NFATc2 bindings sites. Transcription factors which bound to these oligo sequences were purified and analyzed using Western blot. We found that LPS increased the binding of NFATc2 to the PDE4b promotor **(Fig 11A-B).** However, this binding activity was not observed in cells pretreated with INCA-6 or PDE4b promotor constructs lacking the NFATc2 binding sites **(Fig 11A-B)**.

To further corroborate these findings, we transfected BMDM with a PDE4b luciferase promoter construct and determined the increase in promoter activity induced by LPS. Again, we found that LPS markedly increased NFATc2 promoter activity, but this response was abolished in BMDM pretreated with INCA-6 **(Fig 11C)**.

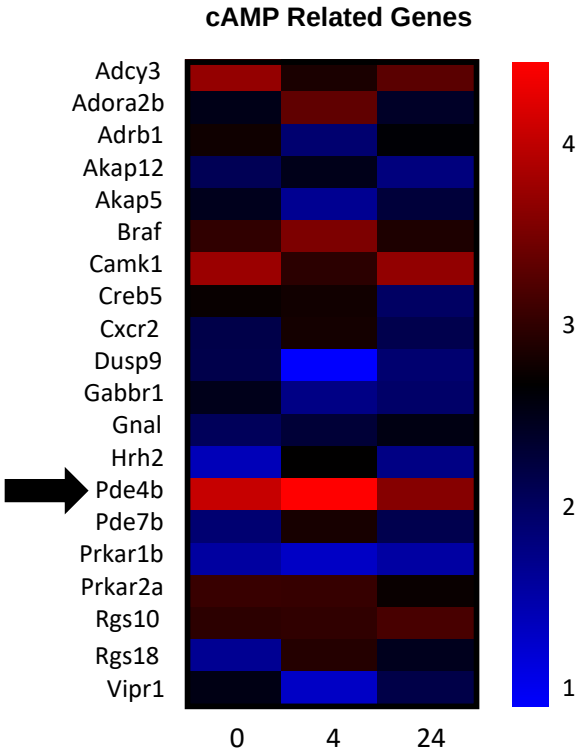

Figure 8. LPS upregulates phosphodiesterase 4b in alveolar macrophage during injury. A) Heatmap of cAMP-regulating genes in $GFP^{+/}Ly6g^{-}/CD64^{+}$ macrophages using bulk RNA sequencing at indicated time points after LPS inhalation. PDE4b (arrow) is the highly expressed and LPS responsive gene during lung injury.

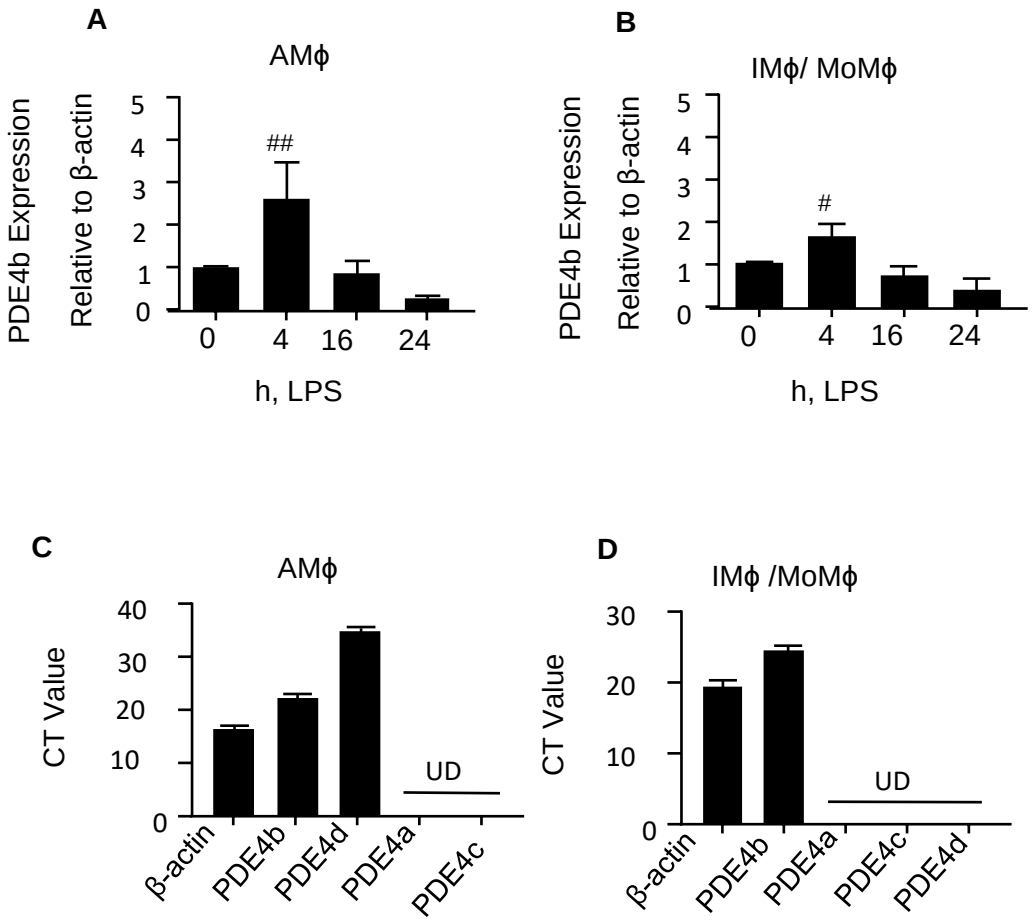

Figure 9. LPS upregulates phosphodiesterase 4b in alveolar macrophage during injury. A-B) Validation of PDE4b mRNA expression in flow sorted AMϕ ($GFP^+/Ly6g^-/CD64^+/SiglecF^+$) (**A**) and IM/Mo-Mϕ ($GFP^+/Ly6g^-/CD64^+/SiglecF^-/CD11b^+$) (B) using RT-QPCR (n=3 sort/group). **C-D** Plots show CT values of PDE4 genes in sorted AMϕ (**C**) and IM/Mo-Mϕ (**D**) using RT-QPCR (n=3 sort/group). Data are shown as means ±SD and represented as # $P < 0.05$ and ## $P < 0.01$ to denote significant difference between LPS exposed and unexposed cells.

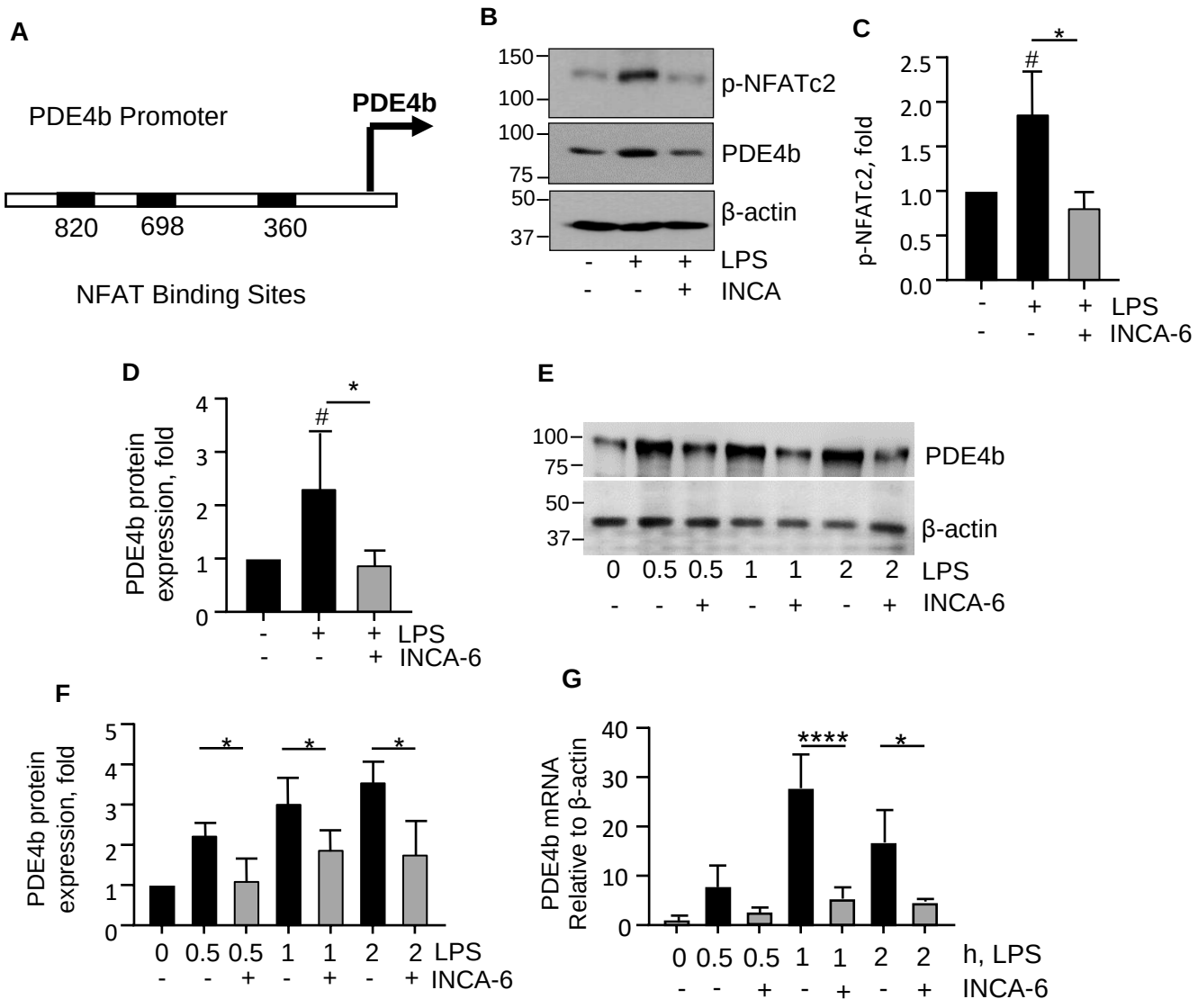

Fig 10. NFAT upregulates PDE4b expression in macrophages. A) Representation of mouse PDE4b promoter region with three NFAT binding sites. Arrow indicate transcription start sites. **B-D)** BMDM were preincubated with 25 μM INCA-6 for 15 min followed by addition of 1μg/mL LPS for another 15 min. NAFTc2 activity was determined using phosphoNFATc2 Ser54 antibody. In addition, PDE4b protein expression was determined using PDE4b antibody. **B,** shows a representative immune blot while plots **C** and **D** shows fold increase in NFATc2 phosphorylation (p-NFATc2) and PDE4b protein expression taking no LPS (-) as the control, experiments performed three times independently, n=3. **E-G)** BMDMs were exposed to LPS for indicated timepoints and PDE4b expression at the level of protein **(E-F)** and mRNA (**G**) was determined using Western blotting **(E-F)** or RT-QPCR (G) (n=3), β–actin was used as a loading control in **E.** The Western blot represent data from experiments that were performed three times independently (n=3). Data are shown as means ±SD and represented as *P < 0.05 and ****P < 0.0001 to denote significant difference between treatment conditions at the same timepoint while #### P<0.0001 denote significant difference between a treatment condition and unstimulated controls.

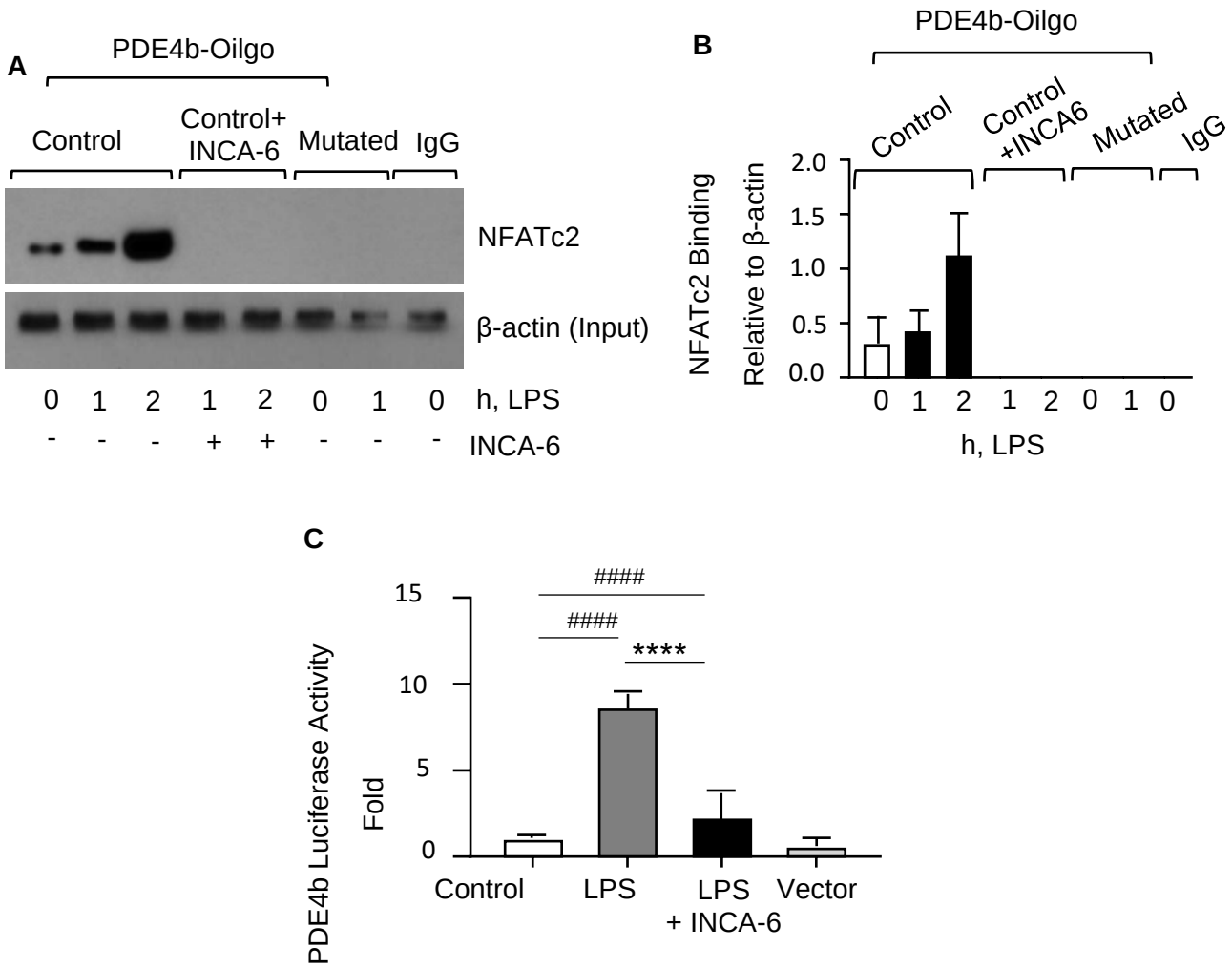

Figure 11. NFAT binds to the promotor of PDE4b and controls transcription in response to LPS. A) Lysates of unstimulated or LPS stimulated BMDM treated without or with INCA-6 were incubated with biotinylated PDE4b promotor oligos containing NFAT binding sites or with these sites removed (mutated) after which complexes were pulled down using streptavidin beads. In parallel, lysates were incubated with oligos containing mutated NFAT binding sites and immunocomplexes were pulled down. Controls included lysates incubated with IgG and PDE4b oligos. A representative Western blot is shown from experiment that was repeated three times. **B)** Densitometry of NFAT binding to PDE4B promoter at indicated times following LPS stimulation of BMDM (n=3). **C)** BMDM were transfected with empty vector or PDE4b luciferase promoter construct. After 48h, cells were exposed to LPS after with or without preexposure with INCA-6. The experiments were repeated three time independently (n=3). Data are shown as means ±SD and represented as *P < 0.05 and ****P < 0.0001 to denote significant difference between treatment conditions at the same timepoint while #### P<0.0001 denote significant difference between a treatment condition and unstimulated controls.

B. Specific Aim 2: Determine whether cAMP reprograms alveolar macrophage reparative phenotype *in vivo*

Results

Inhibition of PDE4b augments AMϕ generation truncating inflammatory lung injury.

CD11b expressing AMϕ are linked to persistent inflammatory states in both mice and humans[95,208,209]. However, we showed that at 24 h 80% of the AMϕ population remained $CD11b^+$ despite the decline in PDE4b expression and resolution of lung injury. We, therefore, surmised that the $SiglecF^+/CD11b^+$ pool also contained a cAMP-sensitive pool of reparative AMϕ. To test this possibility, we inhibited PDE4 activity using rolipram, a well-established inhibitor of PDE4[210], in a therapeutic model of lung injury.

We investigated whether preventing cAMP degradation would skew the $SiglecF^+/CD11b^+$ pool to acquire a homeostatic AMϕ signature ($SiglecF^+/CD11b^-$) and whether this phenotypic shift would also promote resolution of lung injury. Thus, we administered rolipram intratracheally (2.5 mg/kg) 2 h after administration of LPS and assessed AMϕ phenotype and lung edema. We found that the $SiglecF^+/CD11b^-$ AMϕ population constituted a larger percentage of the total resident AMϕ pool in rolipram-treated lungs, increasing by 50% at both 16 h and 24 h but not at 4 h (**Fig 12A-B**). Moreover, rolipram shifted the AMϕ pool from $SiglecF^+/CD11b^+$ to $SiglecF^+/CD11b^-$ **(Fig 13A-B)**. To determine if this increase in AMϕ population was due to proportional changes in AMϕ versus non-AMϕ, we quantified the absolute number of both populations in the lung at each timepoint. While rolipram did not affect the number of non-AMϕ, it did increase the absolute AMϕ number in the lung at 16 and 24 h post-LPS challenge (**Fig 14A-B**).

We next determined if the shift in AMϕ towards the $CD11b^-$ AMϕ lineage reverses lung injury. We first determined cAMP levels in sorted AMϕ following LPS challenge. We found that

rolipram transiently increased cAMP levels in AMϕ by 3-fold within 4 h, which declined to control levels at 16 h (**Fig 15C**). At 4 h, rolipram-treated mice developed lung injury similar to control mice post-LPS challenge (**Fig. 15A-B**). Intriguingly, at 16 h, mice receiving rolipram showed an 80% decrease in lung edema formation and albumin accumulation after LPS challenge relative to control mice (**Fig 15A-B**). Inhibition of PDE4 also massively decreased neutrophil extravasation in the alveolar space at 16 h (**Fig. 16A-B**) without affecting the percentage of peripheral lung neutrophils **(Fig 16C)**. Also, rolipram-treated AMϕ acquired the anti-inflammatory lineage as revealed by markedly suppressed expression of iNOS, IL-6, and IFNγ (**Fig. 17C**). Because AMϕ promote tissue repair by phagocytizing and clearing debris[1], we also assessed whether rolipram treatment enhances AMϕ phagocytic function. To do this, we exposed AMϕ isolated from vehicle or rolipram-treated lungs to fluorescently labeled latex beads and after 45 min determined the phagocytic index. We found that rolipram increased AMϕ phagocytic function by ~1.5 fold **(Fig. 17A-B)**. These results indicate that boosting cAMP levels at the time of peak injury shifts AMϕ into the anti-inflammatory and $CD11b^-$ lineage, thus accelerating the resolution of lung injury.

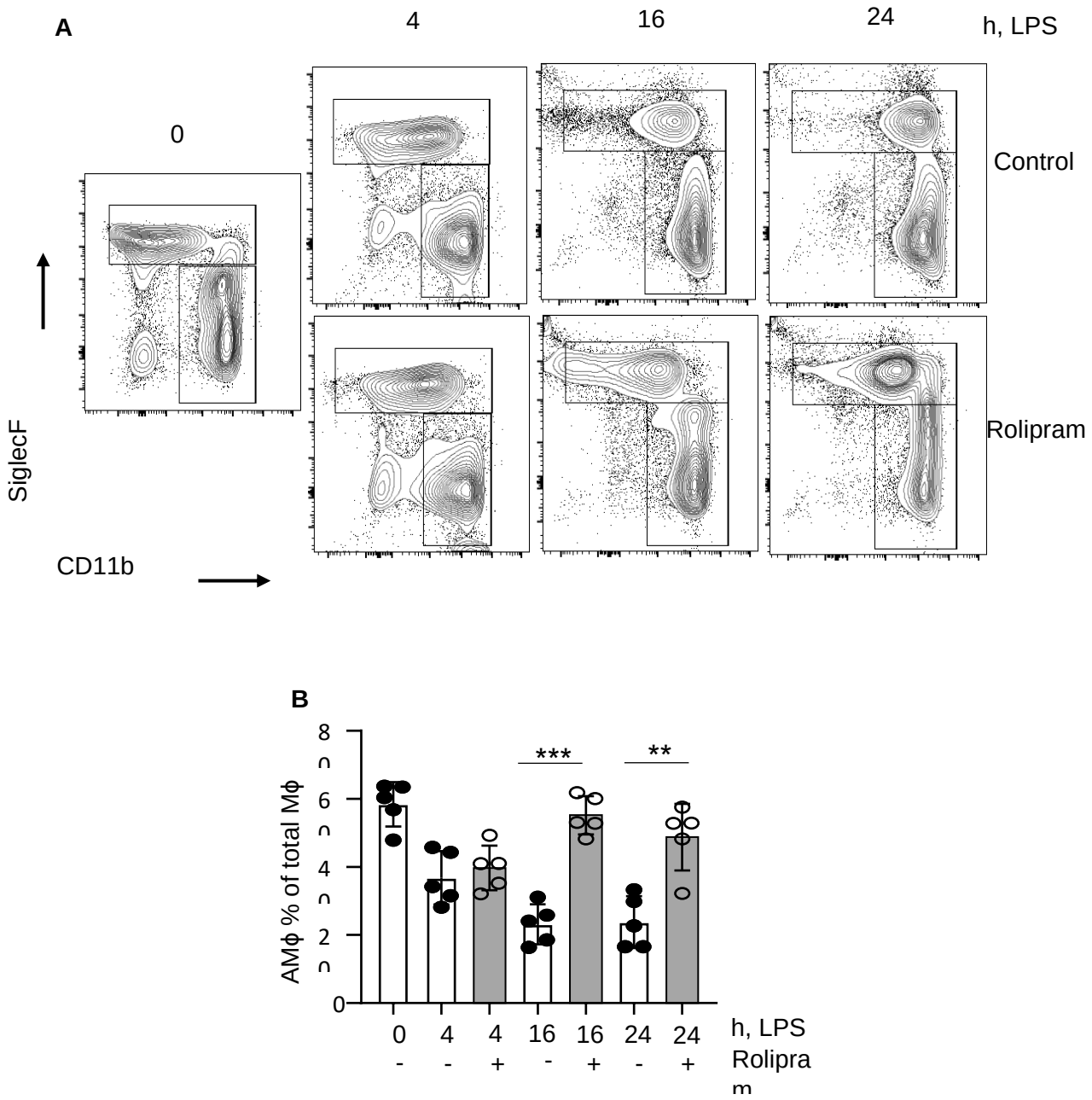

Figure 12. Inhibition of PDE4 sustains higher percentage of alveolar macrophages in the lungs after peak of injury. A) Schematics of assessment of AMϕ phenotype and lung injury following LPS inhalation and non-invasive intratracheal administration of 2.5 mg/kg rolipram or vehicle. **A)** A representative dot plot following gating of GFP+/Ly6g-/CD64+ cells. **B)** AMϕ ($GFP^+/Ly6g^-/CD64^+/SiglecF^+$) as a proportion of the total lung Mϕ pool ($GFP^+/Ly6g^-/CD64^+$) with and without rolipram treatment. Data are shown as means ±SD and represented as *P < 0.05, **P < 0.01, ***P < 0.001, and ****P<0.0001 to denote significant difference between treatment and vehicle control groups at the same timepoint.

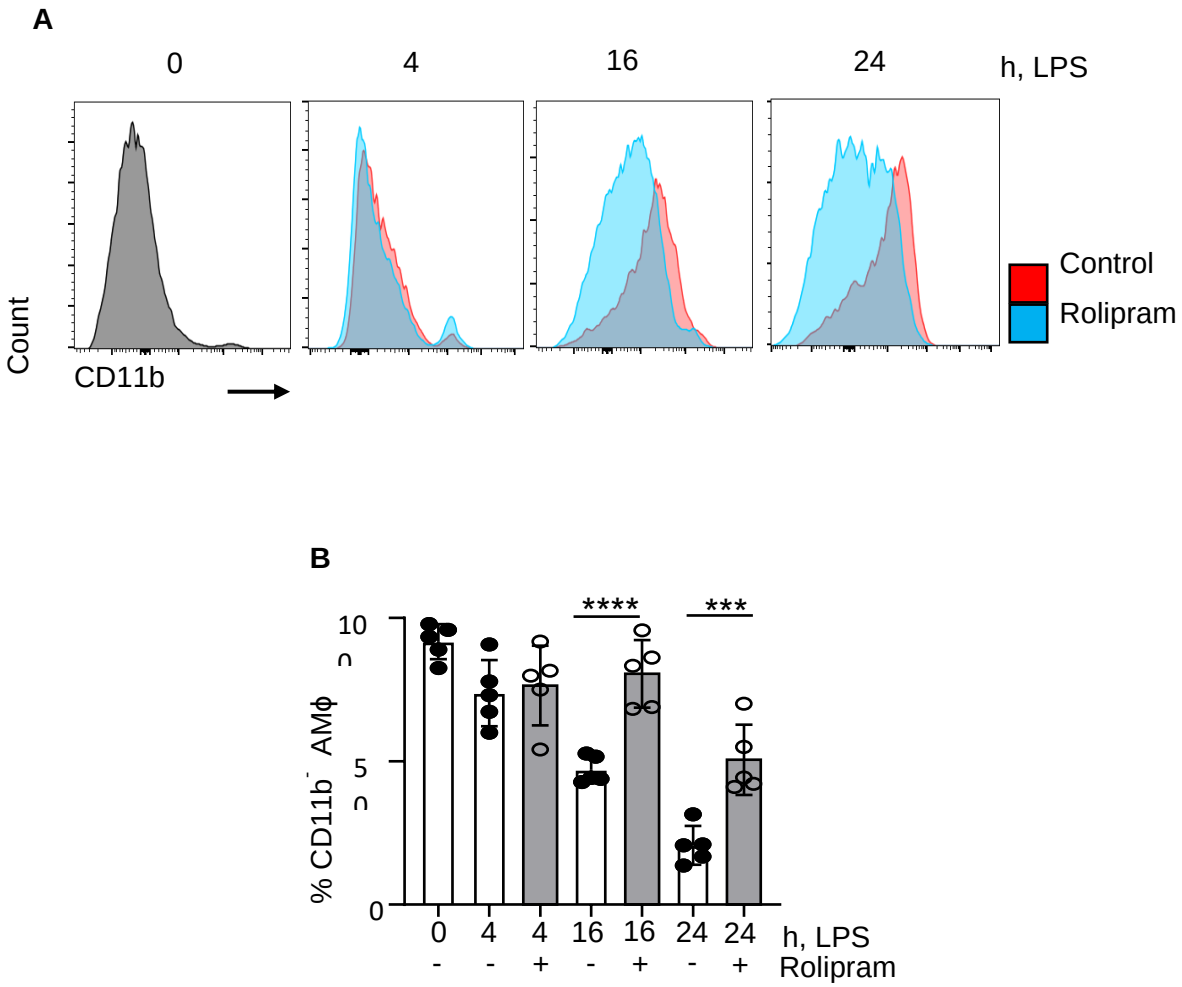

Figure 13. Inhibition of PDE4 restores CD11b^{-} alveolar macrophages in the lungs at peak of injury. A) Histogram comparing shift in CD11b cell-surface expression on AMϕ (GFP^{+}/Ly6g^{-}/CD64^{+}/SiglecF^{+}) following rolipram treatment at each timepoint. **B)** Changes in the percent of AMϕ which are CD11b^{-} following rolipram treatment. Data are shown as means ±SD and represented as *P < 0.05, **P < 0.01, ***P < 0.001, and ****P<0.0001 to denote significant difference between treatment and vehicle control groups at the same timepoint.

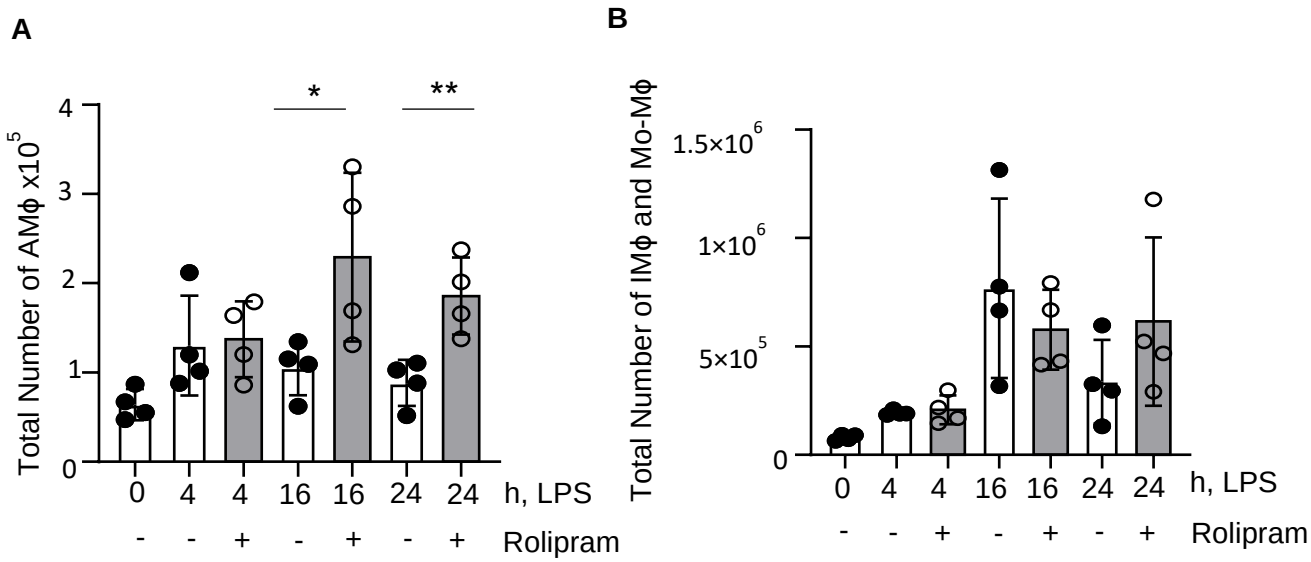

Figure 14. Increase in the proportion of alveolar macrophages after rolipram treatment is due to an increase in the total number of alveolar macrophages. A-B) Quantitation of total number of AMϕ (A) or IM/Mo-Mϕ (B) (n=4). Data are shown as means ±SD and represented as *P < 0.05, **P < 0.01 to denote significant difference between treatment and vehicle control groups at the same timepoint.

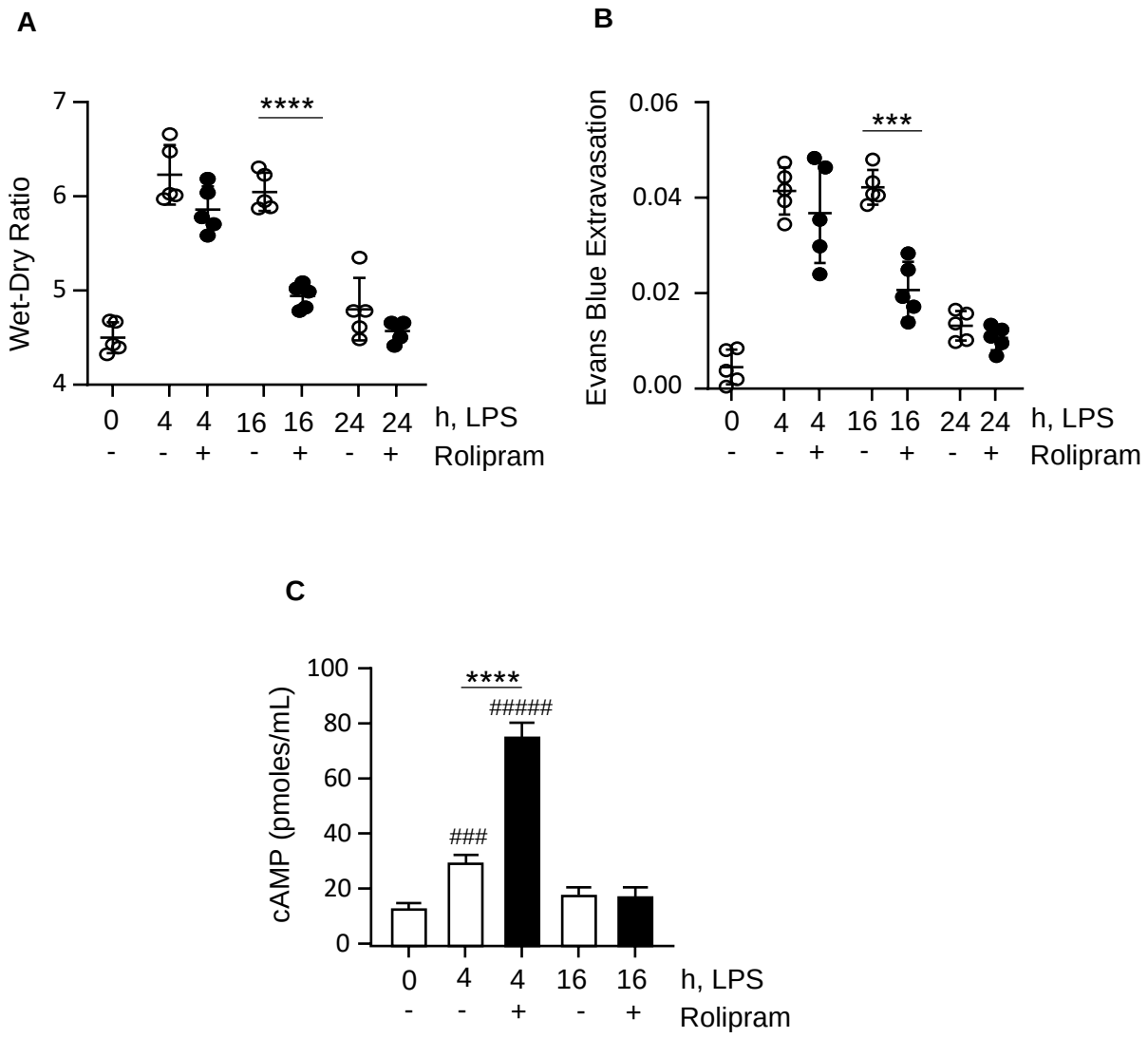

Fig 15. Inhibition of PDE4 rapidly resolves LPS-induced lung vascular inflammatory injury. A) Plot shows changes in cAMP levels in AMϕ post LPS and rolipram treatment determined as described in methods. (n=3). **B-C)** Mice exposed to nebulized LPS (1 mg/ml) for 50 min received rolipram. Thirty minutes before sacrificing the mice at indicated times, Evans blue–labelled albumin was injected retro-orbitally into each mouse. Lung vascular inflammatory injury was determined by measuring lung wet-dry ratio (B) and albumin influx (C). The plot shows individual values along with mean ± SD (n=5). Data shown as means ±SD and represented as *P < 0.05 and ****P<0.0001 to denote significant difference between treatment and vehicle control groups at the same timepoint and ### P < 0.001 and #### P<0.0001 to denote significant difference between experimental conditions and basal cells.

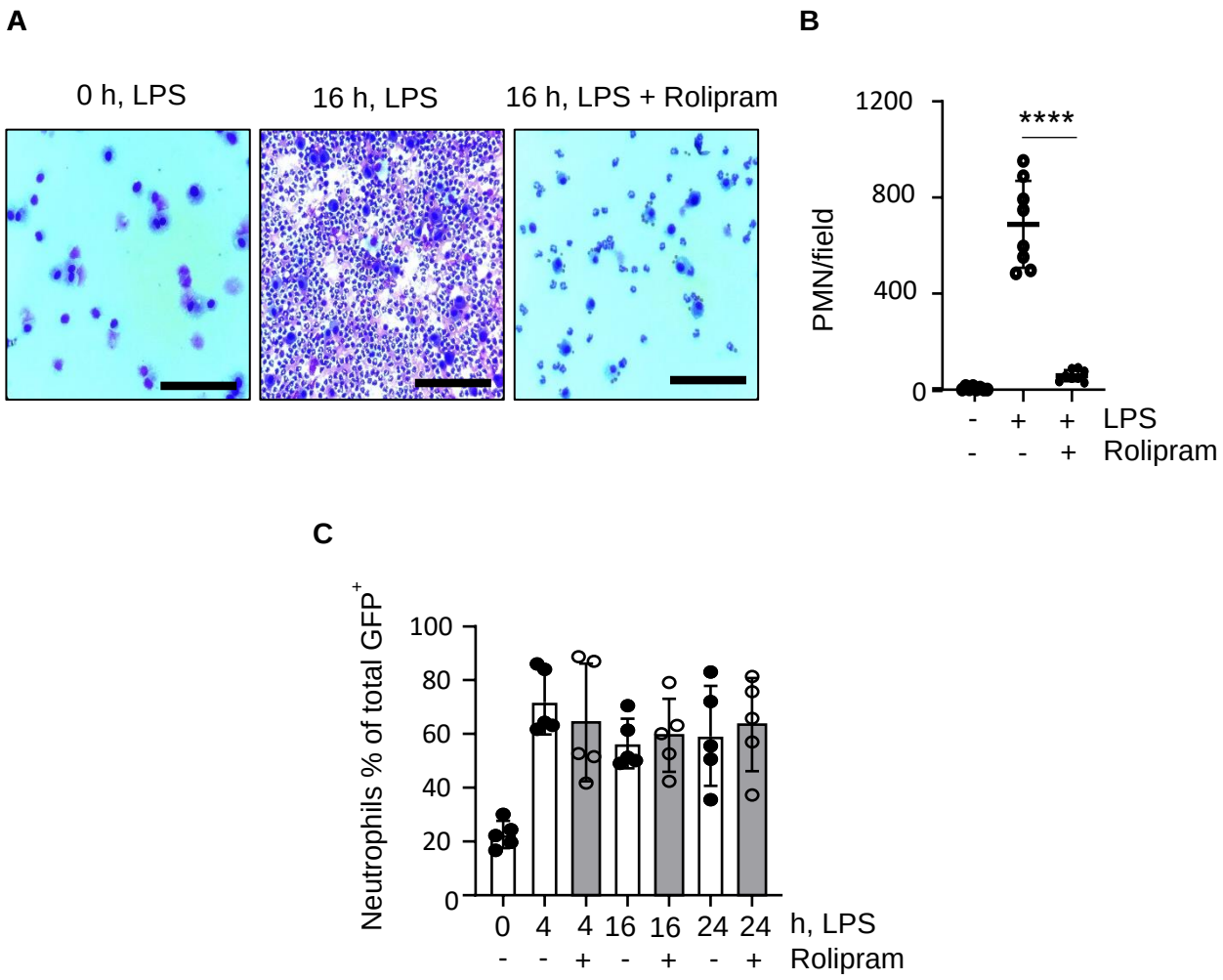

Figure 16. Rolipram treatment prevents recruitment and retention of neutrophils to the airspace. A-B) Neutrophil count was performed (per field) on hematoxylin and eosin stained BAL fluid from indicated conditions. The plot shows individual values with mean ± SD. Scale bar,120 μm. **C)** Dot plot shows neutrophils ($GFP^+/Ly6g^+$) in LPS exposed lungs with or without rolipram treatment as a percent of total GFP^+ cells (n=5) in whole lung. Data shown as means ±SD and represented as $P<0.0001$ to denote significant difference between treatment and vehicle control groups at the same timepoint

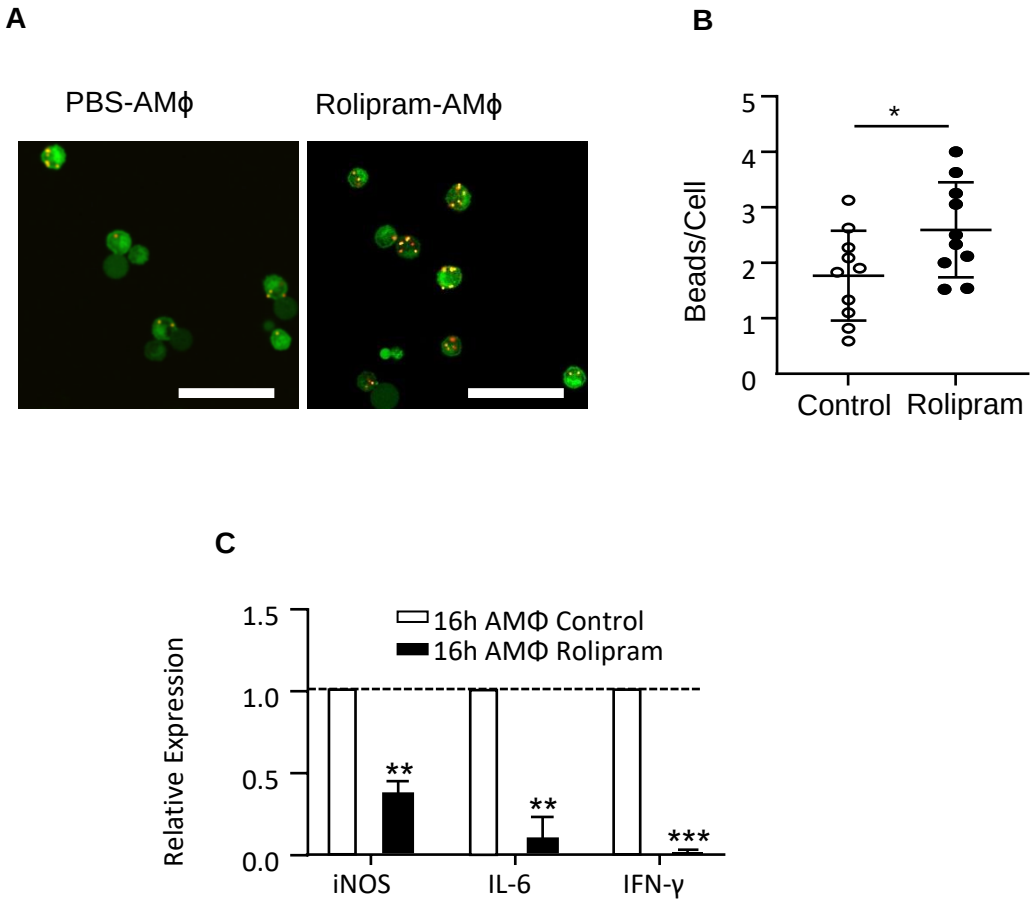

Figure 17. Rolipram treated alveolar macrophages are more phagocytic and express lower levels of inflammatory cytokines. A-B) AMϕ were isolated from bronchoalveolar lavage (BAL) and allowed to adhere on glass bottom dishes for one h. Cells were washed vigorously to remove unadhered cells. Fluorescently labeled latex beads were added at a ratio of 10:1 bead per AMϕ. Cells were fixed after 2h and images were acquired using confocal microscope. Phagocytosis index was measured as average number of beads per cell in each visual field (10 fields/condition, ~10 cells/field). Scale bar, 25 um. **C)** mRNA expression of pro-inflammatory genes in isolated AMϕ using RT-QPCR (n=3). β-actin was used as an internal control. mRNA expression is shown as fold change following rolipram treatment. Data are represented as individual scatter along with mean ± SD with *P < 0.05 denote significant difference between treatment and vehicle controls. Data shown as means ±SD and represented as *P < 0.05

Adoptive transfer of cAMP-programmed alveolar macrophages resolves lung injury.

To examine whether the cAMP-programmed AMϕ population could be used as a cell-therapy in a mouse model of ALI, we adoptively transferred rolipram-educated AMϕ 2 h after exposing WT mice to LPS (**Fig 18A**)[98,178]. To this end, we flow-sorted AMϕ from LysM-GFP mice having received vehicle control (CC) or rolipram (RC) 16 h post-LPS injury. Sorted AMϕ ($2x10^5$ cells) were adoptively transferred into a wildtype mouse by the *i.t.* route two hours after LPS inhalation **(Fig 18A)**, mice received no cells (NC) with or without LPS were used as controls. Lung injury was assessed 16 h after adoptive transfer of AMϕ. We found that adoptive transfer of cAMP programmed AMϕ promoted the resolution of lung injury, whereas this response was not observed in mice receiving no cells or vehicle alone **(Fig 18B)**. We confirmed the presence of adoptively transferred LysM-GFP AMϕ by immunostaining lung sections with SiglecF antibody to identify $GFP^+/SiglecF^+$ cells. **(Fig 19)**. These findings indicate that rolipram-educated AMϕ were capable of repairing lung damage upon transplantation in a diseased mouse.

Recruited monocytes are the source of pro-resolution AMϕ.

AMϕ originate from embryonic precursors that self-maintain throughout their entire lifespan by proliferation[38]. Evidence also indicates that during acute lung injury the AMϕ pool can be replaced by monocytes recruited into the airspace[211]. We, therefore, assessed if rolipram induces proliferation of AMϕ or stimulates differentiation of recruited monocytes into new AMϕ. We injected BrdU into mice receiving vehicle or rolipram 14 h before sacrificing them and assessed AMϕ proliferation using a labeled BrdU antibody. As shown in **Fig. 20A-B**, rolipram did not affect AMϕ proliferation, thus ruling out AMϕ expansion as the cause of the increase in AMϕ number.

To determine whether monocytes contribute to the pro-resolution AMϕ pool after rolipram treatment, we used a mouse model that expresses the human diphtheria-toxin receptor (DTR) under the control of the macrophage-monocyte-specific CD11b promotor[96]. Administration of diphtheria toxin (DT) to DTR mice leads to a rapid depletion of monocytes. Thus, we administered DT to CD11b-DTR mice two hours after initiation of LPS inhalation followed by *i.t.* delivery of rolipram **(Fig 21A)**. As expected, DT induced depletion of monocytes **(Fig 21C)** but had no effect on the gain of CD11b expression in AMϕ or AMϕ themselves (data not shown). Rolipram failed to resolve lung injury in $CD11b^{dep}$ mice **(Fig. 21B)**. However, adoptive transfer of DT-resistant $CD11b^{+}$ monocytes, harvested from LysM-GFP bone marrow, into $CD11b^{dep}$ mice at the same timepoint as DT and rolipram administration resolved injury **(Fig 21B).** Interestingly, we found that compared to vehicle alone, rolipram also increased GFP^{+} macrophages in BAL of $CD11b^{dep}$ mice **(Fig 22A-B)**. We also collected BAL from mice receiving DT and *i.v.* $CD11b^{+}$ LysM-GFP^{+} monocytes at 16 h and quantified adoptively transferred cells using FACS. We show that BAL contains 6% recruited macrophages ($GFP^{+}/CD64^{+}$ cells). Interestingly, of these GFP^{+} macrophages in the airspace, ~14% also acquire SiglecF, while remaining $CD11b^{+}$. Resident AMϕ (Non-GFP^{+}) cells under same conditions amounted to ~90% **(Fig 22C)**. Additionally, GFP^{+} cells recovered in the airspace were both $SiglecF^{+}$ and $CD11b^{+}$ **(Fig 22D)**, indicating adoptive cells gained an AMϕ phenotype. These findings demonstrate that enhancing cAMP levels mobilizes and programs monocytes into reparative AMϕ.

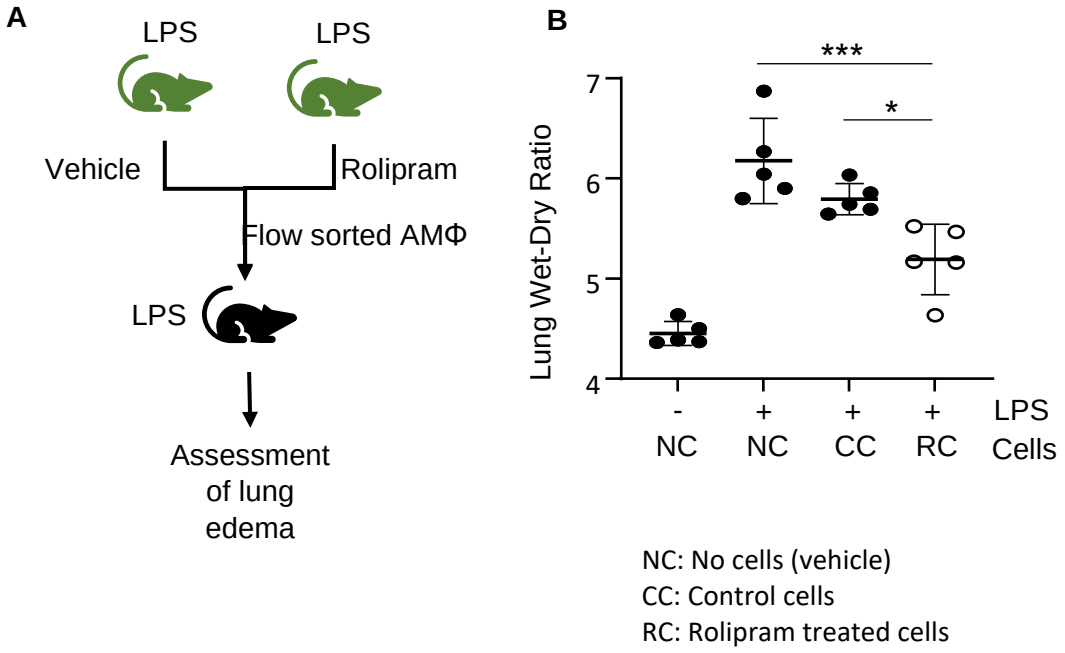

Fig 18. Adoptive transfer of rolipram educated alveolar macrophages is able to resolve lung injury in injured mice. A) Schematic of AMϕ adoptive transfer. LysM-GFP mice exposed to LPS were treated without or with rolipram. At 16 h post LPS challenge, AMϕ were isolated via flow-sorting from vehicle (control cells, CC) or rolipram-treated (RC) lungs. These AMϕ were adoptively transferred into non-GFP mice that had been exposed to LPS two hours prior to receiving cells, control mice received no cells (NC). **B)** Lung edema was measured at 14 h post adoptive transfer of indicated cells, or 16 h post initial LPS exposure. The plot shows individual values along with mean ± SD (n=5).

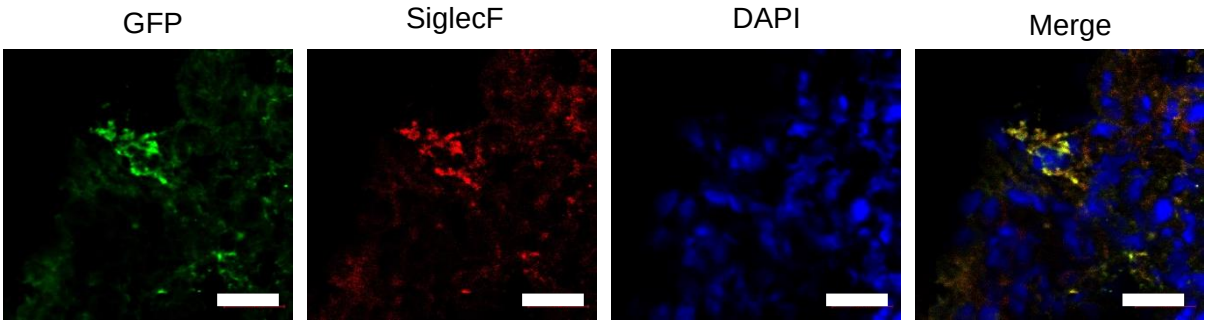

Fig 19. Adoptive transferred rolipram educated alveolar macrophages are retained in the lung after resolution of lung injury. Lung from uncolored WT mice receiving flow sorted LysM-GFP AMϕ were sectioned. Tissue was stained with DAPI and labeled antibodies for GFP and SiglecF to establish that LysM-GFP AMϕ sorted cells were present in lungs 14 h after adoptive transfer. Scale bar, 20μm.

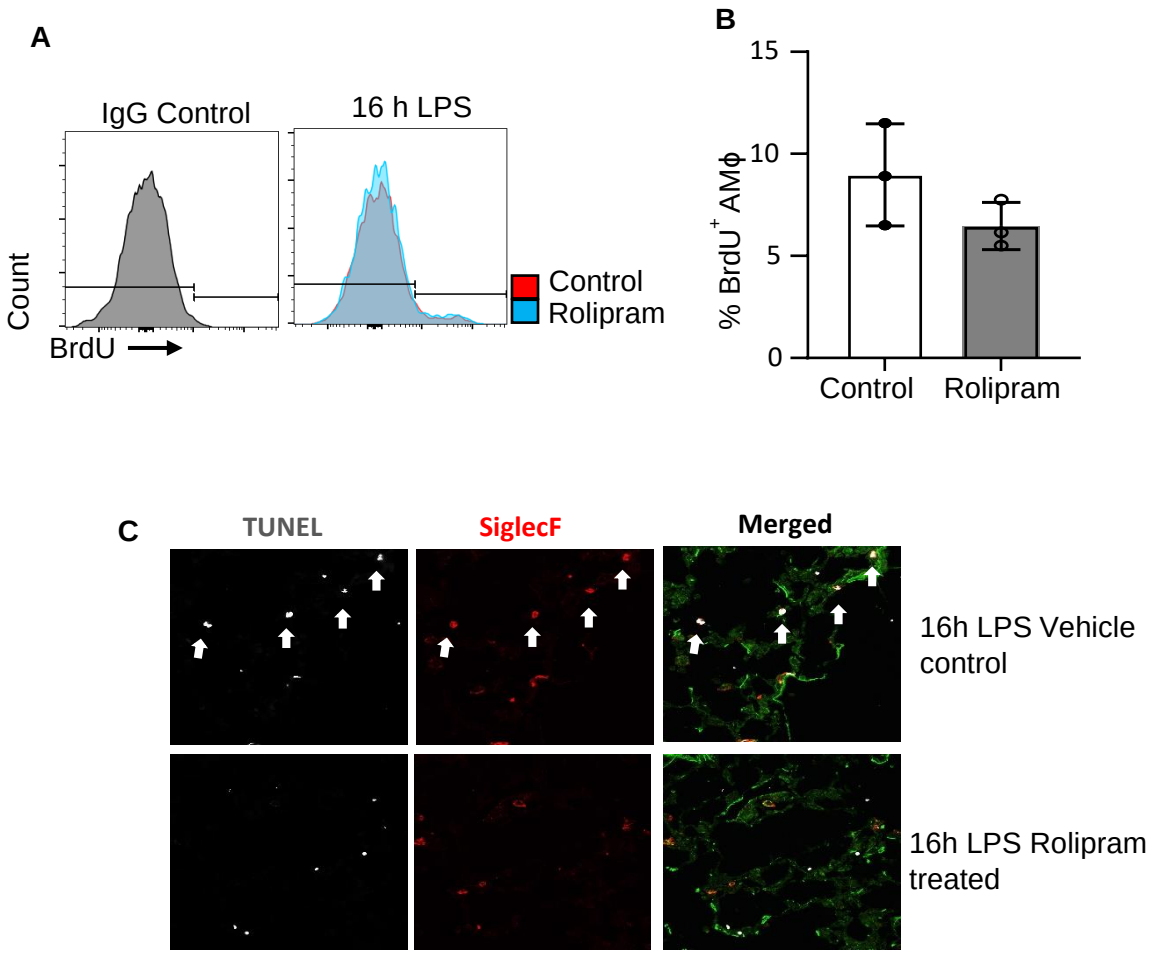

Figure 20. Increase in alveolar macrophage number is not due to proliferation but is impacted by overall cell survival. Histograms (A) shows $BrdU^+$ AMϕ in control or rolipram administered mice to show the proportion of proliferating cells (n=3). **B)** LysM-GFP mice were injected with BrdU 2 h after LPS inhalation. Lung cells were then stained with labeled anti-BrdU antibody and BrdU incorporation was determined in AMϕ ($GFP^+/Ly6g^-/CD64^+/SiglecF^+$) at 16 h using FACS analysis. **C)** Representtiave histological staining of lung sections taken from 16 h LPS exposed LysM-GFP mice treated with rolipram or vehicle, staining for TUNEL and SiglecF.

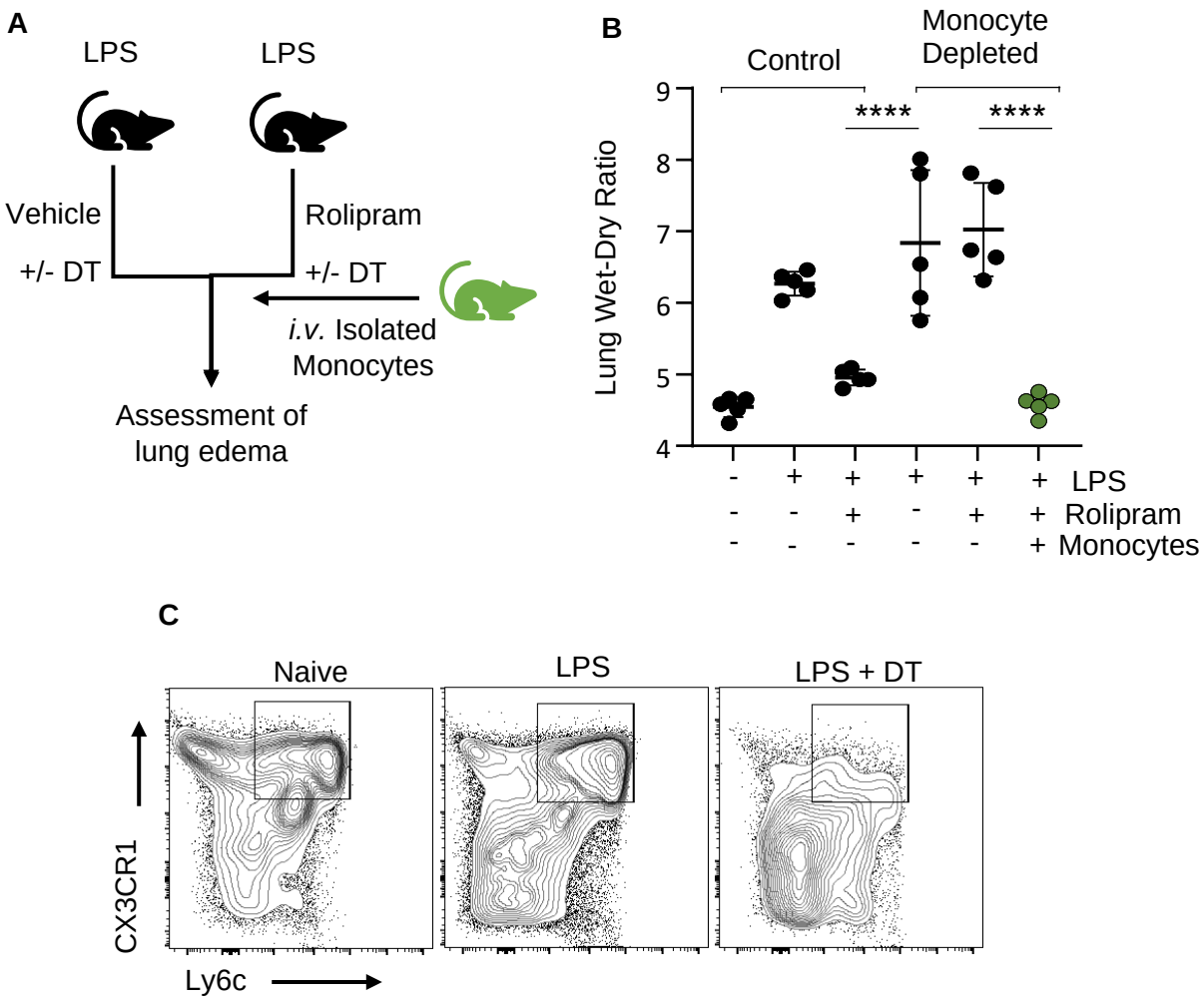

Fig 21. Monocytes are required for the injury restoring effects of rolipram. A) Schematic of rolipram treatment in CD11b-DTR mice. CD11b-DTR mice were expose to LPS as above. After 2h, mice received DT (25 ng/g of mouse *i.p.*). Simultaneously mice were injected with $CD11b^{+}$ monocytes harvested from LysM-GFP mouse bone marrow *i.v.* along with rolipram as above. Lung edema was assessed at 16 h. **B)** Lung edema determined by measuring lung wet-to-dry lung weight ratio. **C)** Representative FACS of $CD45^{+}/Ly6g^{-}/CD62L^{-}/CD11b^{+}/CX3CR1^{+}/Ly6c^{+}$ cells in CD11b-DTR mouse lungs at 16 h with and without DT injection showing depletion of monocytes by DT. Data are shown as means ±SD and represented as ***P < 0.001, and ****P<0.0001 to denote significant difference between treatment and vehicle control groups at the same timepoint.

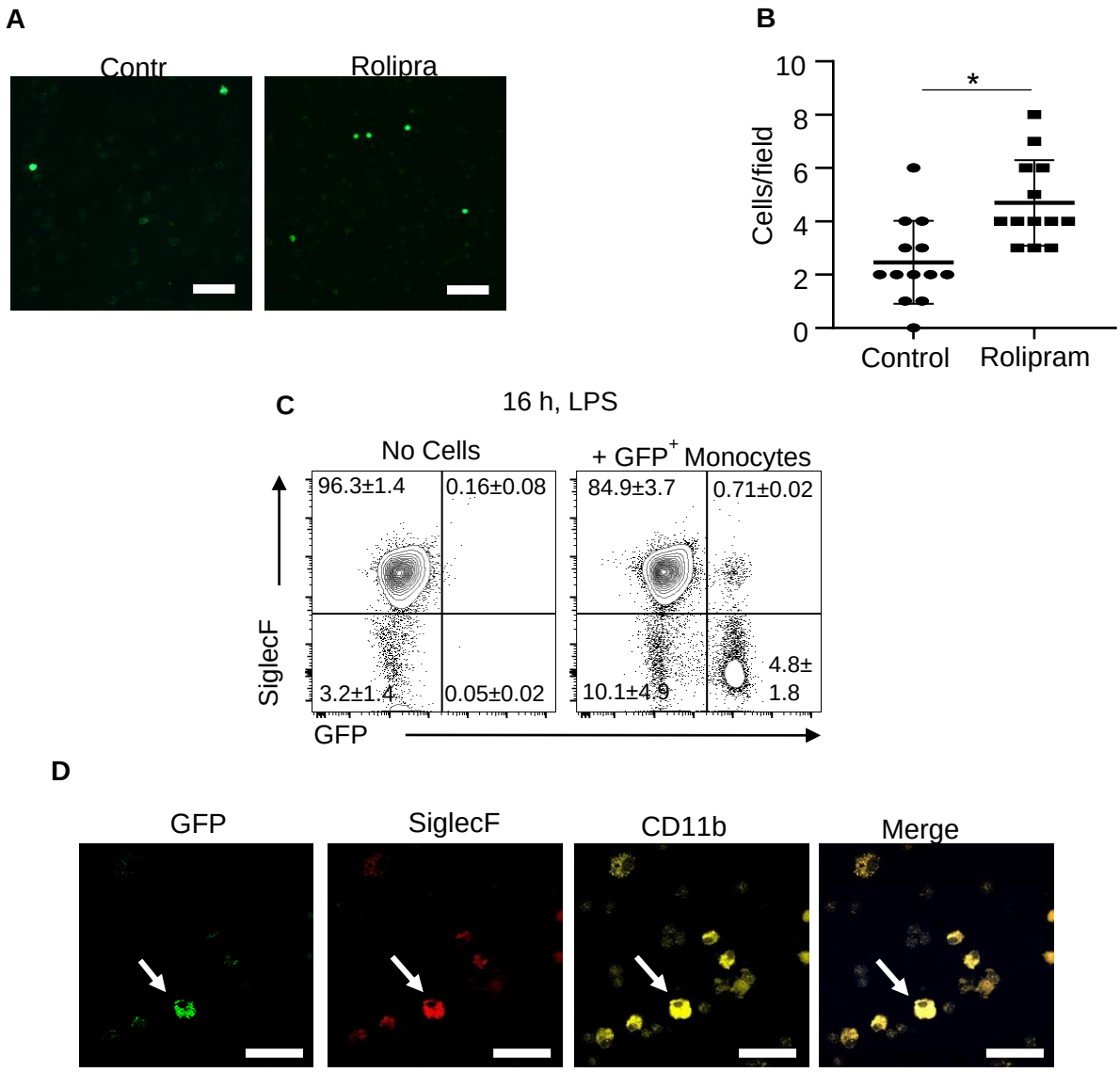

Fig 22. Monocytes are recruited into the airspace by rolipram and take on an alveolar macrophage phenotype. A-B) Epi-fluorescent images of BAL cells from CD11b^{dep} mice receiving either rolipram or vehicle treatment and LysM-GFP bone marrow monocytes. Plot in G shows number of GFP^{+} cells per field. Cells were counted in 15 fields from three independent experiments. Scale bar, 200µm. **C)** FACS dot plot of CD45^{+}/CD64^{+} BAL cells isolated after 16 h from CD11b-DTR mice receiving LPS and DT, with and without *i.v*. LysM-GFP^{+} monocytes. FACS dot plots are representative of 3 independent experiments. **D)** BAL cells obtained from monocyte depleted mice following PBS or adoptive transfer of LysM-GFP monocytes were stained with SiglecF and CD11b antibodies to confirm AMϕ phenotype (merge yellow). A representative image is shown from experiments that were performed multiple times. Scale bar, 50 µm. Data are shown as means ±SD and represented as ***P < 0.001, and ****P<0.0001 to denote significant difference between treatment and vehicle control groups at the same timepoint.

C. Specific Aim 3: Determine whether CREB plays a role in alveolar macrophage reparative phenotype in vivo

Results

Myeloid specific deletion of CREB impairs lung homeostasis

Mice which lacked the CREB gene in macrophages and monocytes ($CREB^{Mye-/-}$) were generated by breeding a LysM-Cre strain with a strain possessing flox site alleles around the 9th axon of the CREB gene. Deletion was confirmed using RT-QPCR of BMDMs **(Fig 23A)**. Flox mice without a Cre gene were used as controls ($CREB^{fl/fl}$) Examination of lung fluid homeostasis was assessed using lung wet-to-dry ratio and EBAE. By both measures, $CREB^{Mye-/-}$ mice exhibited greater vascular permeability in the basal condition **(Fig 23C-D)**. We then measured cytokine levels in the alveolar fluid in the basal state **(Fig 24A-D)**. The AM identity inducing cytokines GM-CSF and TGF-β did not differ between genotypes, nor was IL-6 high in $CREB^{Mye-/-}$ mice. But the homeostatic cytokine IL-10 was significantly lower in $CREB^{Mye-/-}$ mice. Flow analysis of $CREB^{Mye-/-}$ mice reveals that AMϕ represent a smaller proportion of the total macrophage pool under basal conditions, without LPS injury **(Fig 25A)**. Confocal imaging of lung sections also shows fewer $SiglecF^{+}$ cells **(Fig 25B)**.

Loss of CREB results in decreased expression of pyruvate dehydrogenase kinase

A link between IL-10 and metabolic shifting correlating with macrophage homeostatic function has been suggested[212]. Examination of metabolic genes differentially regulated by loss of CREB uncovered pyruvate dehydrogenase kinase 4 (PDK4) as significantly less expressed in $CREB^{Mye-/-}$ mice **(Fig 26A)**. Suggestively, PDK1 and PDK3 were not altered by CREB loss **(Fig 26B).** Pyruvate Dehydrogenase (PDH) is inhibited by phosphorylation by PDK4[194]. To assess

whether loss of PDK4 expression correlated with a change in PDH activity, conversion of pyruvate to acetyl-CoA was assessed in $CREB^{Mye-/-}$ macrophages. Loss of CREB did indeed correlate with increased PDH activity BMDM **(Fig 27A).** Histological examination of BAL isolated AMs revealed decreased phosphorylation of the E3 subunit of PDH, the phosphorylation target of PDK4 **(Fig 27C)**. bioinformatic analysis of the PDK4 promotor shows four CREB binding sites within 2kb of the transcription start site **(Fig 28A)**. transfection of $CREB^{Mye-/-}$ and $CREB^{fl/fl}$ BMDM with a PDK4 luciferase promotor showed that cells without CREB expressed significantly less reporter signal than $CREB^{fl/fl}$ control cells **(Fig28B)**.

Loss of CREB in macrophages compromises lung homeostasis after lung injury.

While in $CREB^{Mye-/-}$ mice exhibited a defect in lung homeostasis we next assessed if this defect impaired recovery from inhaled LPS induced ALI. Examination of lung wet-to-dry ratio and EBAE show that peak injury (4 h) was equal in the case of edema formation **(Fig 29A)**, though vascular permeability was greater in in $CREB^{Mye-/-}$ **(Fig 29B).** Interestingly, in $CREB^{Mye-/-}$ mice were able to partially resolve lung injury by 24 h but resolved to the higher baseline seen in the basal condition **(Fig 29A-B).** Rolipram administration was unable to resolve lung injury at 16h in in $CREB^{Mye-/-}$ **(Fig.30A)**. Flow analysis indicates that after LPS challenge, CREB deficient AMϕ decrease as a proportion of total macrophages **(Fig 30B).** As well, rolipram does not increase the total percentage of AM in $CREB^{Mye-/-}$ as in control mice.

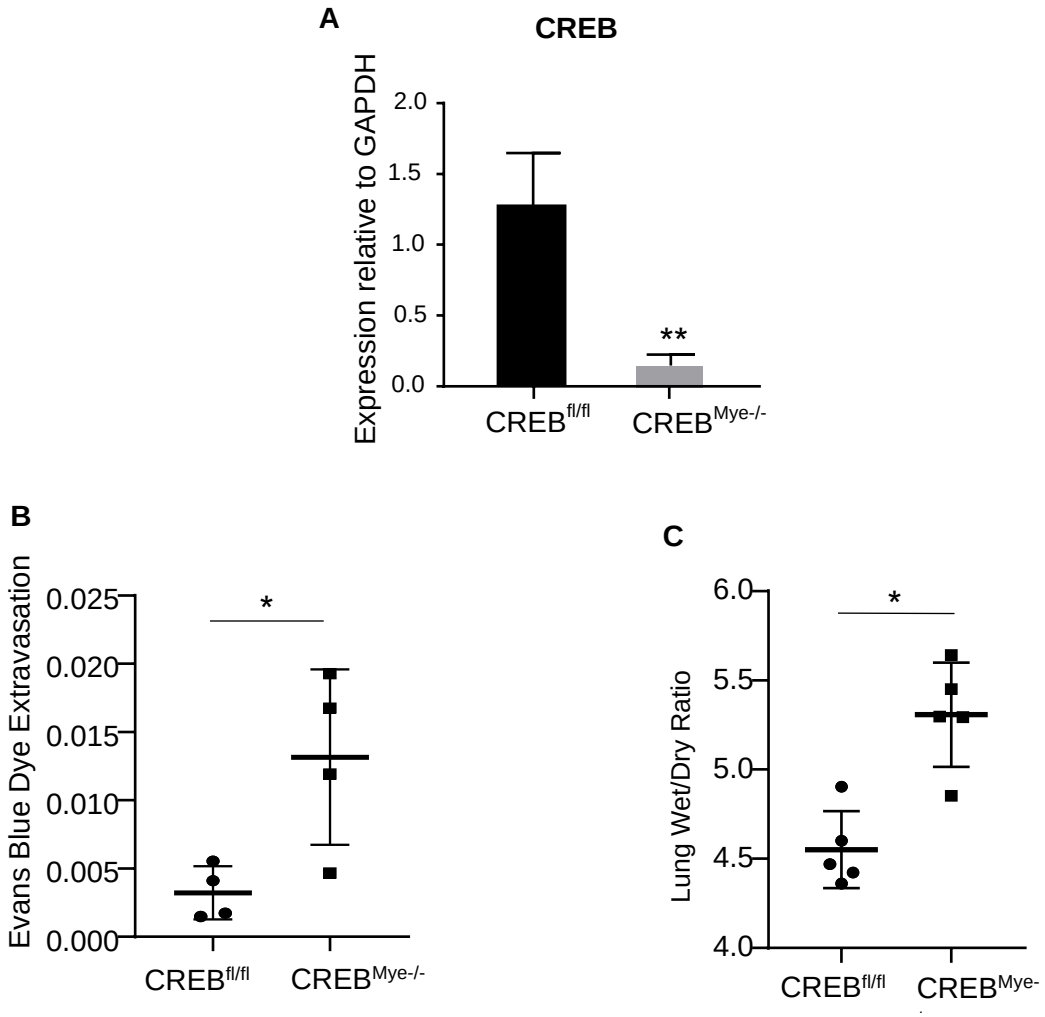

Figure 23. myeloid specific deletion of CREB results in impairment of lung vascular barrier homeostasis. A) Measurement of CREB expression in $CREB^{Mye-/-}$ and $CREB^{fl/fl}$ BMDM, (n=5). **B-C)** Lung vascular inflammatory injury was determined in $CREB^{Mye-/-}$ and $CREB^{fl/fl}$ by measuring lung wet-dry ratio (B) and albumin influx (C). Data are shown as means ±SD and represented as *P < 0.05, **P < 0.01, to denote significant difference between genotypes

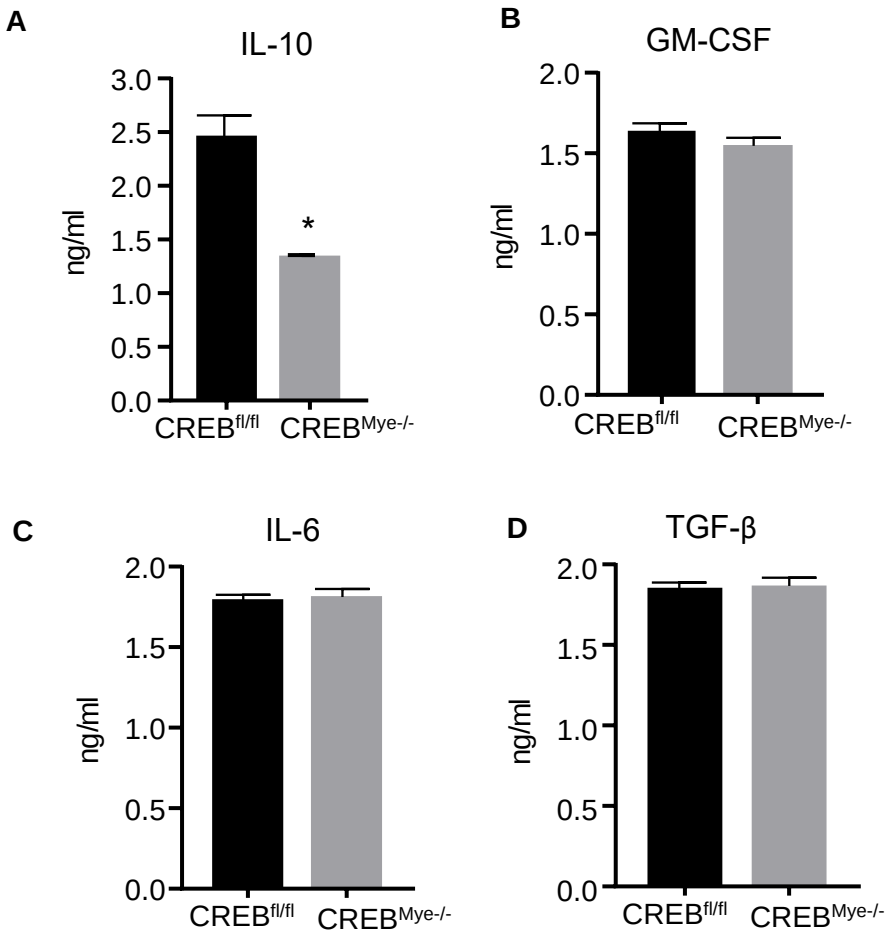

Figure 24. Myeloid specific deletion of CREB results decreased production of IL-10. A-D) Measurement of cytokines in BAL fluid taken from $CREB^{Mye-/-}$ and $CREB^{fl/fl}$ control mice using ELISA, (n=3). Data are shown as means ±SD and represented as *P < 0.05 to denote significant difference between genotypes.

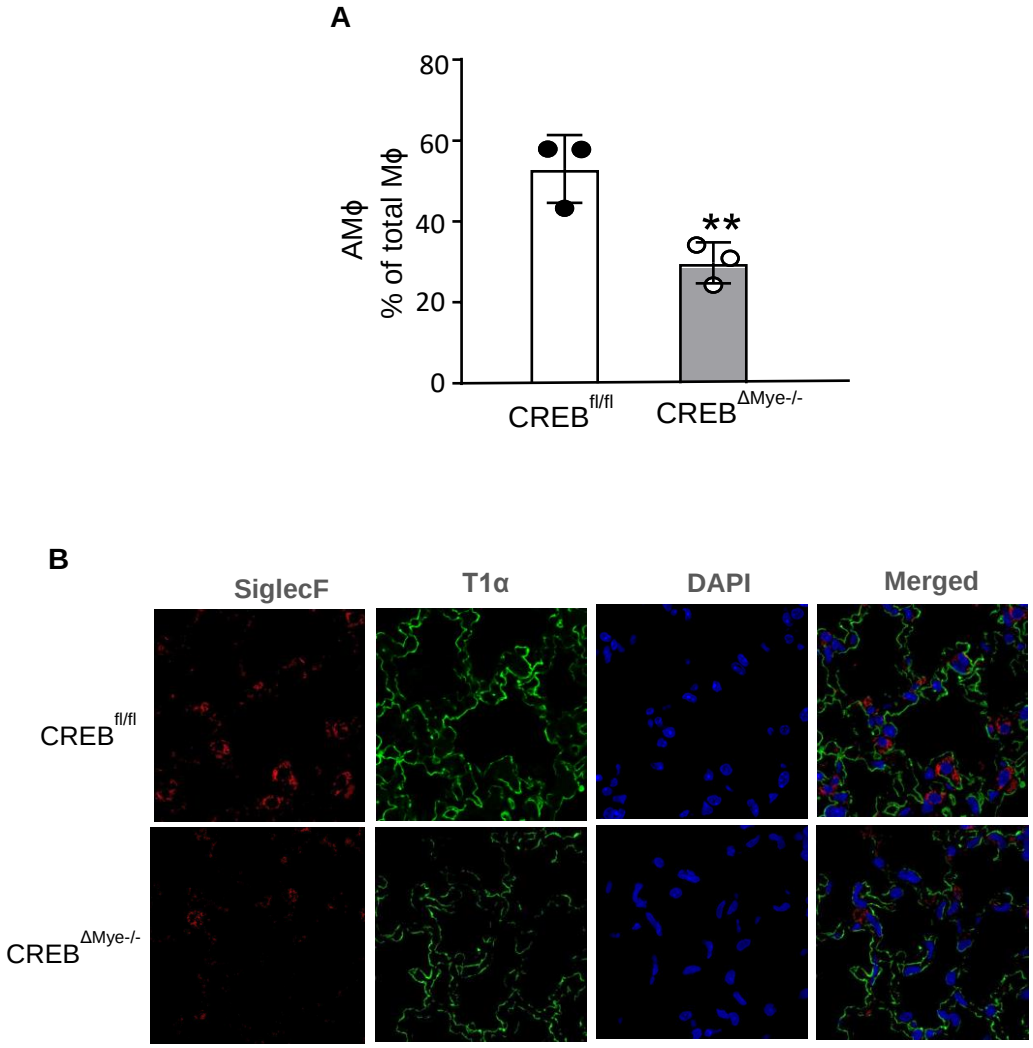

Figure 25. Loss of CREB decreases proportion of AMϕ under basal conditions. A) Percentage of $CD64^{+}/Ly6g^{-}/CD45^{+}$ macrophages which are $SiglecF^{+}$. **B)** Representative confocal image of lungs sections from with $CREB^{Mye-/-}$ and $CREB^{fl/fl}$ mice stained with the AMϕ marker SiglecF and the epithelial marker T1α. Data are shown as means ±SD and represented as $^{**}P < 0.01$.

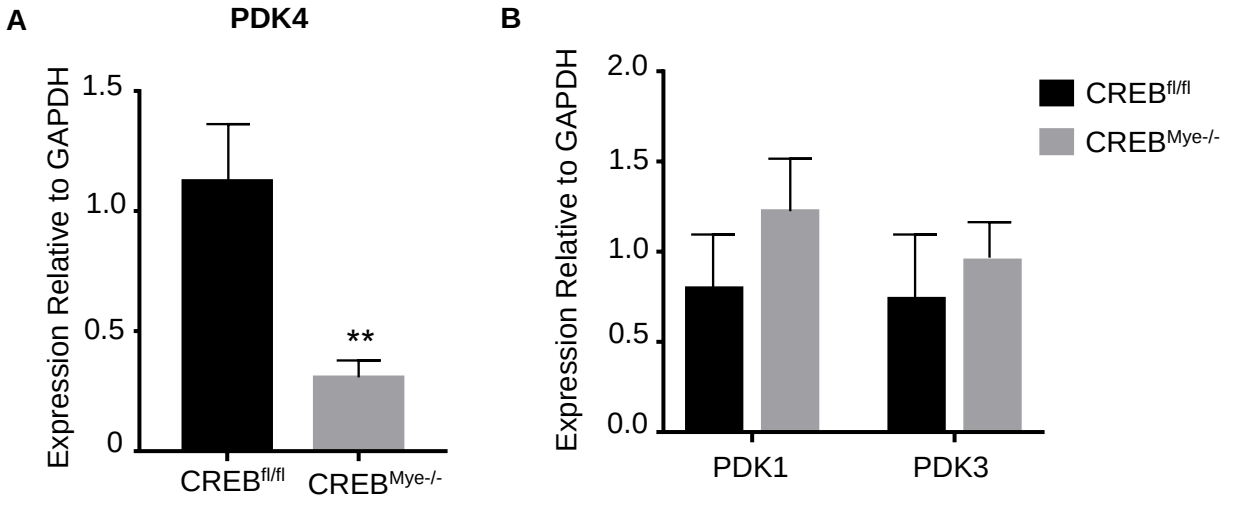

Figure 26. Loss of CREB results in decreased expression of pyruvate dehydrogenase kinase 4. RT-QPCR measurement of gene expression in $CREB^{Mye-/-}$ and $CREB^{fl/fl}$ control BMDM for (**A) PDK4 (B)** PDK1 an PDK3. Data are shown as means ±SD and represented as **P < 0.01 to denote significant difference between genotypes

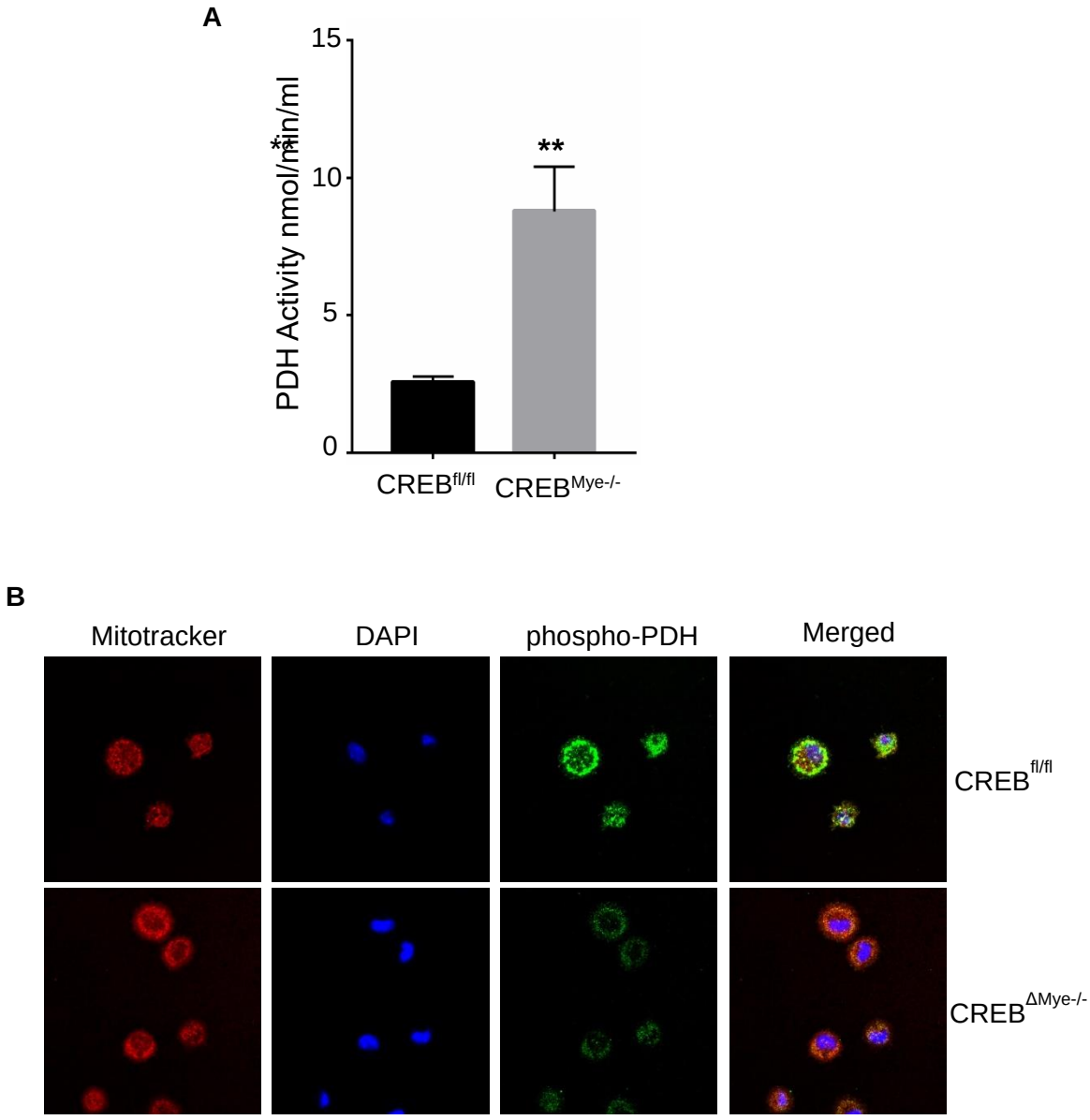

Figure 27. Loss of PDK4 expression results in increased activation of pyruvate dehydrogenase. A-B) Measurement of PDH activity in $CREB^{Mye-/-}$ and $CREB^{fl/fl}$ BMDMs (n=3). **B)** AMϕ isolated from $CREB^{Mye-/-}$ and $CREB^{fl/fl}$ mice by plating BAL fluid. Cells stained with mitotracker and phospho-PDH E3 subunit. Data are shown as means ±SD and represented as **P < 0.01, to denote significant difference between genotypes

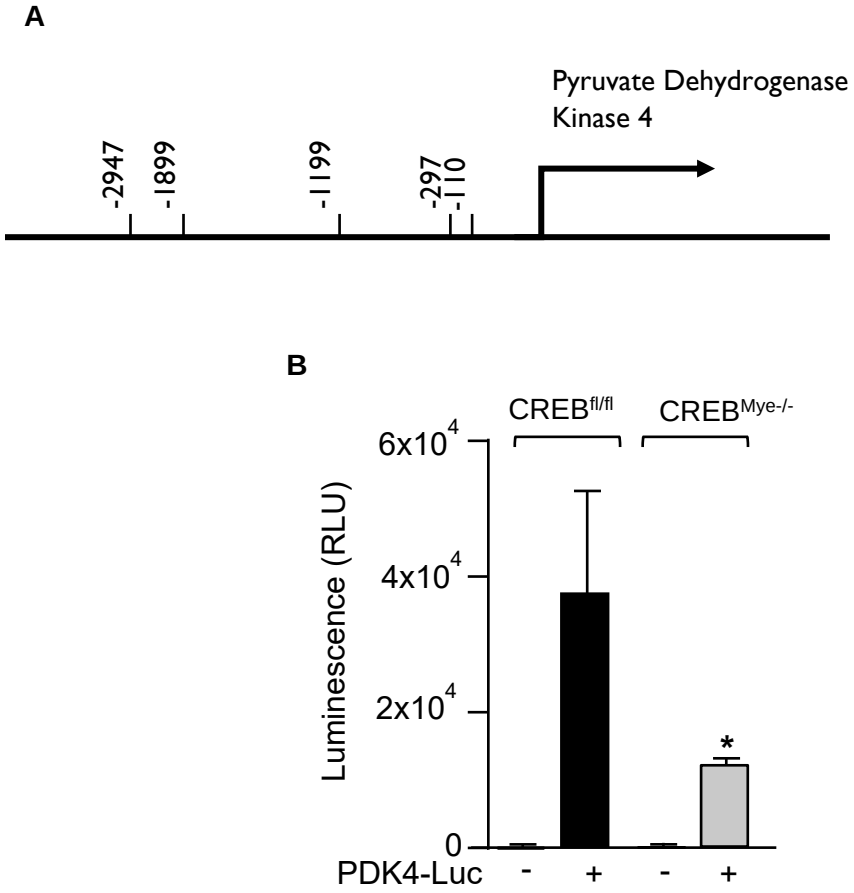

Figure 28. CREB regulates expression of PDK4. A) Representation of mouse PDE4b promoter region with four CREB binding sites. Arrow indicate transcription start sites. **B)** $CREB^{Mye-/-}$ and $CREB^{fl/fl}$ BMDM were transfected with PDK4 promoter luciferase construct. After 48h, luminescence was measured. Data are shown as means ±SD and represented as *P < 0.05, to denote significant difference between genotypes

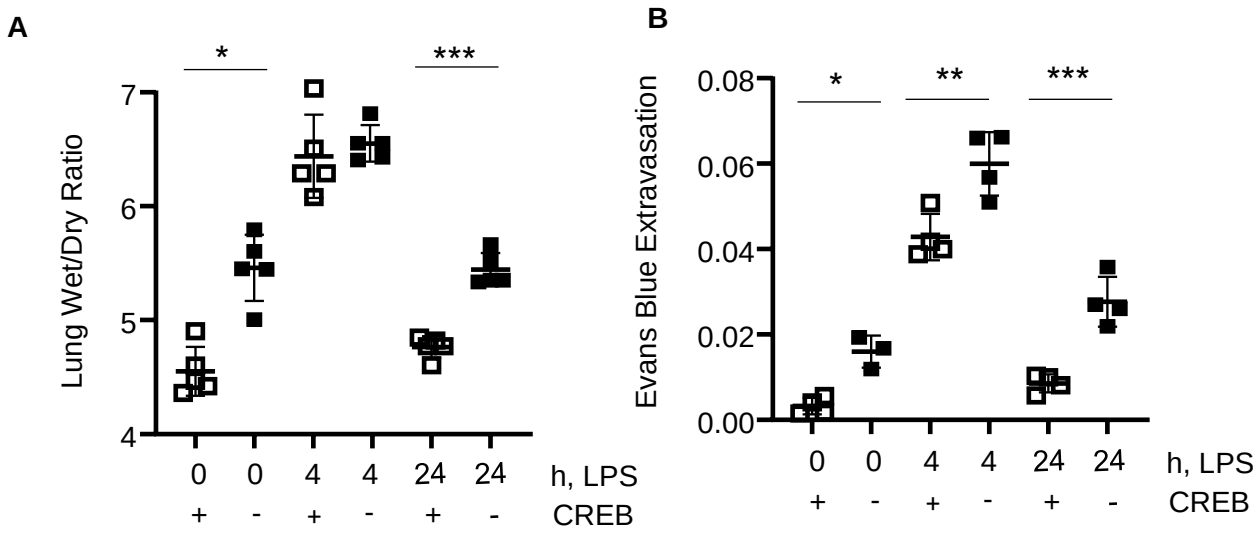

Figure 29. Inhibition of PDE4 sustains higher percentage of alveolar macrophages in the lungs after peak of injury. A-B) $CREB^{Mye-/-}$ and $CREB^{fl/fl}$ mice were exposed to nebulized LPS (1 mg/ml) for 50 min. Lung vascular inflammatory injury was determined by measuring lung wet-dry ratio (A) and albumin influx (B) (n=4-5). Data are shown as means ±SD and represented as *P < 0.05 to denote significant difference between genotypes

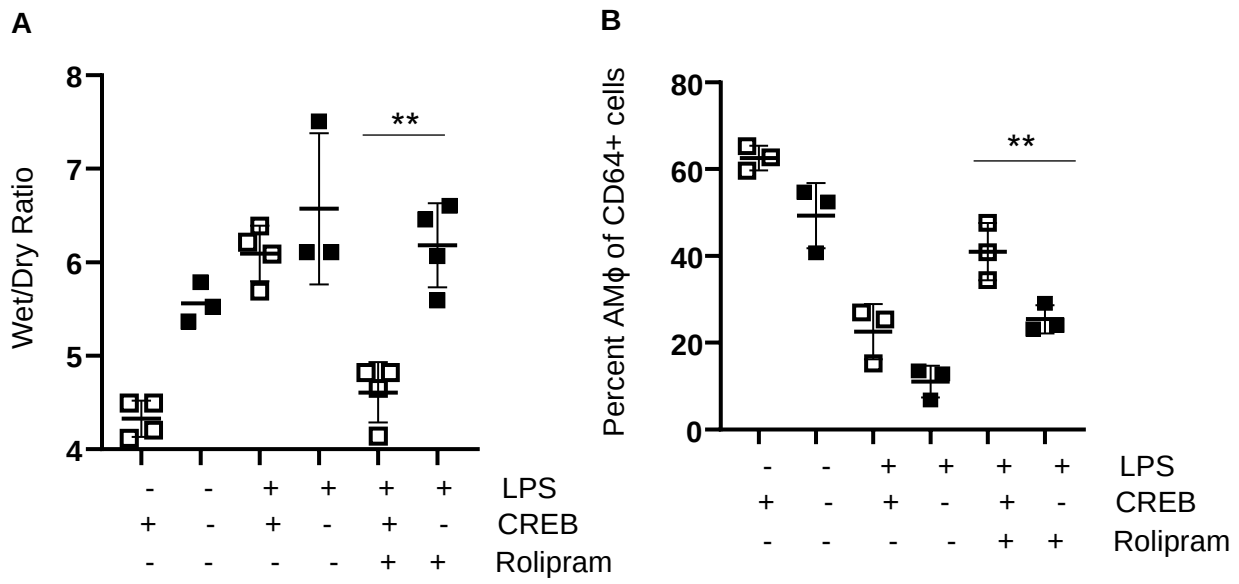

Figure 30. CREB is require for the injury reparative effects of rolipram and generation of alveolar macrophages. $CREB^{Mye-/-}$ and $CREB^{fl/fl}$ mice were exposed to nebulized LPS and treated with either rolipram of vehicle. lung injury and alveolar macrophage proportion was measured at 16h post injury. **A)** Lung vascular inflammatory injury was determined by measuring lung wet-dry ratio (n=3-4). **B)** Percentage of AM ($CD45^{+}/Ly6g^{-}/CD64^{+}/SiglecF^{+}$) as a proportion of the total lung macrophage pool (n=3). Data are shown as means ±SD and represented as **P < 0.01 to denote significant difference between genotypes

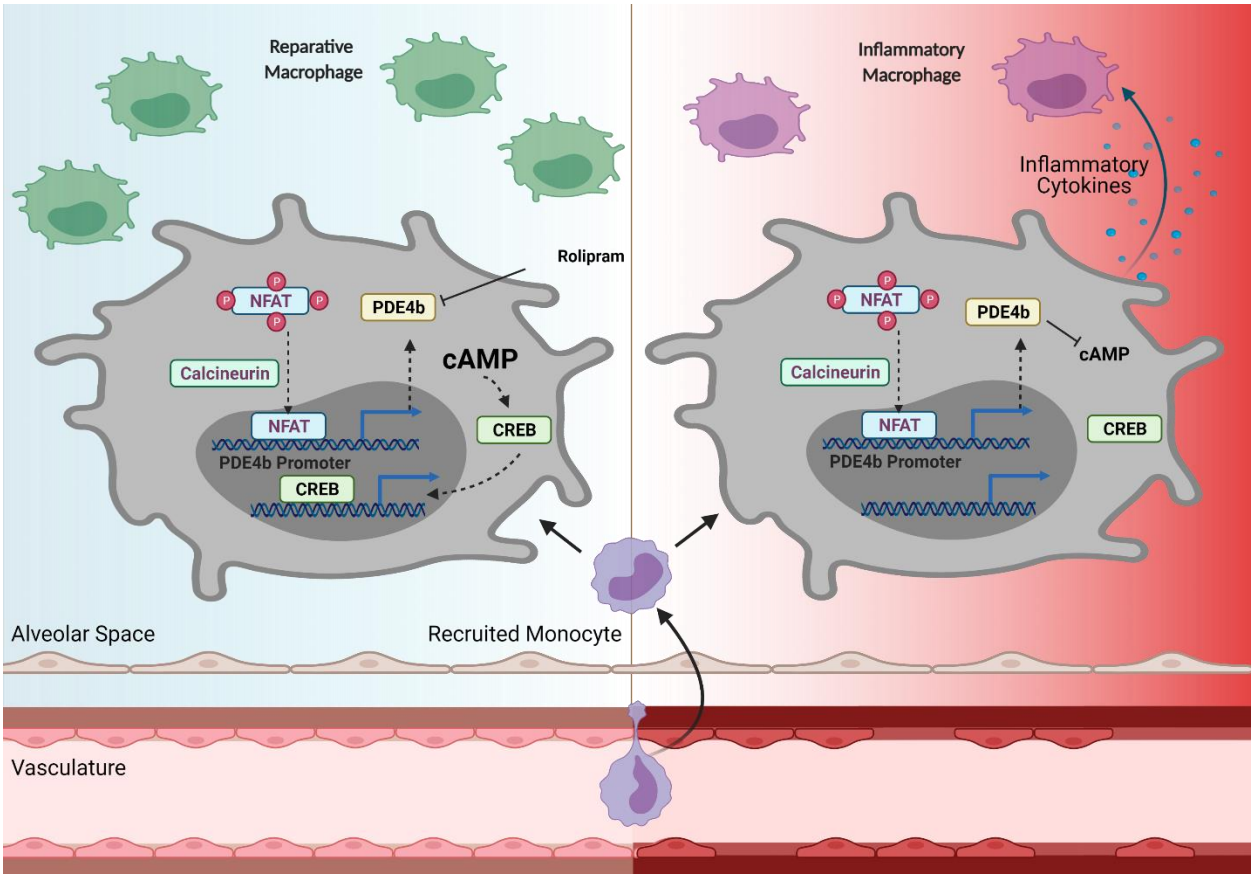

Figure 31. Model of cAMP mediated programming of alveolar macrophage phenotype. Monocytes are recruited into the alveolar space during acute lung injury and differentiates into macrophage. Activation of NFAT induces expression of PDE4b to dampen cAMP signaling to perpetuate inflammatory signaling. Inhibition of PDE4b results in amplification of cAMP signaling, which activates CREB. Transcription of CREB-regulated genes dampens inflammatory signaling and results in programming existing alveolar macrophages to a reparative phenotype.

Discussion

We have demonstrated a key role of PDE4b activity in regulating the *in vivo* programming of Mo-Mϕ into reparative AMϕ through suppression of cAMP-CREB signaling. The targeting of PDE4b activity was able to rapidly program immunosuppressive and reparative AMϕ capable of repairing lung damage endogenously or after adoptive transfer.

These experiments have illustrated four aspects of AMϕ biology in the context of LPS induced acute lung injury. First, PDE4b was identified as the predominant cAMP regulating enzyme expressed in lung resident macrophages and was shown to be upregulated in macrophages in response to LPS challenge via the Ca^{2+}-responsive transcription factor NFATc2. This increase in PDE4b expression was associated with the beginning of a shift in the AMϕ population towards a $CD11b^{+}$ inflammatory phenotype. Secondly, cAMP rose in AMϕ in response to LPS during peak injury, but when PDE4 was inhibited cAMP levels were further enhanced compared to vehicle controls. This indicates that PDE4, principally PDE4b, is responsible for restraining cAMP levels during the acute phase of inflammatory injury. This increase in cAMP signaling led to accelerated resolution of lung injury mediated by a population of reparative AMϕ. Thirdly, this accelerated resolution was contingent on the recruitment of monocytes from the blood into the lungs, whereafter they exhibited a more AMϕ-like signature. Fourth, the injury resolving effects of rolipram was also contingent on CREB expression in myeloid cells.

In the naïve lung, AMϕ are anti-inflammatory and exhibit various phenotypic and genetic markers that are distinct from those of IMϕ or Mo-Mϕ. However, evidence indicates that during lung injury such a distinction between AMϕ and other lung macrophages not always achievable because monocyte-derived AMϕ, resident AMϕ, and Mo-Mϕ lie along a phenotypic continuum with complementary functions and phenotypes[36,95]. In this context, we showed that the basally

CD11b^{-} AMϕ become inflammatory and acquire a CD11b^{+} signature, leading to increased lung vascular injury, as described in several other studies[95,213,214]. However, we also showed that a significant pool of AMϕ remain CD11b^{+} despite the return of lung fluid-homeostasis to the basal state. This raises questions regarding the generally, if tentatively, accepted immunophenotyping of AMϕ[95]. The inflammatory state of macrophages is measured by cytokine expression profile because surface marker expression may not vary between states, but AMϕ are unique in their change in CD11b expression after inflammatory activation. Studies have shown a continuum of CD11b expression on AMϕ of patients suffering from COPD[215], others show CD11b^{+} AMϕ involved in granuloma formation. One possibility may be that CD11b^{+} AMϕ surface expression need not be interpreted as definitively "inflammatory", but rather an indication of prior AMϕ activation. Another possibility may be that the residual subpopulation of CD11b^{lo} AMϕ present during injury is sufficient to restore the anti-inflammatory lung niche despite CD11b^{hi} AMϕ.

To resolve this conundrum, we focused on mechanisms regulating the AMϕ pro-resolution phenotype. Our lab has recently shown that cAMP is an important second messenger that dampens the production of pro-inflammatory cytokines by macrophages[178]. Additionally, the elevation of cAMP has been shown to suppress several lung diseases ranging from asthma to lung injury[168,171,172]. Interestingly, the list of diseases treated by PDE4 inhibitors includes those with pathologies mediated by exaggerated inflammatory signaling as well as inappropriate wound healing, an anti-inflammatory process, in the case of fibrosis. This suggests that PDE4 inhibitors do not function by expressly inducing anti-inflammatory signaling but instead by suppressing immune cell activation.

Our RNAseq data show that PDE4b is an abundantly expressed cAMP regulating gene in lung macrophages even under basal conditions, indicating that cAMP levels are finely tuned for

host-defense functions that arise during normal breathing[216]. We also showed that PDE4b expression increased during injury, but then declined to below the basal level during the resolution phase. In line with these results, while LPS increased cAMP levels in AMϕ by a factor of 2, inhibition of PDE4b increased the cAMP level by a factor of ~5. However, this 5-fold increase in cAMP level did not alter the development of lung injury at 4 h, but rather induced rapid resolution of lung injury at 16 h. Resolution of lung injury was accompanied by marked attenuation of neutrophil influx into the airspace and cytokine generation by AMϕ. Interestingly, in both rolipram and control cells, cAMP levels were both equal to baseline at 16 h. This suggests that increased cAMP signaling potentiates the accelerated resolution of injury without being continually required to maintain.

Importantly, we showed that inhibition of PDE4b subverts the AMϕ signature shift from $CD11b^-$ to $CD11b^+$. Much like the findings reported here, several studies have shown that PDE4b is expressed in immune cells such as eosinophils, monocytes, and neutrophils, and inhibition of PDE4 suppresses lung injury, COPD, and airway hyper-responsiveness[168,171]. However, we have directly shown a novel role of PDE4b in the direct control of AMϕ lineage and functionality *in vivo*. We demonstrate that PDE4 expression and thus activity controls the conversion AMϕ from their anti-inflammatory $CD11b^-$ lineage to a $CD11b^+$ inflammatory lineage, whereby inhibition of PDE4 by rolipram leads to resolution of lung injury and inflammation. This finding is significant due to studies of AMϕ mostly being done *ex vivo* and tend to focus on direct cytokine stimulation as the basis of anti-inflammatory function. Our model of rolipram treatment also differs from many existing studies because we administer intratracheally instead of *i.v.*, bypassing the vasculature and directly exposing macrophages in the alveolar space to the drug.

This leads to the question of how LPS increases PDE4b expression to drive AMϕ into an inflammatory state, thus leading to lung injury. It is known that LPS induces pro-inflammatory cytokine generation through NFκB via TLR4[178,217]. However, our studies showed that inhibition of NFAT using a small molecule inhibitor suppressed PDE4b expression. Further, using an oligonucleotide ChIP assay as well as PDE4b promoter-luciferase activity, we showed that the binding of NFAT to the PDE4b promoter was required for LPS induction of PDE4b transcription. NFAT is a Ca^{2+}-dependent transcription factor well known to regulate T-cell function[218]. However, our lab's previous work shows that LPS activates thrombin generation in Mϕ which then induces Ca^{2+} entry through the TRPV4 channel to promote NFAT activity. Activated NFAT promotes NFκB binding to cytokine promoters leading to increased inflammatory cytokine generation and thereby impairs resolution of inflammation[178]. In the current study, we showed that PDE4b inhibition at the time of peak lung injury augmented cAMP levels, which then suppressed AMϕ inflammatory function as measured by cytokine mRNA levels, phagocytic activity, and injury resolution capacity. LPS induction of NFAT activity and thereby PDE4b transcription in AMϕ could explain the observed alteration in cAMP levels in AMϕ and the increase in inflammatory signaling. These studies, taken together, illustrate that activation of the NFAT-PDE4b circuit 'tunes' the AMϕ inflammatory response to LPS. Our conclusion regarding the importance of PDE4b over other PDE4 family members is supported by research showing that PDE4b knockout mice were protected from LPS induced TNF-α release, while PDE4a and PDE4d knockout mice were not[219].

Our data also show that rolipram treatment leads to an increase in the total number of AMϕ. It is known that during acute lung injury, the resident AMϕ die off through induced programmed cell death during lung injury[59,64]. One notion is that AMϕ can proliferate to restore AMϕ number

during specific inflammatory conditions, but the evidence in support of this idea is limited[94]. Alternatively, new AMϕ can be generated by the differentiation of newly arrived monocytes in the lung[98]. We showed that rolipram did not increase AMϕ proliferation compared to control conditions, thus ruling out the proliferation of AMϕ as the basis for the restoration of AMϕ number after injury. CD11b-DTR mice allowed us to demonstrate that recruited monocytes were responsible for generating reparative AMϕ. PDE4b inhibition by rolipram did not resolve lung injury in monocyte depleted mice (CD11b-DTR mice post DT challenge). However, adoptive transfer of bone marrow monocytes back into $CD11b^{dep}$ mice with rolipram treatment resolved lung injury. Moreover, using GFP^+ monocytes we were able to track newly recruited and differentiated monocyte-derived AMϕ in the airspace. Studies show that recruited monocytes can acquire an inflammatory AMϕ lineage in the lung[211]. However, we showed that PDE4b inhibition programmed monocytes to acquire anti-inflammatory AMϕ lineage thus demonstrating a way to induce reparative AMϕ generation after injury. We inferred from the observation that rolipram instructed AMϕ were more phagocytic that PDE4b inhibition not only mobilizes reparative AMϕ during injury but also instructs these AMϕ to retain their capacity to remove apoptotic neutrophils and thereby release anti-inflammatory mediators[81].

While we showed that monocytes generated reparative AMϕ, our studies were limited in defining whether $CD11b^+$ AMϕ were derived only from monocytes recruited into the airspace or if resident $CD11b^-$ AMϕ switched on CD11b expression. In this context, Gpr84, a free fatty acid receptor has been implicated in transitioning $CD11b^-$ AMϕ to $CD11b^+$ AMϕ[93]. Whether PDE4b regulates the AMϕ inflammatory lineage via Gpr84 activity needs to be clarified. Given that the rolipram-educated AMϕ pool has a greater proportion of $CD11b^-$ cells and can resolve lung injury in injured mice it is possible that $CD11b^+$ monocyte-derived AMϕ, which would be $CD11b^+$,

inhibit the conversion of CD11b-resident AMϕ to $CD11b^{+}$ by affecting their inflammatory activation. Regardless, PDE4b inhibition affects multiple cell types in the lungs[220]. One possibility is that the observed anti-inflammatory AMϕ phenotype observed after PDE4b inhibition may be partly the result of suppression of PDE4b activity in other cell types. However, adoptive transfer of rolipram-treated AMϕ but not vehicle-treated AMϕ repaired lung damage in LPS-exposed mice.

The molecular basis behind cAMP activation of reparative AMϕ generation during lung injury is not clear. cAMP is known to activate protein kinase A (PKA)[103]. PKA phosphorylates CREB, leading to its nuclear transport and transcriptional activity. Thus, we asked whether cAMP activated CREB which then programed the subsequent differentiation of monocytes into reparative AMϕ. This notion is supported by studies in which CREB is shown to induce macrophage polarization into the anti-inflammatory lineage *in vitro*[212,221,222]. We investigated the role of CREB in lung resident macrophages using LysM induced CREB knockout mice. Critically, we found that mice which lacked CREB in myeloid cells were unresponsive to rolipram, indicating not only that CREB mediated the AMϕ reparative phenotype but also that the epithelial and endothelial compartments are not chiefly responsible for the injury resolving effects of PDE4 inhibition in this model.

We also found that $CREB^{Mye-/-}$ mice exhibited a defect in baseline lung fluid homeostasis. While LPS inhalation did lead to increased edema and vascular permeability $CREB^{Mye-/-}$ mice lungs' levels of injury returned to their higher baseline. Suggesting the fault in CREB knockout mice is not in resolution, but homeostasis. Examination of $CREB^{Mye-/-}$ macrophages populations also suggests a defect in the generation of AMϕ at baseline and after injury. Recent research into the role of metabolism in maintaining macrophage tolerogenic function led us to investigate the role of CREB in metabolic regulation. While most other macrophage populations switch to

glycolysis after inflammatory activation[223], AMϕ do not rely on glycolysis to initiate LPS stimulated inflammatory signaling[224]. Analysis of metabolic regulatory genes showed that $CREB^{Mye-/-}$ macrophages lacked expression of PDK4. Direct regulation of PDK4 gene expression by CREB was confirmed using a luciferase assay. PDK4 is a negative regulator of the PDH, the enzyme complex which converts the end-product of glycolysis, pyruvate, into the first step in the TCA cycle, acetyl-CoA. Our measurements showed that macrophages that lacked CREB had far greater PDH activity and acetyl-CoA generation. As PDH has been shown to localize to the nucleus where its acetyl-CoA product is used as a substrate for acetylation of histones, lack of PDK4 may lead to changes in epigenetic regulation, thereby affecting macrophage function. Preliminary experiments show that $CREB^{Mye-/-}$ may have a defect in the generation of normal AMϕ after LPS exposure and the retention of AMϕ after LPS treatment.

In summary, this work has identified NFAT-PDE4b signaling in AMϕ as a key mechanism orchestrating extremely tight control of cAMP levels in AMϕ and their anti-inflammatory function. We have shown that LPS activates PDE4b transcription via NFAT, leading to the generation of inflammatory AMϕ, neutrophil influx, and inflammatory lung injury. Inhibition of PDE4b, therefore, increases cAMP, which educates recruited monocytes into reparative AMϕ through a CREB dependent transcriptional program **(Fig 31)**. These reparative AMϕ are able to resolve lung vascular inflammatory injury. Because of the pivotal role of PDE4b in monocyte differentiation, we suggest that inhibition of PDE4b in AMϕ is a potentially useful approach for the rapid generation of anti-inflammatory AMϕ that subsequently prevent or resolve ALI.

The efficacy of drug therapy to treat inflammatory conditions has been long established. But matters of dosage, side effects, and counterindications make such therapies challenging. Cell-based therapies are an emerging field of medicine whereby cells taken from the patient may be

transplanted or introduced into damaged tissues to treat disease. This work highlights a new direction, in which treated cells can be used to effect positive physiological outcomes, independent of the drug itself. In our study, rolipram-educated resident cells were able to resolve injury in much the same way as drug treatment itself. By understanding how resident macrophage populations transition from an enflamed to a pro-resolving phenotype we can develop easier and more efficient adoptive cell therapies for inflammatory conditions.

Limitations

While this study illustrates that treatment of LPS induced acute lung injury with rolipram leads to an increase in the AMϕ population, further study is needed to characterize the origin of these cells. Enhanced recruitment and differentiation of bloodborne monocytes into AMϕ is likely and suggested by the data. But other explanations include enhanced survival of AMϕ that were resident before injury occurred also contributing to this increased population size. Also, while we show that newly differentiated AMϕ create a niche that can educate existing resident AMϕ to an anti-inflammatory phenotype, what factors or cytokines are released by these monocyte derived AMϕ to create this niche are unknown.

Our studies utilized a fast-resolving LPS-induced acute lung injury model. This model was useful because it allowed us to examine the transition from an inflamed lung to a resolved state. But the results of our study may need to be examined in light of other injury models. Previous studies have shown that rolipram treatment was only partially effective in treating bacterial infection, resulting in reduced lung injury but no decrease in bacterial burden[174]. This result aligns with our work, which further characterizes PDE4 inhibition as being immunomodulatory. While this decreased inflammatory signaling leads to a lessening of tissue injury, it would also counteract the anti-bacterial response, itself an inflammatory process. Thus, the long-term effects of bacterial

burden on rolipram educated AMϕ phenotype remains to be studied. Usage of rolipram in other sterile injury models, such as oxidant damage, may also illustrate similar AMϕ reprogramming by monocyte-derived cells to facilitate enhanced recovery.

Another caveat involves the use of CD11b-DTR mice. In addition to monocytes and macrophages, DT can also deplete other $CD11b^+$ myeloid cells such as neutrophils, IMϕ, and dendritic cells (DC). We have previously used CD11b-DTR mice to deplete both IMϕ and monocytes without affecting neutrophils[98]. Previous studies similarly demonstrated that DT had no effect on neutrophils[33]. However, the effect of DT on $CD11b^+$ dendritic cells remains controversial. While some authors show no alteration in DC after DT injection[96] others have shown partial depletion of DC after DT[225]. Thus, further studies will be required to fully delineate the time course and mechanism of conversion of airspace recruited monocytes/macrophages into AMϕ and the involvement of other lung myeloid populations such as DC and IMϕ in this process.

Future Directions

This project identified PDE4b as the principal PDE4 family member responsible for regulating cAMP signaling in AMϕ exposed to LPS. This has been suggested by existing research but has not been investigated as in our study. The next logical step is to move from a pharmacological model to a genetic model by using a PDE4b specific conditional knockout to differentiate the role of PDE4b in different subpopulations of lung resident macrophage populations and myeloid cell types.

We have shown that recruited monocytes are required for the beneficial effects of rolipram in lung injury. But the recruitment of monocytes that differentiate into AMϕ over the course of lung injury may not fully account for the shift in CD11b expression and increase in AMϕ number

seen in our study. Further experiments are required to trace the lineage of AMϕ over the course of injury to determine if this pro-resolution mixed $CD11b^+$ and $CD11b^-$ AMϕ population actually represents a cluster of subpopulations with different roles and ontogenies. This question can be addressed using single-cell RNA sequencing. By isolating monocyte/macrophages from the alveolar space of injured mice with and without rolipram treatment and determining their RNA signature we may further characterize the anti-inflammatory reprogramming of AMϕ. This would also allow us to focus on the transcriptional signature of those 'anti-inflammatory niche creating' Mo-Mϕ and the resident cells which are reprogrammed to accelerate injury resolution.

Related to this, while we have clearly shown that AMϕ programmed by enhanced cAMP signaling has the potential to dampen lung injury without continual conditioning with cAMP-increasing drugs. We also showed that these cells are more phagocytic and less inflammatory, but what remains to be revealed is the specific mediators that cAMP programmed AMϕ secrete to dampen tissue inflammation and encourage regeneration of the alveolar and epithelial barriers. Transcriptional analysis of rolipram educated AMϕ, either through RT-QPCR or single-cell RNA sequencing, may also reveal upregulated genes which are important to communication between AMϕ and other lung cells. Important considerations for these experiments are the time and conditions of the collected cells. We see that cAMP signaling after rolipram treatment is maximal at the peak of injury, but lung injury does not resolve for some time. Critical events may be occurring at the onset of rolipram treatment, in the midpoint transition between the peak of injury, and at the point at which enhanced resolution of injury was measured, generally 16 h post LPS induced injury in our experiments.

Another important next step is tracing the lineage of AMϕ after injury and how this is altered after rolipram treatment. Parabiosis of LysM-GFP and wildtype mice or usage of bone

marrow transplant to label monocytes would allow a more detailed tracing of monocytes into the airspace during injury and how rolipram affects the dynamics of this process. Further, we may investigate the ontogeny of recruited AMϕ through the adoptive transfer of fetal liver monocytes, the direct precursors of adult AMϕ, instead of bone marrow-derived monocytes. These more primitive cells may more readily generate anti-inflammatory AMϕ or be retained in higher numbers. Coupling lineage tracing with single-cell RNA sequencing would allow us to define the continuum of macrophage phenotypic signatures between resident and recruited macrophages as rolipram drives their reprogramming.

Preliminary results using LysM-CREB mice have given us a host of promising data to pursue. The deletion of CREB in myeloid cells is now established to impact lung fluid homeostasis. But because LysM is expressed in several myeloid lineage cell types a more specific Cre-promoter, such as the putative AMϕ specific driver CD169, is needed to interrogate the role of CREB in isolated lung macrophage populations. The dysregulation of PDK4 in CREB null BMDMs is particularly intriguing, as this critical metabolic bottleneck is dysregulated in a cell type whose metabolism undergoes dramatic shifts under inflammatory stimuli. Additionally, the overabundance of acetyl-CoA may also impact histone acetylation processes. Recent research has demonstrated that PDH is capable of translocating to the nucleus, where acetyl-CoA would be used as a substrate for histone acetylation and epigenetic regulation. Studying the epigenetic changes caused by the lack of CREB could reveal links between CREB and macrophage plasticity.

Literature Cited

1. Grabiec AM, Hussell T. The role of airway macrophages in apoptotic cell clearance following acute and chronic lung inflammation. *Semin Immunopathol*. 2016;38(4):409-423. doi:10.1007/s00281-016-0555-3

2. Lu YC, Yeh WC, Ohashi PS. LPS/TLR4 signal transduction pathway. *Cytokine*. 2008;42(2):145-151. doi:10.1016/j.cyto.2008.01.006

3. Stout RD, Suttles J. Functional plasticity of macrophages: reversible adaptation to changing microenvironments. *J Leukoc Biol*. 2004;76(3):509-513. doi:10.1189/jlb.0504272

4. Wynn TA, Vannella KM. Macrophages in Tissue Repair, Regeneration, and Fibrosis. *Immunity*. 2016;44(3):450-462. doi:10.1016/j.immuni.2016.02.015

5. Hoeksema MA, Glass CK. Nature and nurture of tissue-specific macrophage phenotypes. *Atherosclerosis*. 2019;281:159-167. doi:10.1016/j.atherosclerosis.2018.10.005

6. Fang P, Li X, Dai J, et al. Immune cell subset differentiation and tissue inflammation. *J Hematol Oncol*. 2018;11(1):97. doi:10.1186/s13045-018-0637-x

7. Gantner F, Kupferschmidt R, Schudt C, Wendel A, Hatzelmann A. In vitro differentiation of human monocytes to macrophages: Change of PDE profile and its relationship to suppression of tumour necrosis factor-α release by PDE inhibitors. *Br J Pharmacol*. 1997;121(2):221-231. doi:10.1038/sj.bjp.0701124

8. Hoeksema MA, de Winther MPJ. Epigenetic Regulation of Monocyte and Macrophage Function. *Antioxid Redox Signal*. 2016;25(14):758-774. doi:10.1089/ars.2016.6695

9. Uhlenhaut NH, Barish GD, Yu RT, et al. Insights into Negative Regulation by the Glucocorticoid Receptor from Genome-wide Profiling of Inflammatory Cistromes. *Mol Cell*. 2013;49(1):158-171. doi:10.1016/j.molcel.2012.10.013

10. Van Den Bossche J, Neele AE, Hoeksema MA, De Winther MPJ. Macrophage polarization: the epigenetic point of view. *Curr Opin Lipidol*. 2014;25(5):367-373. doi:10.1097/MOL.0000000000000109

11. Lavin Y, Winter D, Blecher-Gonen R, et al. Tissue-resident macrophage enhancer landscapes are shaped by the local microenvironment. *Cell*. 2014;159(6):1312-1326. doi:10.1016/j.cell.2014.11.018

12. Haldar M, Kohyama M, So AYL, et al. Heme-mediated SPI-C induction promotes monocyte differentiation into iron-recycling macrophages. *Cell*. 2014;156(6):1223-1234. doi:10.1016/j.cell.2014.01.069

13. Rosas M, Davies LC, Giles PJ, et al. The transcription factor Gata6 links tissue macrophage phenotype and proliferative renewal. *Science (80-)*. 2014;344(6184):645-648. doi:10.1126/science.1251414

14. Schultze JL, Schmidt S V. Molecular features of macrophage activation. *Semin Immunol*. 2015;27(6):416-423. doi:10.1016/j.smim.2016.03.009

15. Murray PJ, Allen JE, Biswas SK, et al. Macrophage Activation and Polarization: Nomenclature and Experimental Guidelines. *Immunity*. 2014;41(1):14-20. doi:10.1016/j.immuni.2014.06.008

16. Sica A, Mantovani A. Macrophage plasticity and polarization: In vivo veritas. *J Clin Invest*. 2012;122(3):787-795. doi:10.1172/JCI59643

17. Chávez-Galán L, Olleros ML, Vesin D, Garcia I. Much More than M1 and M2 Macrophages, There are also CD169(+) and TCR(+) Macrophages. *Front Immunol*. 2015;6:263. doi:10.3389/fimmu.2015.00263

18. Rhee SH, Hwang D. Murine TOLL-like receptor 4 confers lipopolysaccharide responsiveness as determined by activation of NFκB and expression of the inducible cyclooxygenase. *J Biol Chem*. 2000;275(44):34035-34040. doi:10.1074/jbc.M007386200

19. Janssens S, Beyaert R. A universal role for MyD88 in TLR/IL-1R-mediated signaling. *Trends Biochem Sci*. 2002;27(9):474-482. doi:10.1016/S0968-0004(02)02145-X

20. Smith TD, Tse MJ, Read EL, Liu WF. Regulation of macrophage polarization and plasticity by complex activation signals. *Integr Biol (United Kingdom)*. 2016;8(9):946-955. doi:10.1039/c6ib00105j

21. Ohmori Y, Hamilton TA. IL-4-induced STAT6 suppresses IFN-gamma-stimulated STAT1-dependent transcription in mouse macrophages. *J Immunol*. 1997;159(11):5474-5482. http://www.ncbi.nlm.nih.gov/pubmed/9548487. Accessed March 17, 2020.

22. Venkataraman C, Leung S, Salvekar A, Mano H, Schindler U. Repression of IL-4-induced gene expression by IFN-γ requires Stat1 activation. *J Immunol*. 1999;162(7):4053-4061.

23. Morales-Nebreda L, Misharin A V., Perlman H, Scott Budinger GR. The heterogeneity of lung macrophages in the susceptibility to disease. *Eur Respir Rev*. 2015;24(137):505-509. doi:10.1183/16000617.0031-2015

24. Cai Y, Sugimoto C, Arainga M, Alvarez X, Didier ES, Kuroda MJ. In Vivo Characterization of Alveolar and Interstitial Lung Macrophages in Rhesus Macaques: Implications for Understanding Lung Disease in Humans. *J Immunol*. 2014;192(6):2821-2829. doi:10.4049/jimmunol.1302269

25. Garbi N, Lambrecht BN. Location, function, and ontogeny of pulmonary macrophages during the steady state. *Pflugers Arch Eur J Physiol*. 2017;469(3-4):561-572. doi:10.1007/s00424-017-1965-3

26. Aegerter H, Kulikauskaite J, Crotta S, et al. Influenza-induced monocyte-derived alveolar macrophages confer prolonged antibacterial protection. *Nat Immunol*. 2020;21(2):145-157. doi:10.1038/s41590-019-0568-x

27. Fujimori T, Grabiec AM, Kaur M, et al. The Axl receptor tyrosine kinase is a discriminator of macrophage function in the inflamed lung. *Mucosal Immunol*. 2015;8(5):1021-1030. doi:10.1038/mi.2014.129

28. Zaynagetdinov R, Sherrill TP, Kendall PL, et al. Identification of myeloid cell subsets in murine lungs using flow cytometry. *Am J Respir Cell Mol Biol*. 2013;49(2):180-189.

doi:10.1165/rcmb.2012-0366MA

29. Singer BD, Mock JR, D 'alessio FR, et al. Flow-cytometric method for simultaneous analysis of mouse lung epithelial, endothelial, and hematopoietic lineage cells. *Am J Physiol - Lung Cell Mol Physiol*. 2016;310(9). http://ajplung.physiology.org/content/310/9/L796.long. Accessed July 17, 2017.

30. Hussell T, Bell TJ. Alveolar macrophages: plasticity in a tissue-specific context TL - 14. *Nat Rev Immunol*. 2014;14 VN-r(2):81-93. doi:10.1038/nri3600

31. Barnes PJ. Alveolar macrophages as orchestrators of COPD. *COPD*. 2004;1(1):59-70. doi:10.1081/COPD-120028701

32. Aggarwal NR, King LS, D'Alessio FR, et al. Diverse macrophage populations mediate acute lung inflammation and resolution. *Am J Physiol Lung Cell Mol Physiol*. 2014;306(8):L709-25. doi:10.1152/ajplung.00341.2013

33. Franke-Ullmann G, Pförtner C, Walter P, Steinmüller C, Lohmann-Matthes ML, Kobzik L. Characterization of murine lung interstitial macrophages in comparison with alveolar macrophages in vitro. *J Immunol*. 1996;157(7):3097-3104. http://www.jimmunol.org/content/157/7/3097. Accessed January 12, 2018.

34. Gibbings SL, Thomas SM, Atif SM, et al. Three Unique Interstitial Macrophages in the Murine Lung at Steady State. *Am J Respir Cell Mol Biol*. 2017;57(1):66-76. doi:10.1165/rcmb.2016-0361OC

35. Florentin J, Dutta P. Origin and production of inflammatory perivascular macrophages in pulmonary hypertension. *Cytokine*. 2017;100:11-15. doi:10.1016/j.cyto.2017.08.015

36. Johnston LK, Rims CR, Gill SE, McGuire JK, Manicone AM. Pulmonary macrophage subpopulations in the induction and resolution of acute lung injury. *Am J Respir Cell Mol Biol*. 2012;47(4):417-426. doi:10.1165/rcmb.2012-0090OC

37. Jakubzick C, Gautier EL, Gibbings SL, et al. Minimal differentiation of classical monocytes as they survey steady-state tissues and transport antigen to lymph nodes. *Immunity*. 2013;39(3):599-610. doi:10.1016/j.immuni.2013.08.007

38. van de Laar L, Saelens W, De Prijck S, et al. Yolk Sac Macrophages, Fetal Liver, and Adult Monocytes Can Colonize an Empty Niche and Develop into Functional Tissue-Resident Macrophages. *Immunity*. 2016;44(4):755-768. doi:10.1016/j.immuni.2016.02.017

39. Yu X, Buttgereit A, Lelios I, et al. The Cytokine TGF-β Promotes the Development and Homeostasis of Alveolar Macrophages. *Immunity*. November 2017. doi:10.1016/j.immuni.2017.10.007

40. Lemaire I, Yang H, Lauzon W, Gendron N. M-CSF and GM-CSF promote alveolar macrophage differentiation into multinucleated giant cells with distinct phenotypes. *J Leukoc Biol*. 1996;60(4):509-518. doi:10.1002/jlb.60.4.509

41. Ginhoux F. Fate PPAR-titioning: PPAR-gamma "instructs" alveolar macrophage development. *Nat Immunol*. 2014;15(11):1005-1007. doi:10.1038/ni.3011

42. Ebina-Shibuya R, Watanabe-Matsui M, Matsumoto M, et al. The double knockout of Bach1 and Bach2 in mice reveals shared compensatory mechanisms in regulating alveolar macrophage function and lung surfactant homeostasis. *J Biochem*. 2016;160(6):333-344. doi:10.1093/jb/mvw041

43. McVerry BJ, Garcia JGN. In vitro and in vivo modulation of vascular barrier integrity by sphingosine 1-phosphate: Mechanistic insights. *Cell Signal*. 2005;17(2):131-139. doi:10.1016/j.cellsig.2004.08.006

44. Bhattacharya J, Matthay MA. Regulation and Repair of the Alveolar-Capillary Barrier in Acute Lung Injury. *Annu Rev Physiol*. 2013;75(1):593-615. doi:10.1146/annurev-physiol-030212-183756

45. Matthay MA, Zimmerman GA. Acute lung injury and the acute respiratory distress syndrome: Four decades of inquiry into pathogenesis and rational management. *Am J Respir Cell Mol Biol*. 2005;33(4):319-327. doi:10.1165/rcmb.F305

46. Bhatia M, Moochhala S. Role of inflammatory mediators in the pathophysiology of acute respiratory distress syndrome. *J Pathol*. 2004;202(2):145-156. doi:10.1002/path.1491

47. Ma X, Xu D, Ai Y, Ming G, Zhao S. Fas inhibition attenuates lipopolysaccharide-induced apoptosis and cytokine release of rat type II alveolar epithelial cells. *Mol Biol Rep*. 2010;37(7):3051-3056. doi:10.1007/s11033-009-9876-9

48. Budinger GRS, Mutlu GM, Urich D, et al. Epithelial cell death is an important contributor to oxidant-mediated acute lung injury. *Am J Respir Crit Care Med*. 2011;183(8):1043-1054. doi:10.1164/rccm.201002-0181OC

49. Ware L, Matthay M. The acute respiratory distress syndrome. *N Engl J Med*. 2000;342(18):1334-1349. doi:10.1056/NEJM200005043421806

50. Ranieri VM, Rubenfeld GD, Thompson BT, et al. Acute respiratory distress syndrome: The Berlin definition. *JAMA - J Am Med Assoc*. 2012;307(23):2526-2533. doi:10.1001/jama.2012.5669

51. Matute-Bello G, Frevert CW, Martin TR. Animal models of acute lung injury. *Am J Physiol - Lung Cell Mol Physiol*. 2008;295(3):L379. doi:10.1152/ajplung.00010.2008

52. Tauseef M, Knezevic N, Chava KR, et al. TLR4 activation of TRPC6-dependent calcium signaling mediates endotoxininduced lung vascular permeability and inflammation. *J Exp Med*. 2012;209(11):1953-1968. doi:10.1084/jem.20111355

53. Kawano H, Kayama H, Nakama T, Hashimoto T, Umemoto E, Takeda K. IL-10-producing lung interstitial macrophages prevent neutrophilic asthma. *Int Immunol*. 2016;28(10):489-501. doi:10.1093/intimm/dxw012

54. Neupane AS, Willson M, Chojnacki AK, et al. Patrolling Alveolar Macrophages Conceal Bacteria from the Immune System to Maintain Homeostasis. *Cell*. 2020;183(1):110-125.e11. doi:10.1016/j.cell.2020.08.020

55. Westphalen K, Gusarova GA, Islam MN, et al. Sessile alveolar macrophages communicate with alveolar epithelium to modulate immunity. *Nature*.

2014;506(7489):503-506. doi:10.1038/nature12902

56. Snelgrove RJ, Goulding J, Didierlaurent AM, et al. A critical function for CD200 in lung immune homeostasis and the severity of influenza infection. *Nat Immunol*. 2008;9(9):1074-1083. doi:10.1038/ni.1637

57. Thepen T, Van Rooijen N, Kraal G. Alveolar macrophage elimination in vivo is associated with an increase in pulmonary immune response in mice. *J Exp Med*. 1989;170(2):499-509. doi:10.1084/jem.170.2.499

58. Rayees S, Rochford I, Joshi JC, Joshi B, Banerjee S, Mehta D. Macrophage TLR4 and PAR2 Signaling: Role in Regulating Vascular Inflammatory Injury and Repair. *Front Immunol*. 2020;11. doi:10.3389/fimmu.2020.02091

59. Wu DD, Pan PH, Liu B, et al. Inhibition of alveolar macrophage pyroptosis reduces lipopolysaccharide-induced acute lung injury in mice. *Chin Med J (Engl)*. 2015;128(19):2638-2645. doi:10.4103/0366-6999.166039

60. Preston JA, Bewley MA, Marriott HM, et al. Alveolar Macrophage Apoptosis-Associated Bacterial Killing Helps Prevent Murine Pneumonia. *Am J Respir Crit Care Med*. 2019;200(1):rccm.201804-0646OC. doi:10.1164/rccm.201804-0646OC

61. Orning P, Lien E, Fitzgerald KA. Gasdermins and their role in immunity and inflammation. *J Exp Med*. 2019:jem.20190545. doi:10.1084/jem.20190545

62. Latz E, Xiao TS, Stutz A. Activation and regulation of the inflammasomes. *Nat Rev Immunol*. 2013;13(6):397-411. doi:10.1038/nri3452

63. Ganter MT, Roux J, Miyazawa B, et al. Interleukin-1β causes acute lung injury via αvβ5 and αvβ6 integrin-dependent mechanisms. *Circ Res*. 2008;102(7):804-812. doi:10.1161/CIRCRESAHA.107.161067

64. He X, Qian Y, Li Z, et al. TLR4-Upregulated IL-1β and IL-1RI Promote Alveolar Macrophage Pyroptosis and Lung Inflammation through an Autocrine Mechanism. *Sci Rep*. 2016;6. doi:10.1038/srep31663

65. Martinon F, Burns K, Tschopp J. The Inflammasome: A Molecular Platform Triggering Activation of Inflammatory Caspases and Processing of proIL-1b. *Mol Cell*. 2004;10(2):417-426. doi:10.1016/s1097-2765(02)00599-3

66. Herold S, Mayer K, Lohmeyer J. *Acute Lung Injury: How Macrophages Orchestrate Resolution of Inflammation and Tissue Repair*. Vol 2.; 2011. doi:10.3389/fimmu.2011.00065

67. Vadász I, Raviv S, Sznajder JI. Alveolar epithelium and Na,K-ATPase in acute lung injury. *Intensive Care Med*. 2007;33(7):1243-1251. doi:10.1007/s00134-007-0661-8

68. Eaton DC, Helms MN, Koval M, Hui FB, Jain L. The contribution of epithelial sodium channels to alveolar function in health and disease. *Annu Rev Physiol*. 2009;71:403-423. doi:10.1146/annurev.physiol.010908.163250

69. Dickie AJ, Rafii B, Piovesan J, et al. Preventing endotoxin-stimulated alveolar

macrophages from decreasing epithelium Na+ channel (ENaC) mRNA levels and activity. *Pediatr Res*. 2000;48(3):304-310. doi:10.1203/00006450-200009000-00007

70. Laskin DL, Weinberger B, Laskin JD. Functional heterogeneity in liver and lung macrophages. *J Leukoc Biol*. 2001;70(August):163-170. doi:10.1189/JLB.70.2.163

71. Blázquez-Prieto J, López-Alonso I, Huidobro C, M. Albaiceta G. The Emerging Role of Neutrophils in Repair after Acute Lung Injury. *Am J Respir Cell Mol Biol*. 2018;59(3):rcmb.2018-0101PS. doi:10.1165/rcmb.2018-0101PS

72. Zheng DJ, Taka MA, Heit B. Role of apoptotic cell clearance in pneumonia and inflammatory lung disease. *Pathogens*. 2021;10(2):1-32. doi:10.3390/pathogens10020134

73. Krysko O, Vandenabeele P, Krysko D V., Bachert C. Impairment of phagocytosis of apoptotic cells and its role in chronic airway diseases. *Apoptosis*. 2010;15(9):1137-1146. doi:10.1007/s10495-010-0504-x

74. Reddy SM, Hsiao K-HK, Abernethy VE, et al. Phagocytosis of Apoptotic Cells by Macrophages Induces Novel Signaling Events Leading to Cytokine-Independent Survival and Inhibition of Proliferation: Activation of Akt and Inhibition of Extracellular Signal-Regulated Kinases 1 and 2. *J Immunol*. 2002;169(2):702-713. doi:10.4049/jimmunol.169.2.702

75. Huang S, Zhu B, Cheon IS, et al. PPAR-γ in macrophages limits pulmonary inflammation and promotes host recovery following respiratory viral infection. *J Virol*. February 2019:JVI.00030-19. doi:10.1128/JVI.00030-19

76. Schneider C, Nobs SP, Kurrer M, Rehrauer H, Thiele C, Kopf M. Induction of the nuclear receptor PPAR-γ 3 by the cytokine GM-CSF is critical for the differentiation of fetal monocytes into alveolar macrophages. *Nat Immunol*. 2014;15(11):1026-1037. doi:10.1038/ni.3005

77. Yoon YS, Kim SY, Kim MJ, Lim JH, Cho MS, Kang JL. PPARγ activation following apoptotic cell instillation promotes resolution of lung inflammation and fibrosis via regulation of efferocytosis and proresolving cytokines. *Mucosal Immunol*. 2015;8(5):1031-1046. doi:10.1038/mi.2014.130

78. Melloni B, Lesur O, Bouhadiba T, Cantin A, Martel M, Bégin R. Effect of exposure to silica on human alveolar macrophages in supporting growth activity in type II epithelial cells. *Thorax*. 1996;51(8):781-786. doi:10.1136/thx.51.8.781

79. Granata F, Frattini A, Loffredo S, et al. Production of Vascular Endothelial Growth Factors from Human Lung Macrophages Induced by Group IIA and Group X Secreted Phospholipases A 2. *J Immunol*. 2010;184(9):5232-5241. doi:10.4049/jimmunol.0902501

80. Golpon HA, Fadok VA, Taraseviciene-Stewart L, et al. Life after corpse engulfment: phagocytosis of apoptotic cells leads to VEGF secretion and cell growth. *FASEB J*. 2004;18(14):1716-1718. doi:10.1096/fj.04-1853fje

81. Morimoto K, Amano H, Sonoda F, et al. Alveolar macrophages that phagocytose apoptotic neutrophils produce hepatocyte growth factor during bacterial pneumonia in mice. *Am J Respir Cell Mol Biol*. 2001;24(5):608-615. doi:10.1165/ajrcmb.24.5.4292

82. Leslie CC, McCormick-Shannon K, Shannon JM, et al. Heparin-binding EGF-like Growth Factor is a Mitogen for Rat Alveolar Type II Cells. *Am J Respir Cell Mol Biol*. 1997;16(4):379-387. doi:10.1165/ajrcmb.16.4.9115748

83. Herold S, Tabar TS, Janßen H, et al. Exudate macrophages attenuate lung injury by the release of IL-1 receptor antagonist in gram-negative pneumonia. *Am J Respir Crit Care Med*. 2011;183(10):1380-1390. doi:10.1164/rccm.201009-1431OC

84. Evren E, Ringqvist E, Tripathi KP, et al. Distinct developmental pathways from blood monocytes generate human lung macrophage diversity. *Immunity*. 2020;0(0). doi:10.1016/j.immuni.2020.12.003

85. Ural BB, Yeung ST, Damani-Yokota P, et al. Identification of a nerve-associated, lung-resident interstitial macrophage subset with distinct localization and immunoregulatory properties. *Sci Immunol*. 2020;5(45):8756. doi:10.1126/sciimmunol.aax8756

86. García-Sastre A, Lucas D, Forsberg EC, et al. Tissue-resident macrophages self-maintain locally throughout adult life with minimal contribution from circulating monocytes. *Immunity*. 2013;38(4):792-804. doi:10.1016/j.immuni.2013.04.004

87. Misharin A V., Morales-Nebreda L, Reyfman PA, et al. Monocyte-derived alveolar macrophages drive lung fibrosis and persist in the lung over the life span. *J Exp Med*. 2017:1-18. doi:10.1084/jem.20162152

88. Landsman L, Varol C, Jung S. Distinct Differentiation Potential of Blood Monocyte Subsets in the Lung. *J Immunol*. 2007;178(4):2000-2007. doi:10.4049/jimmunol.178.4.2000

89. Landsman L, Jung S. Lung Macrophages Serve as Obligatory Intermediate between Blood Monocytes and Alveolar Macrophages. *J Immunol*. 2007;179(6):3488-3494. doi:10.4049/jimmunol.179.6.3488

90. Duan M, Li WC, Vlahos R, Maxwell MJ, Anderson GP, Hibbs ML. Distinct Macrophage Subpopulations Characterize Acute Infection and Chronic Inflammatory Lung Disease. *J Immunol*. 2012;189(2):946-955. doi:10.4049/jimmunol.1200660

91. Srivastava M, Jung S, Wilhelm J, et al. The Inflammatory versus Constitutive Trafficking of Mononuclear Phagocytes into the Alveolar Space of Mice Is Associated with Drastic Changes in Their Gene Expression Profiles. *J Immunol*. 2005;175(3):1884-1893. doi:10.4049/jimmunol.175.3.1884

92. Vijayaraj P, Gomperts BN. The aCCR(2)ual of M2 Macrophages Provides Some Breathing Room. *Cell Stem Cell*. 2017;21(1):1-3. doi:10.1016/j.stem.2017.06.006

93. Yin C, Cheng L, Pan J, et al. Regulatory role of Gpr84 in the switch of alveolar macrophages from CD11blo to CD11bhi status during lung injury process. *Mucosal Immunol*. July 2020:1-16. doi:10.1038/s41385-020-0321-7

94. Huaux F, Lo Re S, Giordano G, et al. IL-1α induces CD11blow alveolar macrophage proliferation and maturation during granuloma formation. *J Pathol*. 2015;235(5):698-709. doi:10.1002/path.4487

95. Duan M, Steinfort D, Smallwood D, et al. CD11b immunophenotyping identifies inflammatory profiles in the mouse and human lungs. *Mucosal Immunol*. 2015;9. doi:10.1038/mi.2015.84

96. Stoneman V, Braganza D, Figg N, et al. Monocyte/macrophage suppression in CD11b diphtheria toxin receptor transgenic mice differentially affects atherogenesis and established plaques. *Circ Res*. 2007;100(6):884-893. doi:10.1161/01.RES.0000260802.75766.00

97. Moldobaeva A, Zhong Q, Eldridge L, Wagner EM. CD11b + interstitial macrophages are required for ischemia-induced lung angiogenesis. *Physiol Rep*. 2018;6(11). doi:10.14814/phy2.13721

98. Joshi JC, Joshi B, Rochford I, et al. SPHK2-Generated S1P in CD11b+ Macrophages Blocks STING to Suppress the Inflammatory Function of Alveolar Macrophages. *Cell Rep*. 2020;30(12):4096-4109.e5. doi:10.1016/j.celrep.2020.02.112

99. Liu H, Moura-Alves P, Pei G, et al. cGAS facilitates sensing of extracellular cyclic dinucleotides to activate innate immunity. *EMBO Rep*. 2019;20(4). doi:10.15252/embr.201846293

100. Ohkuri T, Kosaka A, Ishibashi K, et al. Intratumoral administration of cGAMP transiently accumulates potent macrophages for anti-tumor immunity at a mouse tumor site. *Cancer Immunol Immunother*. 2017;66(6):705-716. doi:10.1007/s00262-017-1975-1

101. Polouliakh N, Nock R, Nielsen F, Kitano H. G-protein coupled receptor signaling architecture of mammalian immune cells. *PLoS One*. 2009;4(1). doi:10.1371/journal.pone.0004189

102. Rahman N, Buck J, Levin LR. pH sensing via bicarbonate-regulated "soluble" adenylyl cyclase (sAC). *Front Physiol*. 2013;4 NOV. doi:10.3389/fphys.2013.00343

103. Delghandi MP, Johannessen M, Moens U. The cAMP signalling pathway activates CREB through PKA, p38 and MSK1 in NIH 3T3 cells. *Cell Signal*. 2005;17(11):1343-1351. doi:10.1016/j.cellsig.2005.02.003

104. Shirshev S V. Role of Epac proteins in mechanisms of cAMP-dependent immunoregulation. *Biochem*. 2011;76(9):981-998. doi:10.1134/S000629791109001X

105. Insel PA, Ostrom RS. Forskolin as a tool for examining adenylyl cyclase expression, regulation, and G protein signaling. *Cell Mol Neurobiol*. 2003;23(3):305-314. doi:10.1023/A:1023684503883

106. Morinobu S, Fujimaki K, Okuyama N, Takahashi M, Duman RS. Stimulation of adenylyl cyclase and induction of brain-derived neurotrophic factor and TrkB mRNA by NKH477, a novel and potent forskolin derivative. *J Neurochem*. 1999;72(5):2198-2205. doi:10.1046/j.1471-4159.1999.0722198.x

107. Toyoshima H, Nasa Y, Kohsaka Y, et al. The effect of chronic treatment with trandolapril on cyclic AMP- and cyclic GMP-dependent relaxations in aortic segments of rats with chronic heart failure. *Br J Pharmacol*. 1998;123(2):344-352. doi:10.1038/sj.bjp.0701635

108. Reiter E, Lefkowitz RJ. GRKs and β-arrestins: roles in receptor silencing, trafficking and signaling. *Trends Endocrinol Metab*. 2006;17(4):159-165. doi:10.1016/j.tem.2006.03.008

109. Lazar AM, Irannejad R, Baldwin TA, et al. G protein-regulated endocytic trafficking of adenylyl cyclase type 9. *Elife*. 2020;9:1-24. doi:10.7554/eLife.58039

110. Smith FD, Esseltine JL, Nygren PJ, et al. Local protein kinase A action proceeds through intact holoenzymes. *Science (80-)*. 2017;356(6344):1288-1293. doi:10.1126/science.aaj1669

111. Baillie GS. Compartmentalized signalling: Spatial regulation of cAMP by the action of compartmentalized phosphodiesterases. *FEBS J*. 2009;276(7):1790-1799. doi:10.1111/j.1742-4658.2009.06926.x

112. Omori K, Kotera J. Overview of PDEs and their regulation. *Circ Res*. 2007;100(3):309-327. doi:10.1161/01.RES.0000256354.95791.f1

113. Conti M, Beavo J. Biochemistry and physiology of cyclic nucleotide phosphodiesterases: Essential components in cyclic nucleotide signaling. *Annu Rev Biochem*. 2007;76:481-511. doi:10.1146/annurev.biochem.76.060305.150444

114. Francis SH, Blount MA, Corbin JD. Mammalian cyclic nucleotide phosphodiesterases: Molecular mechanisms and physiological functions. *Physiol Rev*. 2011;91(2):651-690. doi:10.1152/physrev.00030.2010

115. Martinez SE, Wu AY, Glavas NA, et al. The two GAF domains in phosphodiesterase 2A have distinct roles in dimerization and in cGMP binding. *Proc Natl Acad Sci U S A*. 2002;99(20):13260-13265. doi:10.1073/pnas.192374899

116. Cedervall P, Aulabaugh A, Geoghegan KF, McLellan TJ, Pandit J. Engineered stabilization and structural analysis of the autoinhibited conformation of PDE4. *Proc Natl Acad Sci*. 2015;112(12):201419906. doi:10.1073/pnas.1419906112

117. Burgin AB, Magnusson OT, Singh J, et al. Design of phosphodiesterase 4D (PDE4D) allosteric modulators for enhancing cognition with improved safety. *Nat Biotechnol*. 2010;28(1):63-70. doi:10.1038/nbt.1598

118. Richter W, Conti M. Dimerization of the type 4 cAMP-specific phosphodiesterases is mediated by the upstream conserved regions (UCRs). *J Biol Chem*. 2002;277(43):40212-40221. doi:10.1074/jbc.M203585200

119. Baillie GS, Sood A, McPhee I, et al. β-arrestin-mediated PDE4 cAMP phosphodiesterase recruitment regulates β-adrenoceptor switching from Gs to Gi. *Proc Natl Acad Sci U S A*. 2003;100(3):940-945. doi:10.1073/pnas.262787199

120. Baillie GS, Houslay MD. Arrestin times for compartmentalised cAMP signalling and phosphodiesterase-4 enzymes. *Curr Opin Cell Biol*. 2005;17(2):129-134. doi:10.1016/j.ceb.2005.01.003

121. Richter W, Conti M. The oligomerization state determines regulatory properties and inhibitor sensitivity of type 4 cAMP-specific phosphodiesterases. *J Biol Chem*. 2004;279(29):30338-30348. doi:10.1074/jbc.M312687200

122. Houslay MD, Adams DR. Putting the lid on phosphodiesterase 4. *Nat Biotechnol*. 2010;28(1):38-40. doi:10.1038/nbt0110-38

123. Sette C, Conti M. Phosphorylation and activation of a cAMP-specific phosphodiesterase by the cAMP-dependent protein kinase. Involvement of serine 54 in the enzyme activation. *J Biol Chem*. 1996;271(28):16526-16534. doi:10.1074/jbc.271.28.16526

124. Manning CD, Mclaughlin MM, Livi GP, Cieslinski LB, Torphy TJ, Barnette MS. Prolonged beta adrenoceptor stimulation up-regulates cAMP phosphodiesterase activity in human monocytes by increasing mRNA and protein for phosphodiesterases 4A and 4B. *J Pharmacol Exp Ther*. 1996;276(2):810-818.

125. Conti M, Richter W, Mehats C, Livera G, Park J-Y, Jin C. Cyclic AMP-specific PDE4 Phosphodiesterases as Critical Components of Cyclic AMP Signaling. *J Biol Chem*. 2003;278(8):5493-5496. doi:10.1074/jbc.r200029200

126. Houslay MD, Baillie GS. The role of ERK2 docking and phosphorylation of PDE4 cAMP phosphodiesterase isoforms in mediating cross-talk between the cAMP and ERK signalling pathways. In: *Biochemical Society Transactions*. Vol 31. Portland Press Ltd; 2003:1186-1190. doi:10.1042/bst0311186

127. Krishnan J, Choi S. Systems Biological Approaches Reveal Non-additive Responses and Multiple Crosstalk Mechanisms between TLR and GPCR Signaling. *Genomics Inform*. 2012;10(3):153. doi:10.5808/gi.2012.10.3.153

128. Chopra M, Reuben JS, Sharma AC. Acute Lung Injury:Apoptosis and Signaling Mechanisms. *Exp Biol Med*. 2009;234(4):361-371. doi:10.3181/0811-MR-318

129. Chen Y, Wen JG, Feng JJ, et al. Forskolin attenuates the NLRP3 inflammasome activation and IL-1β secretion in human macrophages. *Pediatr Res*. May 2019:1. doi:10.1038/s41390-019-0418-4

130. Lee G-SS, Subramanian N, Kim AI, et al. The calcium-sensing receptor regulates the NLRP3 inflammasome through Ca2+ and cAMP. *Nature*. 2012;492(7427):123-127. doi:10.1038/nature11588

131. Fan EKY, Fan J. Regulation of alveolar macrophage death in acute lung inflammation. *Respir Res*. 2018;19(1). doi:10.1186/s12931-018-0756-5

132. You T, Cheng Y, Zhong J, et al. Roflupram, a Phosphodiesterase 4 Inhibitior, Suppresses Inflammasome Activation through Autophagy in Microglial Cells. *ACS Chem Neurosci*. 2017;8(11):2381-2392. doi:10.1021/acschemneuro.7b00065

133. Yang JX, Hsieh KC, Chen YL, et al. Phosphodiesterase 4B negatively regulates endotoxin-activated interleukin-1 receptor antagonist responses in macrophages. *Sci Rep*. 2017;7. doi:10.1038/srep46165

134. Bryn T, Mahic M, Enserink JM, Schwede F, Aandahl EM, Taskén K. The Cyclic AMP-Epac1-Rap1 Pathway Is Dissociated from Regulation of Effector Functions in Monocytes but Acquires Immunoregulatory Function in Mature Macrophages. *J Immunol*. 2006;176(12):7361-7370. doi:10.4049/jimmunol.176.12.7361

135. Jin S-LC, Conti M. Induction of the cyclic nucleotide phosphodiesterase PDE4B is essential for LPS-activated TNF- responses. *Proc Natl Acad Sci*. 2002;99(11):7628-7633. doi:10.1073/pnas.122041599

136. Gobejishvili L, Barve S, Joshi-Barve S, McClain C. Enhanced PDE4B expression augments LPS-inducible TNF expression in ethanol-primed monocytes: Relevance to alcoholic liver disease. *Am J Physiol - Gastrointest Liver Physiol*. 2008;295(4). doi:10.1152/ajpgi.90232.2008

137. Erdely A, Kepka-Lenhart D, Clark M, et al. Inhibition of phosphodiesterase 4 amplifies cytokine-dependent induction of arginase in macrophages. *Am J Physiol Cell Mol Physiol*. 2005;290(3):L534-L539. doi:10.1152/ajplung.00326.2005

138. Ernst O, Failayev H, Athamna M, He H, Tsfadia Y, Zor T. A dual and conflicting role for imiquimod in inflammation: A TLR7 agonist and a cAMP phosphodiesterase inhibitor. *Biochem Pharmacol*. 2020;182:114206. doi:10.1016/j.bcp.2020.114206

139. Ariga M, Neitzert B, Nakae S, et al. Nonredundant Function of Phosphodiesterases 4D and 4B in Neutrophil Recruitment to the Site of Inflammation. *J Immunol*. 2014;173(12):7531-7538. doi:10.4049/jimmunol.173.12.7531

140. Perazzona B, Isabel G, Preat T, Davis RL. The role of cAMP response element-binding protein in Drosophila long-term memory. *J Neurosci*. 2004;24(40):8823-8828. doi:10.1523/JNEUROSCI.4542-03.2004

141. Antony N, Weir JR, McDougall ARA, et al. cAMP Response Element Binding Protein1 Is Essential for Activation of Steroyl Co-Enzyme A Desaturase 1 (Scd1) in Mouse Lung Type II Epithelial Cells. *PLoS One*. 2013;8(4). doi:10.1371/journal.pone.0059763

142. Wen AY, Sakamoto KM, Miller LS. The Role of the Transcription Factor CREB in Immune Function. *J Immunol*. 2010;185(11):6413-6419. doi:10.4049/jimmunol.1001829

143. Impey S, McCorkle SR, Cha-Molstad H, et al. Defining the CREB regulon: A genome-wide analysis of transcription factor regulatory regions. *Cell*. 2004;119(7):1041-1054. doi:10.1016/j.cell.2004.10.032

144. Mayr B, Montminy M. Transcriptional regulation by the phosphorylation-dependent factor CREB. *Nat Rev Mol Cell Biol*. 2001;2(8):599-609. doi:10.1038/35085068

145. Thomson DM, Herway ST, Fillmore N, et al. AMP-activated protein kinase phosphorylates transcription factors of the CREB family. *J Appl Physiol*. 2008;104:429-438. doi:10.1152/japplphysiol.00900.2007.—AMP

146. Parker D, Ferreri K, Nakajima T, et al. Phosphorylation of CREB at Ser-133 induces complex formation with CREB-binding protein via a direct mechanism. *Mol Cell Biol*. 1996;16(2):694-703. doi:10.1128/mcb.16.2.694

147. Cho EE-C, Mitton B, Sakamoto KM. CREB and leukemogenesis. *Crit Rev Oncog*. 2011;16(1-2):37-46. doi:10.1615/CritRevOncog.v16.i1-2.50

148. Sandoval S, Kraus C, Cho EC, et al. Sox4 cooperates with CREB in myeloid transformation. *Blood*. 2012;120(1):155-165. doi:10.1182/blood-2011-05-357418

149. Brenner S, Prösch S, Schenke-Layland K, Riese U, Gausmann U, Platzer C. cAMP-induced interleukin-10 promoter activation depends on CCAAT/enhancer-binding protein expression and monocytic differentiation. *J Biol Chem*. 2003;278(8):5597-5604. doi:10.1074/jbc.M207448200

150. Sabatel C, Radermecker C, Fievez L, et al. Exposure to Bacterial CpG DNA Protects from Airway Allergic Inflammation by Expanding Regulatory Lung Interstitial Macrophages. *Immunity*. 2017;46(3):457-473. doi:10.1016/j.immuni.2017.02.016

151. Luan B, Yoon Y-S, Le Lay J, Kaestner KH, Hedrick S, Montminy M. CREB pathway links PGE2 signaling with macrophage polarization. *Proc Natl Acad Sci U S A*. 2015;112(51):15642-15647. doi:10.1073/pnas.1519644112

152. Bystrom J, Evans I, Newson J, et al. Resolution-phase macrophages possess a unique inflammatory phenotype that is controlled by cAMP. *Blood*. 2008;112(10):4117-4127. doi:10.1182/blood-2007-12-129767

153. Hayakawa K, Wang X, Lo EH. CD200 increases alternatively activated macrophages through CREB - C/EBP-beta signaling. *J Neurochem*. 2015. doi:10.1111/jnc.13492

154. Shenkar R, Yum HK, Arcaroli J, Kupfner J, Abraham E. Interactions between CBP, NF-kappaB, and CREB in the lungs after hemorrhage and endotoxemia. *Am J Physiol Lung Cell Mol Physiol*. 2001;281(2):L418-26. http://ajplung.physiology.org/content/ajplung/281/2/L418.full.pdf. Accessed September 13, 2017.

155. Sohal SS, Reid D, Soltani A, et al. Reticular basement membrane fragmentation and potential epithelial mesenchymal transition is exaggerated in the airways of smokers with chronic obstructive pulmonary disease. *Respirology*. 2010;15(6):930-938. doi:10.1111/j.1440-1843.2010.01808.x

156. Welte T, Groneberg DA. Asthma and COPD. *Exp Toxicol Pathol*. 2006;57(SUPPL. 2):35-40. doi:10.1016/j.etp.2006.02.004

157. Giembycz MA, Maurice DH. Cyclic nucleotide-based therapeutics for chronic obstructive pulmonary disease. *Curr Opin Pharmacol*. 2014;16(1):89-107. doi:10.1016/j.coph.2014.04.001

158. Bender AT, Beavo JA. Cyclic nucleotide phosphodiesterases: Molecular regulation to clinical use. *Pharmacol Rev*. 2006;58(3):488-520. doi:10.1124/pr.58.3.5

159. Dillard J, Meng X, Nelin L, Liu Y, Chen B. Nitric oxide activates AMPK by modulating PDE3A in human pulmonary artery smooth muscle cells. *Physiol Rep*. 2020;8(17). doi:10.14814/phy2.14559

160. Rybalkin SD, Yan C, Bornfeldt KE, Beavo JA. Cyclic GMP phosphodiesterases and regulation of smooth muscle function. *Circ Res*. 2003;93(4):280-291. doi:10.1161/01.RES.0000087541.15600.2B

161. Perez-Zoghbi JF, Bai Y, Sanderson MJ. Nitric oxide induces airway smooth muscle cell relaxation by decreasing the frequency of agonist-induced Ca2+ oscillations. *J Gen Physiol*. 2010;135(3):247-259. doi:10.1085/jgp.200910365

162. Andersson KE. PDE5 inhibitors – pharmacology and clinical applications 20 years after sildenafil discovery. *Br J Pharmacol*. 2018;175(13):2554-2565. doi:10.1111/bph.14205

163. Ghofrani HA, Osterloh IH, Grimminger F. Sildenafil: From angina to erectile dysfunction to pulmonary hypertension and beyond. *Nat Rev Drug Discov*. 2006;5(8):689-702. doi:10.1038/nrd2030

164. Abbott-Banner KH, Page CP. Dual PDE3/4 and PDE4 inhibitors: Novel treatments for COPD and other inflammatory airway diseases. *Basic Clin Pharmacol Toxicol*. 2014;114(5):365-376. doi:10.1111/bcpt.12209

165. BinMahfouz H, Borthakur B, Yan D, George T, Giembycz MA, Newton R. Superiority of combined phosphodiesterase PDE3/PDE4 inhibition over PDE4 inhibition alone on glucocorticoid- And long-acting β-adrenoceptor agonist -induced gene expression in human airway epithelial cells. *Mol Pharmacol*. 2015;87(1):64-76. doi:10.1124/mol.114.093393

166. Milara J, Navarro A, Almudéver P, Lluch J, Morcillo EJ, Cortijo J. Oxidative stress-induced glucocorticoid resistance is prevented by dual PDE3/PDE4 inhibition in human alveolar macrophages. *Clin Exp Allergy*. 2011;41(4):535-546. doi:10.1111/j.1365-2222.2011.03715.x

167. Blease K, Burke-Gaffney A, Hellewell PG. Modulation of cell adhesion molecule expression and function on human lung microvascular endothelial cells by inhibition of phosphodiesterases 3 and 4. *Br J Pharmacol*. 1998;124(1):229-237. doi:10.1038/sj.bjp.0701833

168. Brown WM. Treating COPD with PDE 4 inhibitors. *Int J Chron Obstruct Pulmon Dis*. 2007;2(4):517-533. http://www.ncbi.nlm.nih.gov/pubmed/18268925. Accessed April 8, 2019.

169. Jeffery P. Phosphodiesterase 4-selective inhibition: Novel therapy for the inflammation of COPD. *Pulm Pharmacol Ther*. 2005;18(1):9-17. doi:10.1016/j.pupt.2004.09.027

170. Milara J, Morcillo E, Monleon D, Tenor H, Cortijo J. Roflumilast prevents the metabolic Effects of bleomycin-induced fibrosis in a murine model. *PLoS One*. 2015;10(7). doi:10.1371/journal.pone.0133453

171. Seimetz M, Parajuli N, Pichl A, et al. Cigarette smoke-induced emphysema and pulmonary hypertension can be prevented by phosphodiesterase 4 and 5 inhibition in mice. *PLoS One*. 2015;10(6):e0129327. doi:10.1371/journal.pone.0129327

172. Peng CK, Huang KL, Wu CP, Wu YK, Tzeng IS, Lan CC. Phosphodiesterase-4 Inhibitor Roflumilast Attenuates Pulmonary Air Emboli–Induced Lung Injury. *J Surg Res*. 2019;241:24-30. doi:10.1016/j.jss.2019.03.028

173. Ma H, Shi J, Wang C, et al. Blockade of PDE4B limits lung vascular permeability and lung inflammation in LPS-induced acute lung injury. *Biochem Biophys Res Commun*. 2014;450(4):1560-1567. doi:10.1016/j.bbrc.2014.07.024

174. Tavares LP, Garcia CC, Vago JP, et al. Inhibition of phosphodiesterase-4 during pneumococcal pneumonia reduces inflammation and lung injury in mice. *Am J Respir Cell*

Mol Biol. 2016;55(1):24-34. doi:10.1165/rcmb.2015-0083OC

175. Kosutova P, Mikolka P, Kolomaznik M, et al. Reduction of lung inflammation, oxidative stress and apoptosis by the PDE4 inhibitor roflumilast in experimental model of acute lung injury. *Physiol Res*. 2018;67(Supplementum 4):S645-S654. doi:10.33549/physiolres.934047

176. Martorana PA, Beume R, Lucattelli M, Wollin L, Lungarella G. Roflumilast fully prevents emphysema in mice chronically exposed to cigarette smoke. *Am J Respir Crit Care Med*. 2005;172(7):848-853. doi:10.1164/rccm.200411-1549OC

177. Mihara K, Ramachandran R, Saifeddine M, et al. Thrombin-mediated direct activation of proteinase-activated Receptor-2: Another target for thrombin signaling. *Mol Pharmacol*. 2016;89(5):606-614. doi:10.1124/mol.115.102723

178. Rayees S, Joshi JCJCJC, Tauseef M, et al. PAR2-Mediated cAMP Generation Suppresses TRPV4-Dependent Ca 2+ Signaling in Alveolar Macrophages to Resolve TLR4-Induced Inflammation. *Cell Rep*. 2019;27(3):793-805.e4. doi:10.1016/j.celrep.2019.03.053

179. Sato Y, Sato S, Yamamoto T, Ishikawa S, Onizuka M, Sakakibara Y. Phosphodiesterase type 4 inhibitor reduces the retention of polymorphonuclear leukocytes in the lung. *Am J Physiol Cell Mol Physiol*. 2015;282(6):L1376-L1381. doi:10.1152/ajplung.00433.2001

180. Bradley KK, Bradley ME. Phosphodiesterase 4 inhibitors prevent cytokine secretion by T lymphocytes by inhibiting nuclear factor-κB and nuclear factor of activated T cells activation. *J Pharmacol Exp Ther*. 2001;299(2):753-759. http://jpet.aspetjournals.org. Accessed November 4, 2019.

181. MacKenzie SJ, Houslay MD. Action of rolipram on specific PDE4 cAMP phosphodiesterase isoforms and on the phosphorylation of cAMP-response-element-binding protein (CREB) and p38 mitogen-activated protein (MAP) kinase in U937 monocytic cells. *Biochem J*. 2000;347(2):571-578. doi:10.1042/0264-6021:3470571

182. Covarrubias AJ, Aksoylar HI, Horng T. Control of macrophage metabolism and activation by mTOR and Akt signaling. *Semin Immunol*. 2015;27(4):286-296. doi:10.1016/j.smim.2015.08.001

183. Freemerman AJ, Johnson AR, Sacks GN, et al. GLUCOSE TRANSPORTER 1 (GLUT1)-MEDIATED GLUCOSE METABOLISM DRIVES A S PROINFLAMMATORY PHENOTYPE. *J Biol Chem*. 2014;289(11):7884-7896. doi:10.1074/jbc.M113.522037

184. Koo SJ, Chowdhury IH, Szczesny B, Wan X, Garg NJ. Macrophages promote oxidative metabolism to drive nitric oxide generation in response to Trypanosoma cruzi. *Infect Immun*. 2016;84(12):3527-3541. doi:10.1128/IAI.00809-16

185. Van den Bossche J, Baardman J, Otto NA, et al. Mitochondrial Dysfunction Prevents Repolarization of Inflammatory Macrophages. *Cell Rep*. 2016;17(3):684-696. doi:10.1016/j.celrep.2016.09.008

186. Ip WKE, Hoshi N, Shouval DS, Snapper S, Medzhitov R. Anti-inflammatory effect of IL-10 mediated by metabolic reprogramming of macrophages. http://science.sciencemag.org/content/sci/356/6337/513.full.pdf. Accessed May 18, 2017.

187. Mills EL, Kelly B, Logan A, et al. Succinate Dehydrogenase Supports Metabolic Repurposing of Mitochondria to Drive Inflammatory Macrophages. *Cell*. 2016;167(2):457-470.e13. doi:10.1016/j.cell.2016.08.064

188. Seim GL, Britt EC, John S V., et al. Two-stage metabolic remodelling in macrophages in response to lipopolysaccharide and interferon-γ stimulation. *Nat Metab*. 2019;1(7):731-742. doi:10.1038/s42255-019-0083-2

189. Huang SC-CCC, Smith AMM, Everts B, et al. Metabolic Reprogramming Mediated by the mTORC2-IRF4 Signaling Axis Is Essential for Macrophage Alternative Activation. *Immunity*. 2016;45(4):817-830. doi:10.1016/j.immuni.2016.09.016

190. Jiang D-S, Bian Z-Y, Zhang Y, et al. Role of Interferon Regulatory Factor 4 in the Regulation of Pathological Cardiac Hypertrophy. *Hypertension*. 2013;61(6):1193-1202. doi:10.1161/HYPERTENSIONAHA.111.00614

191. Lumeng CN, Bodzin JL, Saltiel AR. Obesity induces a phenotypic switch in adipose tissue macrophage polarization. *J Clin Invest*. 2007;117(1):175-184. doi:10.1172/JCI29881

192. Feng J, Li L, Ou Z, et al. IL-25 stimulates M2 macrophage polarization and thereby promotes mitochondrial respiratory capacity and lipolysis in adipose tissues against obesity. *Cell Mol Immunol*. 2017. doi:10.1038/cmi.2016.71

193. Kolobova E, Tuganova A, Boulatnikov I, Popov KM. Regulation of pyruvate dehydrogenase activity through phosphorylation at multiple sites. *Biochem J*. 2001;358(1):69-77. doi:10.1042/0264-6021:3580069

194. Zhang S, Hulver MW, McMillan RP, Cline MA, Gilbert ER. The pivotal role of pyruvate dehydrogenase kinases in metabolic flexibility. *Nutr Metab*. 2014;11(1). doi:10.1186/1743-7075-11-10

195. Holness MJ, Sugden MC. Regulation of pyruvate dehydrogenase complex activity by reversible phosphorylation. In: *Biochemical Society Transactions*. Vol 31. ; 2003:1143-1151. doi:10.1042/bst0311143

196. Meiser J, Krämer L, Sapcariu SC, et al. Pro-inflammatory macrophages sustain pyruvate oxidation through pyruvate dehydrogenase for the synthesis of itaconate and to enable cytokine expression. *J Biol Chem*. 2016;291(8):3932-3946. doi:10.1074/jbc.M115.676817

197. De Boer VCJ, Houten SM. A mitochondrial expatriate: Nuclear pyruvate dehydrogenase. *Cell*. 2014;158(1):9-10. doi:10.1016/j.cell.2014.06.018

198. Sutendra G, Kinnaird A, Dromparis P, et al. A nuclear pyruvate dehydrogenase complex is important for the generation of Acetyl-CoA and histone acetylation. *Cell*. 2014;158(1):84-97. doi:10.1016/j.cell.2014.04.046

199. Matsuhashi T, Hishiki T, Zhou H, et al. Activation of pyruvate dehydrogenase by dichloroacetate has the potential to induce epigenetic remodeling in the heart. *J Mol Cell Cardiol*. 2015;82:116-124. doi:10.1016/j.yjmcc.2015.02.021

200. Na YR, Jung D, Song J, Park JW, Hong JJ, Seok SH. Pyruvate dehydrogenase kinase is a negative regulator of interleukin-10 production in macrophages. *J Mol Cell Biol*.

2020;12(7):543-555. doi:10.1093/jmcb/mjz113

201. Jha MK, Song GJ, Lee MG, et al. Metabolic Connection of Inflammatory Pain: Pivotal Role of a Pyruvate Dehydrogenase Kinase-Pyruvate Dehydrogenase-Lactic Acid Axis. *J Neurosci*. 2015;35(42):14353-14369. doi:10.1523/JNEUROSCI.1910-15.2015

202. Semba H, Takeda N, Isagawa T, et al. HIF-1α-PDK1 axis-induced active glycolysis plays an essential role in macrophage migratory capacity. *Nat Commun*. 2016;7:11635. doi:10.1038/ncomms11635

203. Bertram A, Zhang H, von Vietinghoff S, et al. Protein Kinase C-θ Is Required for Murine Neutrophil Recruitment and Adhesion Strengthening under Flow. *J Immunol*. 2012;188(8):4043-4051. doi:10.4049/jimmunol.1101651

204. Sheldon KE, Shandilya H, Kepka-Lenhart D, Poljakovic M, Ghosh A, Morris SM. Shaping the Murine Macrophage Phenotype: IL-4 and Cyclic AMP Synergistically Activate the Arginase I Promoter. *J Immunol*. 2013;191(5):2290-2298. doi:10.4049/jimmunol.1202102

205. Pehote G, Bodas M, Brucia K, Vij N. Cigarette Smoke Exposure Inhibits Bacterial Killing via TFEB-Mediated Autophagy Impairment and Resulting Phagocytosis Defect. *Mediators Inflamm*. 2017;2017:1-14. doi:10.1155/2017/3028082

206. Lea S, Metryka A, Li J, et al. The modulatory effects of the PDE4 inhibitors CHF6001 and roflumilast in alveolar macrophages and lung tissue from COPD patients. *Cytokine*. 2019;123:154739. doi:10.1016/j.cyto.2019.154739

207. Round JL, Humphries LA, Tomassian T, Mittelstadt P, Zhang M, Miceli MC. Scaffold protein Dlgh1 coordinates alternative p38 kinase activation, directing T cell receptor signals toward NFAT but not NF-κB transcription factors. *Nat Immunol*. 2007;8(2):154-161. doi:10.1038/ni1422

208. Lafuse WP, Rajaram MVS, Wu Q, et al. Identification of an Increased Alveolar Macrophage Subpopulation in Old Mice That Displays Unique Inflammatory Characteristics and Is Permissive to Mycobacterium tuberculosis Infection. *J Immunol*. 2019;203(8):2252-2264. doi:10.4049/jimmunol.1900495

209. St-Laurent J, Turmel V, Boulet LP, Bissonnette E. Alveolar macrophage subpopulations in bronchoalveolar lavage and induced sputum of asthmatic and control subjects. *J Asthma*. 2009;46(1):1-8. doi:10.1080/02770900802444211

210. Lucia Gonçalves de Moraes V, Singer M, Boris Vargaftig B, et al. Effects of rolipram on cyclic AMP levels in alveolar macrophages and lipopolysaccharide-induced inflammation in mouse lung. *Br J Pharmacol*. 2005;123(4):631-636. doi:10.1038/sj.bjp.0701649

211. Maus UA, Janzen S, Wall G, et al. Resident alveolar macrophages are replaced by recruited monocytes in response to endotoxin-induced lung inflammation. *Am J Respir Cell Mol Biol*. 2006;35(2):227-235. doi:10.1165/rcmb.2005-0241OC

212. Sanin DE, Prendergast CT, Mountford AP. IL-10 Production in Macrophages Is Regulated by a TLR-Driven CREB-Mediated Mechanism That Is Linked to Genes Involved in Cell Metabolism. *J Immunol*. 2015;195(3):1218-1232. doi:10.4049/jimmunol.1500146

213. Gamage AM, Zhu F, Ahn M, et al. Immunophenotyping monocytes, macrophages and granulocytes in the Pteropodid bat Eonycteris spelaea. *Sci Rep*. 2020;10(1). doi:10.1038/s41598-019-57212-1

214. Kirby AC, Raynes JG, Kaye PM. CD11b regulates recruitment of alveolar macrophages but not pulmonary dendritic cells after pneumococcal challenge. *J Infect Dis*. 2006;193(2):205-213. doi:10.1086/498874

215. Löfdahl JM, Wahlström J, Sköld CM. Different inflammatory cell pattern and macrophage phenotype in chronic obstructive pulmonary disease patients, smokers and non-smokers. *Clin Exp Immunol*. 2006;145(3):428-437. doi:10.1111/j.1365-2249.2006.03154.x

216. Zasłona Z, Przybranowski S, Wilke C, et al. Resident Alveolar Macrophages Suppress, whereas Recruited Monocytes Promote, Allergic Lung Inflammation in Murine Models of Asthma. *J Immunol*. 2014;193(8):4245-4253. doi:10.4049/jimmunol.1400580

217. Cao S, Zhang X, Edwards JP, Mosser DM. NF-κB1 (p50) homodimers differentially regulate pro- and anti-inflammatory cytokines in macrophages. *J Biol Chem*. 2006;281(36):26041-26050. doi:10.1074/jbc.M602222200

218. Hogan PG. Calcium–NFAT transcriptional signalling in T cell activation and T cell exhaustion. *Cell Calcium*. 2017;63:66-69. doi:10.1016/j.ceca.2017.01.014

219. Jin S-LLC, Lan L, Zoudilova MM, Conti M. Specific Role of Phosphodiesterase 4B in Lipopolysaccharide-Induced Signaling in Mouse Macrophages. *J Immunol*. 2014;175(3):1523-1531. doi:10.4049/jimmunol.175.3.1523

220. Sun J gang, Deng Y mei, Wu X, et al. Inhibition of phosphodiesterase activity, airway inflammation and hyperresponsiveness by PDE4 inhibitor and glucocorticoid in a murine model of allergic asthma. *Life Sci*. 2006;79(22):2077-2085. doi:10.1016/j.lfs.2006.07.001

221. MacKenzie KF, Clark K, Naqvi S, et al. PGE2 Induces Macrophage IL-10 Production and a Regulatory-like Phenotype via a Protein Kinase A-SIK-CRTC3 Pathway. *J Immunol*. 2013;190(2):565-577. doi:10.4049/jimmunol.1202462

222. Avni D, Ernst O, Philosoph A, Zor T. Role of CREB in modulation of TNFα and IL-10 expression in LPS-stimulated RAW264.7 macrophages. *Mol Immunol*. 2010;47(7-8):1396-1403. doi:10.1016/j.molimm.2010.02.015

223. Galván-Peña S, O'Neill LAJ. Metabolic reprograming in macrophage polarization. *Front Immunol*. 2014;5(SEP):420. doi:10.3389/fimmu.2014.00420

224. Woods PS, Kimmig LM, Meliton AY, et al. Tissue Resident Alveolar Macrophages Do Not Rely on Glycolysis for LPS-induced Inflammation. *Am J Respir Cell Mol Biol*. August 2019. doi:10.1165/rcmb.2019-0244oc

225. Dhaliwal K, Scholefield E, Ferenbach D, et al. Monocytes control second-phase neutrophil emigration in established lipopolysaccharide-induced murine lung injury. *Am J Respir Crit Care Med*. 2012;186(6):514-524. doi:10.1164/rccm.201112-2132OC

Vita

Ian Rochford

EDUCATION

University of Illinois at Chicago — Chicago, IL
PhD in Pharmacology and Regenerative Medicine — May 2021

University of Missouri at Kansas City — Kansas City, MO
Master of Science in Biochemistry and Molecular Biology — May 2014

University of Nebraska at Lincoln — Lincoln, NE
Bachelor of Arts and Sciences in Biological Sciences — August 2012

RESEARCH PUBLICATIONS

Rochford I, Joshi JC, Rayees S, Yalagala V, Anwar M, Mehta D. PDE4b suppresses alveolar macrophage generation and anti-inflammatory function. *AJP Lung.* PUBLICATION PENDING

Rayees S, **Rochford I**, Joshi JC, Joshi B, Banerjee S, Mehta D. Macrophage TLR4 and PAR2 signaling: Role in regulating vascular inflammatory injury and repair. *Front Immunol*. 2020; 11: 2091.

Joshi JC, Joshi B, **Rochford I**, Rayees S, et al. SPHK2-generated S1P in $CD11b^{+}$ macrophages blocks STING to suppress the inflammatory function of alveolar macrophages. *Cell Rep*. 2020; 30(12):4096-4109.e5.

Rayees S, Joshi JC, Tauseef M, Anwar M, Baweja S, **Rochford I**, et al. PAR2-mediated cAMP generation suppresses TRPV4-dependent Ca^{2+} signaling in alveolar macrophages to resolve TLR4-induced inflammation. *Cell Rep*. 2019; 27(3):793-805.e4.

AWARDS

Federation of American Societies for Experimental Biology Travel Award. 2017

National Institute of Health Lung Biology and Pathophysiology Training Grant. 2016-1018

PRESENTATIONS

PDE4b regulates alveolar macrophage pyroptosis
Poster Presentation, UIC Pharmacology Department Research Retreat
Chicago, 2019

Novel role of CREB in regulating alveolar macrophage generation and function
Oral Presentation, Graduate Education in Medical Sciences (GEMS) Research Symposium
Chicago, 2018

Novel role of CREB in regulating maturation of alveolar macrophages and maintaining lung-fluid balance
Poster Presentation Experimental Biology Conference
San Diego, 2018

Macrophage lineage during acute lung injury and resolution: Role of epigenetic mechanisms
Oral Presentation, Experimental Biology Conference
Chicago, 2017

Epigenetic regulation of macrophage linage during acute lung injury and resolution
Poster Presentation, Experimental Biology Conference
Chicago, 2017

Macrophage cAMP-response element binding protein regulates metabolic reprogramming, mitochondrial function, and lung-fluid homeostasis
Poster Presentation, UIC Pharmacology Department Research Retreat
Chicago, 2017

VOLUNTEER WRITING

COVID-19: Redefining Lung Disease
Science Unsealed blog, Illinois Science Council
September 2020

Cancer Immunotherapy: Living Drugs and Immune Catalysts
Science Unsealed blog, Illinois Science Council
July 2020

LEADERSHIP EXPERIENCE

Graduate Education in Medical Sciences Student Association (GEMSSA) Leadership Board
Career Development Coordinator, 2016-2020
University of Illinois College of Medicine

'Your Future in Science' Seminar Series Planning Committee
Committee Member, 2017-2020
University of Illinois College of Medicine

GEMSSA Research Symposium Planning Committee
Committee Member, 2017-2019
University of Illinois College of Medicine

MEMBERSHIPS

American Medical Writer's Association
Student Member

ADDITIONAL TRAINING

CommSci Conference Writing Workshop
Northwestern University, 2019

Writing in the Sciences
Coursera Online Course, Stanford University, 2018

Foundational Skills for Communicating About Health
Coursera Online Course, University of Michigan, 2021